Systematic revision of the genus *Jorunna* (Nudibranchia: Discodorididae) in Europe with a focus on the *J. tomentosa* species complex

Master of Science in Marine Biology

Jenny Neuhaus

Department of Biological Sciences

University of Bergen, Norway

September 2020

Acknowledgements

I would like to start off by saying thank you to my supervisor Manuel A. E. Malaquias for introducing me to the field of integrative systematics in nudibranch molluscs. The sea slugs have taken me on an inspiring journey across many countries and I am grateful for this opportunity and for all your guidance and patience. I would also like to give a special thanks to Cessa Rauch for being an excellent and ever supportive supervisor, helping me with illustrations, literature research, and giving me lots of great field work experience. I am deeply grateful to Marta Pola from the University Autónoma of Madrid, Spain for being an extraordinary teacher, spending weeks to guide me through the world of sea slug anatomy. It was a great pleasure being able to dissect and draw my specimens in your lab facilities, thank you for all your guidance and patience.

I wish to thank all the people that provided me with slug samples and photographs for this project: Nils Aukan, Anders Schouw, Erling Svensen, Bernard Picton, Torkild Bakken, Tine Kinn Kvamme, Heine Jensen, Juan Lucas Cervera, Marina Poddubetskaia, Jessica A. Toms, and Bernhard Hausdorf. A special thanks to Terrence M. Gosliner and Elizabeth Kools at the California Academy of Sciences (CAS) for allowing me to visit the facilities and gather material for my studies. Furthermore, I wish to thank everyone that helped me at the Biodiversity Laboratory (BDL, DNA lab) at the University of Bergen and contributed to a pleasant work environment. A special thanks goes to Louise M. Lindblom for introducing me to the DNA lab facilities, guiding me through the steps of the molecular work throughout my entire thesis and helping me troubleshoot difficult samples. Thank you, Kenneth Meland and Solveig Thorkildsen, for always answering my questions about practicalities in the DNA lab. I also wish to thank Irene Heggstad for her guidance and patience with the scanning electron microscope images. A big thank you to the staff at the UiB University library at the Faculty of Mathematics and Natural Sciences for providing me with historic literature from all over the world.

Furthermore, I would like to express my gratitude to the Sea Slugs of Southern Norway project (SSOSN) for funding my studies and making it possible for me to present my research at the World Congress of Malacology 2019 in Monterey Bay, California. It was an amazing experience to be part of an international conference and I am ever grateful for this opportunity. Thanks to the Norwegian Taxonomy Initiative (Artsdatabanken, project nr. 812038) for in turn funding the SSOSN project. Thank you to the University of Bergen from whom I received a travel grand which funded a substantial part of my attendance at the World Congress of Malacology. Finally, I would like to thank Paul, my family, and friends for all your support. I

could certainly not have done this without you, especially with regard to the COVID-19 pandemic and the social restrictions it brought along.

Cover photograph: *Jorunna tomentosa sensu lato* (ZMBN 127657). Photo taken in Egersund, Norway by Erling Svensen (2019).

Abstract

Jorunna is a genus of Nudibranchia in the family Discodorididae, currently comprising 21 recognized valid species with a worldwide coastal distribution in the four main biogeographical regions Eastern and Western Atlantic, Eastern Pacific and the Indo-West Pacific. This study presents a systematic revision of the currently valid European species *J. tomentosa*, *J. efe*, *J. evansi*, *J. onubensis*, and *J. spazzola* in addition to a generic assessment of *Gargamella lemchei*, former *Jorunna lemchei*. The taxonomic status of *J. tomentosa sensu lato* was revised using an integrative approach combining morpho-anatomical studies with molecular phylogenetics. Two mitochondrial genes, cytochrome *c* oxidase subunit I (COI) and 16S ribosomal RNA (16S), as well as the nuclear gene histone 3 (H3), were amplified and sequenced (*n = 114* novel sequences). The phylogenetic relationships were inferred using Bayesian and maximum likelihood analyses. The molecular species delimitation method Automatic Barcode Gap Discovery was used to aid delimiting species. Genetic uncorrected *p*-distances based on the gene COI were estimated between and within species. Animals were dissected for the reproductive system, radulae, and labial cuticles using a stereo microscope. Scanning electron microscopy was employed to study ultrastructural elements of anatomical characters. The results revealed the first record of cryptic speciation in *Jorunna*, disclosing the pseudo-cryptic species *Jorunna* sp. nov. and a possible case of incipient speciation in *J. tomentosa*, with the genes COI and 16S supporting the occurrence of two lineages, namely *J. tomentosa* A and *J. tomentosa* B (interspecific COI uncorrected *p*-distance = 3.2–5.0%). *Jorunna* sp. nov. was found to be 9.0–12.3% genetically distinct from its sister species *J. tomentosa* and is characterized by a white to yellow background colour with irregularly placed small brown spots, smooth radular teeth and a copulatory spine up to 600 µm longer compared to *J. tomentosa*. No distinct morphological differences could be found between *J. tomentosa* lineage A and B. The generic assignment of *J. lemchei* to the genus *Gargamella* is questioned because of the presence of a copulatory spine, a feature absent in all other species of this genus.

Table of contents

1. Introduction

Understanding biodiversity patterns is of great importance for evolutionary ecology, conservation biology and to address theoretical questions of speciation and evolution (Bickford *et al.*, 2007; Marrone *et al.*, 2013; Korshunova *et al.*, 2017). A considerable proportion of diversity is hidden and often seemingly impossible to detect by morphological examination alone (Korshunova *et al.*, 2020), highlighting the necessity of adding molecular methods to traditional morphology-based taxonomy to delimit species (Nylander *et al.*, 2004; Puillandre *et al.*, 2012; Coates, Byrne & Moritz, 2018). Over the past decades, integrative taxonomy approaches, *i.e.*, classical morpho-anatomical studies combined with DNA analytical methods and scanning electron microscopy (SEM), have induced numerous revisions of the taxonomic status of taxa and increased our knowledge on species diversity. Adding the molecular dimension has not only challenged our understanding of traditional systematics (Camacho-García & Gosliner, 2008; Capa, Hutchings & Peart, 2012; Weiss *et al.*, 2014; Kienberger *et al.*, 2016), but also improved the differentiation of morphologically similar species (Bickford *et al.*, 2007). The definition of a species is a matter, sometimes of contentious debate, reflected in the large number of concepts available with over 30 definitions (see de Queiroz, 2007 for species conceptualizations; Zachos, 2016). The concept adopted here is consistent with the Phylogenetic Species Concept (PSC), defining a species as a group of organisms that constitutes a divergent monophyletic lineage and shares at least one unique derived character (Nixon & Wheeler, 1990; Wheeler & Meier, 2000). In sympatry, *i.e.*, species living in the same area, the PSC is concordant with the Biological Species Concept (Mayr, 1942; Bickford *et al.*, 2007; de Queiroz, 2007), because isolation is assumed to be attained by lack of interbreeding followed by lineage sorting over time. Regarding allopatry, *i.e.*, species occurring in separate geographies, however, the PSC is more problematic because the lack of interbreeding is not as easy to test. Here it is assumed that concordant phylogenetic patterns in two or more genetic markers or genetically determined morphological characters are indicative for that reproductive isolation has most likely been achieved (Avise & Wollenberg, 1997).

When two or more discrete species are wrongly classified under one species name because they appear morphologically indistinguishable despite genetic disparity, species are commonly referred to as being cryptic (Bickford *et al.*, 2007; Korshunova *et al.*, 2019). Besides the term cryptic species, a range of other denotations are applied in literature to describe several grades of cryptic diversity. Pseudo-cryptic/semi-cryptic species are species with subtle but detectable morphologically differences (Korshunova *et al.*, 2017). To find such traits, one may need to

study different life stages. A classic example is the species complex in the butterfly *Astraptes fulgerator* (Walch, 1775) which is morphologically indistinguishable from another in the adult stage but clearly distinguishable as caterpillars (Hebert *et al.*, 2004). Another grade of cryptic diversity are hyper-cryptic species, defined as any taxon currently regarded as a single species which turns out to consist of many valid, yet undiagnosed species (Adams *et al.*, 2014; Meyer-Wachsmuth, Galletti & Jondelius, 2014). Some authors refer to species being morphologically cryptic, *i.e.*, when a valid and accepted species pair displays morphological differences, but shows strong genetic similarity (Stuart, Inger & Voris, 2006; Dong *et al.*, 2012; Korshunova *et al.*, 2017). At last, the term cryptic may also be applied in ecological studies, referring to well-camouflaged species, and is not to be confused with the cryptic species complexes elaborated here (Todd, 1981; Franks & Noble, 2004). As an example, Wägele & Klussmann-Kolb (2005; Fig. 8B) address the cryptic appearance of *Jorunna tomentosa* (Cuvier, 1804), mimicking the unpalatable sponge of the genus *Halichondria* Fleming, 1828.

Reflected by the drastic increase in scientific publications (Pfenninger & Schwenk, 2007; Struck *et al.*, 2018), the discovery and systematic revisions of cryptic species have disclosed hidden biodiversity across a large variety of taxa, such as Scyphozoa (Dawson & Jacobs, 2001), Platyhelminthes (Scarpa *et al.*, 2016), Polychaeta (Nygren, Eklöf & Pleijel, 2010), Amphipoda (Beermann *et al.*, 2018), Lepidoptera (Hebert *et al.*, 2004), and Pisces (Adams *et al.*, 2014). Among the Nudibranchia, many studies have revealed the occurrence of cryptic speciation. For example, Gosliner & Fahey (2011) described 20 new species of *Dermatobranchus* van Hasselt, 1824, depicting remarkably diverse radular morphologies. Carmona *et al.* (2014) detected a cryptic species complex in *Anteaeolidiella indica* (Bergh, 1888), with three lineages recognized, showing consistent variations in colour pattern and internal anatomy. Pola, Roldán & Padilla (2014) described a new cryptic species of the genus *Okenia* Menke, 1830. Multiple cryptic species were detected among the genus *Pteraeolidia* Bergh, 1875, a group of photosynthetic nudibranchs from the Indo-Pacific (Wilson & Burghardt, 2015), and the common *Aeolidia papillosa* (Linnaeus, 1761) was shown to hide two pseudo-cryptic species when Kienberger *et al.* (2016) applied DNA analytical methods. In addition, Sørensen *et al.* (2020) just recently revealed a cryptic species in the nudibranch genus *Polycera* Cuvier, 1816 in Norwegian waters.

Prior to this study it had never been questioned whether the various colour morphs occurring in the dorid nudibranch *Jorunna tomentosa* (Cuvier, 1804) are part of the intraspecific variability of the species or in fact represent putative cryptic lineages, and whether its polychromatic

variation is linked with geographical localities or occurs randomly. The European species *J. tomentosa* might hide yet another example of cryptic diversity and is investigated here for the first time, contributing to a better understanding of nudibranch diversity.

1.1 Background: On the biology and ecology of nudibranch gastropods

Nudibranch gastropods (Nudibranchia Cuvier, 1817) constitute a prominent group of marine invertebrates and are commonly referred to as sea slugs. They are well known to both scientists and amateurs for their flamboyant colours and aesthetically attractive appearance (Korshunova *et al.*, 2017). Nudibranchs are characterized by loss of the shell during metamorphosis and the concurrent expansion of the notum over the dorsal body surface. Their head is fused with their prolate body, which is attached to the foot upon which they glide (Wägele & Willan, 2000; Alvim & Pimenta, 2013). To interact with the environment and compensate for their lack of sight, sea slugs are equipped with two chemosensory rhinophores, two oral tentacles, and, for some, one pair of labial tentacles (Dean & Prinsep, 2017).

Globally, nudibranchs inhabit a large range of habitats, from shallow-water coastlines to the deep sea (Cordeiro *et al.*, 2015; Valdés *et al.*, 2017). Whereas nearly all species belong to the epibenthic fauna (Todd, 1983), some are found to be pelagic (*e.g.*, Fam. Glaucidae Gray, 1827; Churchill, Valdés & Ó Foighil, 2014). As adults, nudibranchs range in size from 2 mm (*e.g.*, *Pseudovermis salamandrops* Ev. Marcus, 1953; Jörger *et al.*, 2014) to more than 43 cm (*e.g.*, *Hexabranchus* sp. and *Melibe viridis* (Kelaart, 1858); Yonow, 2015; Tibiriçá, Pola & Cervera, 2017; Tibiriçá *et al.*, 2019), though most species measure less than 3 cm (Wägele & Willan, 2000) and some are categorized as meiofauna (Swedmark, 1964; Flammensbeck *et al.*, 2019). Their geographical range spans from the Arctic Ocean around Spitsbergen to the Ross Sea off Antarctica (Cattaneo-Vietti, 1991; Wägele, 1991; Ekimova *et al.*, 2015).

Almost all nudibranch species are marine, however, the recently described *Bohuslania matsmichaeli* Korshunova, Lundin, Malmberg, Picton & Martynov, 2018 lives in brackish water (Korshunova *et al.*, 2018). Their shell-less body has enabled sea slugs to gain a high degree of plasticity, which has facilitated the occupation of many ecological niches (Thompson, 1988). To protect their soft bodies from predatory attacks, species have developed a variety of adaptations such as the utilization of toxins which they accumulate from prey, *de novo* synthesis of deterrent chemical compounds, colour signaling, camouflage, endoskeletal spicules, and kleptoplasty of cnidarian nematocysts (Thompson, 1960; Fuhrman, Fuhrman & DeRiemer, 1979; Mebs, 1985; Fahey & Garson, 2002; Wägele, 2004).

Reproduction and life cycles

Nearly all nudibranchs are simultaneous hermaphrodites with internal fertilization, reciprocally donating and receiving sperm (Gosliner, 1994). Some species, however, show exceptions to this typical copulatory behavior. For instance, in *Aeolidiella glauca* (Alder & Hancock, 1845) spermatophores (sperm packets) are externally exchanged by attachment to the body surface of the mate. The lining of the spermatophores then dissolves and the sperm migrates upon the epidermis towards the gonopore (Karlsson & Haase, 2002). In *Aeolidia papillosa* (Linnaeus, 1761), spermatophores are reciprocally placed onto and around everted genital cones. Sperm packets placed onto the cone are so drawn into the female duct when the penis retracts. Misplaced packets remain attached to the epidermis for a few days until they dissolve (Longley & Longley, 1984; Pola & González Duarte, 2008). The nudibranch *Polycera quadrilineata* (O.F. Müller, 1776), simultaneously exchanges spermatophores by depositing these within the genital system of their mate (von Ihering, 1886; Pola & González Duarte, 2008). Others, such as *Palio zosterae* (O'Donoghue, 1924) and *P. dubia* (M. Sars, 1829), copulate by hypodermic injection piercing the body wall with a barbed penial cirrus (Rivest, 1984).

All nudibranch species are oviparous and, once attained maturity, typically produce several spawn masses during a single reproductive event and copulate repeatedly between spawnings (Eyster, 1981; Todd, Lambert & Davies, 2001). Their life cycles are assumed to correlate with the availability of their prey, being either perennial (*e.g.*, sponges, anemones, bryozoans) or ephemeral (*e.g.*, seasonal hydrozoans) (Miller, 1962; Thompson, 1976; Todd, 1981; Eyster, 1981; Picton & Morrow, 1994). Nearly all nudibranchs are semelparous, *i.e.*, oviposition during a single reproductive event is followed by death (Todd, 1981). In the course of evolution, species have developed different life history strategies (Davies, 1993). Most species, such as *Adalaria proxima* (Alder & Hancock, 1854) and *Onchidoris bilamellata* (Linnaeus, 1767) have an annual life cycle as they undergo one discrete spawning period during a life span of one year (Todd, 1981). Other species, such as *Armina tigrina* Rafinesque, 1814 and *Trinchesia foliata* (Forbes & Goodsir, 1839), are sub-annual, generating two or more overlapping generations per year with a life span of a couple of months (Eyster, 1981; Todd, 1981). Again others, such as *Doris pseudoargus* Rapp, 1827 and *Tritonia hombergii* Cuvier, 1803, have a biennial life cycle and live for two years, reproducing only in their second year (Todd, 1981; Todd, Lambert & Davies, 2001). Besides these three common life cycles, some species such as *Cadlina laevis* (Linnaeus, 1767), are known to live for more than two years and are categorized as perennial.

Contrary to the aforementioned life history strategies, *C. laevis* is iteroparous, *i.e.*, undergoes repetitive reproductive events over several years (Davies, 1993).

The majority of nudibranchs has an indirect life cycle and hatches as shell-bearing planktonic veliger larvae. Most species, such as *Onchidoris muricata* (O. F. Müller, 1776) and *D. pseudoargus*, develop as type I planktotrophic veliger larvae. They hatch from eggs with a respective size of 90 µm and 150 µm as veliger larvae with a small foot and lack both eyes and a propodium (the anterior portion of the foot). To grow and develop, the veligers feed on plankton during a swimming phase of approximately nine to 28 days (Thompson, 1966; Todd & Havenhand, 1985; Davies, 1993). Other species, such as *A. proxima* and *T. hombergii*, hatch from eggs with a size range of 165 to 210 µm at a late stage of development as type II pelagic lecithotrophic veliger larvae. Being more advanced compared to the type I veliger, they possess a well-developed foot with propodium and carry eyes. Yolk reserves in their digestive gland enable the larvae to complete their development without the necessity to feed and their swimming phase does rarely exceed two days (Thompson, 1967; Todd & Havenhand, 1985). In both developmental types, the planktonic veliger phase is followed by metamorphosis and the loss of their shells. Some species, however, have developed a direct life cycle (type III) and hatch as fully developed post-veliger benthic juveniles after a long embryonic period of up to 50 days, crawling away from the egg masses already as benthic slugs. Examples of species with a direct life cycle are *C. laevis* and *Vayssierea elegans* (Baba, 1930) (Thompson, 1967; Davies, 1993; Todd, Lambert & Davies, 2001).

Ecology

Many sea slugs feed by means of their radula, a rasping tongue covered with numerous backward-pointing teeth, an apomorphy of the phylum Mollusca. Some slugs, however, have lost their radula in the course of evolution and developed anatomical modifications in the foregut adapted for suctorial feeding (Valdés, 2003). Some species of nudibranchs show well-defined dietary specificities often limited to a single type of prey, hinting where the species is most likely to be found. For example, *T. hombergii* is almost exclusively encountered on its prey, the anthozoan *Alcyonium digitatum* Linnaeus, 1758 (Salvini-Plawen, 1972; McDonald & Nybakken, 1997), and *O. bilamellata* mainly feeds on the barnacle *Balanus balanoides* (Linnaeus, 1767) growing on and below rocks in the upper littoral (Todd, 1979). On the other hand, several studies on feeding behavior and gut content have shown that many species feed on a variety of prey items, including their own kind. For example, species of the genus

Gymnodoris Stimpson, 1855 feed on a large range of opisthobranchs (Nakano & Hirose, 2011). Others, such as *Tyrannodoris europaea* (García-Gómez, 1985), predate on polycerids and even on individuals of its own species, depicting cannibalistic behavior (Megina & Cervera, 2003). Again other species such as *Prodoris clavigera* (Thiele, 1912), *Bathydoris hodgsoni* Eliot, 1907, and *Kalinga ornata* Alder & Hancock, 1864 are found to feed upon a variety of echinoderms (Wägele, 1989; Nakano *et al.*, 2011).

Systematics of Nudibranchia

Nudibranchs were traditionally grouped under the subclass Opisthobranchia (Rudman & Willan, 1998), however, the advent of molecular phylogenetics since the 1990s revealed that Opisthobranchia constitutes a polyphyletic group. The systematics of "opisthobranchs" underwent dramatic taxonomic re-arrangements and the group is now placed together with the pulmonates and other small marine shelled forms in the clade Heterobranchia (Wägele *et al.*, 2014). Nevertheless, despite the now accepted polyphyly of "opisthobranchs", the monophyletic status of its main traditional evolutionary lineages [Acochlidiacea Odhner, 1937; Aplysiida (P. Fischer, 1883); Cephalaspidea P. Fischer, 1883; Gymnosomata Blainville, 1824; Nudibranchia Cuvier, 1817; Pleurobranchida (Pelseneer, 1906); Sacoglossa (Bergh, 1876); Umbraculida Odhner, 1939] stands robust (Jörger *et al.*, 2010). The Order Nudibranchia consists of about 3000 described species (Sales *et al.*, 2013) assigned to the two evolutionary lineages Cladobranchia and Doridina. According to Bouchet *et al.* (2017), the present status of dorid phylogeny (Doridina) is largely unresolved . Until recent, the Cryptobranchiata, *i.e.*, species capable of retracting their gills into a branchial pocket, were divided into two major clades, the Porostomata Bergh, 1891 and the Labiostomata Valdés, 2002, referring to the absence or presence of a radular structure, respectively (Valdés, 2002; Penney, 2008; Wägele *et al.*, 2014). Currently, the colloquially known "doridaceans" (Infraorder Doridoidei) are divided into five superfamilies: Doridoidea Rafinesque, 1815 (= Cryptobranchia, = Eudoridoidea, = Labiostomata), Polyceroidea Alder & Hancock, 1845, Chromodoridoidea Bergh, 1891, Onchidoridoidea Gray 1827, and Phyllidioidea Rafinesque, 1814 (= Porostomata) (MolluscaBase, 2020a). In addition, the family Okadaiidae Baba, 1930 would be nested within the suborder Doridina, but is currently not assigned to any of the superfamilies indicated above (Bouchet *et al.*, 2017; MolluscaBase, 2020b). Approximately 2000 species belong to the Doridoidea which is grouped into the two families Dorididae Rafinesque, 1815 and Discodorididae Bergh, 1891. The genus *Jorunna* Bergh, 1876 is placed within the Discodorididae (MolluscaBase, 2020c).

1.2 Common characters of the genus *Jorunna* Bergh, 1876

Species of *Jorunna* Bergh, 1876 are usually found in coastal shallow-water habitats. Their oval-elongate body depicts a range of background colours varying from white, grey-white to yellow-orange, reddish-brown, and pink-purple. Their notum may be covered with larger dark brown blotches, dark rings, and irregularly distributed spots from pale brown to almost black, varying in size and colour intensity (see Camacho-García & Gosliner, 2008, fig. 1; Edmunds, 2011, figs 9 a, b; Alvim & Pimenta, 2013, figs 1, 2; Ortea *et al.*, 2014, fig. 10; Ortea & Moro, 2016, figs 4–6, 9; Tibiriçá, Pola & Cervera, 2017, fig. 18). The genus is characterized by having a mantle covered with numerous, densely spaced caryophyllidia, *i.e.*, highly specialized tubercles carrying four to seven vertical spicules arranged in a circular crown, surrounding a spherical, ciliated knob (Kress, 1981; Foale & Willan, 1987; Gosliner, 1994; Valdés & Gosliner, 2001). The caryophyllidia cover the entire dorsal mantle surface, except for the outermost dorsal mantle margin, which is surrounded by a single row of rounded, irregularly shaped knobs termed mantle rim organs (Foale & Willan, 1987; Wägele, 1998). Both the caryophyllidia and mantle rim organs were named and described for the very first time in the genera *Jorunna* and *Rostanga* Bergh, 1897 by the respective authors Labbé (1929; 1933) and Foale & Willan (1987).

Most species of *Jorunna* have their anterior border of the foot grooved and notched, and the posterior foot extends from the mantle edge when in motion. In all species, the rhinophores are lamellated, terminating in a vertical knob (Figure 1). The gills are unipinnate to tripinnate. Both the rhinophoral and branchial leaves can be fully retracted in low sheaths. Their radula bears a homogenous set of hook-shaped teeth with a broad base. The innermost teeth may be smooth or denticulate. The outermost teeth are elongate, sickle-shaped, with a thinner base, and may carry denticles. All species lack rachidian teeth. The labial cuticle may be smooth or armed with rodlets, also called jaw elements. They possess a large prostate, clearly divided into two differentiated sections. The accessory gland is large and equipped with a copulatory spine. Both the vagina and the penis are unarmed in all currently recognized valid species (Bergh, 1893; Ev. Marcus, 1976; Camacho-García & Gosliner, 2008).

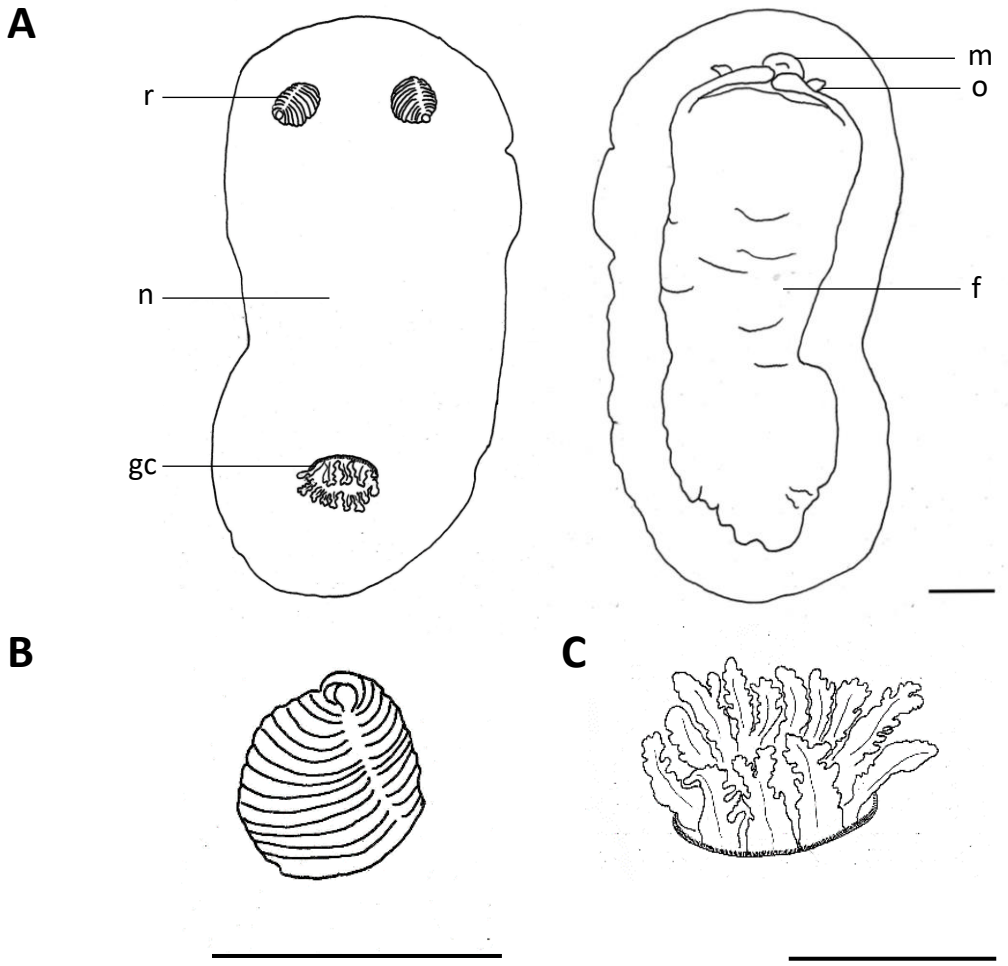

Figure 1. General external morphology of *Jorunna tomentosa sensu lato* **A.** Dorsal (left) and ventral (right) view **B.** Detailed drawing of lamellated rhinophore with apical knob **C.** Detailed drawing of gill circlet with 13 branchial leaves. Both the rhinophores and gills can be fully retracted in low sheaths. Abbreviations: r = rhinophore; n = notum; gc = gill circlet; m = mouth; o = oral tentacle; f = foot. Scale bars = 1 mm.

Diversity and taxonomy of Jorunna

The genus *Jorunna* Bergh, 1876 (Discodorididae Bergh, 1891) comprises 21 valid species with a worldwide coastal distribution in the four main biogeographical marine regions Eastern Pacific, Indo-West Pacific, Western Atlantic, and Eastern Atlantic (MolluscaBase, 2020d). Four species [*J. alisonae* Ev. Marcus, 1976; *J. osae* Camacho-García & Gosliner, 2008; *J. pardus* Behrens & Henderson, 1981; *J. tempisquensis* Camacho-García & Gosliner, 2008] are recorded from the Eastern Pacific, ranging from California, USA in the North to Costa Rica in the South. Seven species occur in the Indo-West Pacific [*J. funebris* (Kelaart, 1859); *J. hartleyi* (Burn, 1958); *J. labialis* (Eliot, 1908); *J. pantherina* (Angas, 1864); *J. parva* (Baba, 1938); *J. ramicola* M. C. Miller, 1996; *J. rubescens* (Bergh, 1876)], ranging from the Marshall Islands in the East to the archipelago of the Seychelles in the West. In the Western Atlantic,

four species [*J. coloradilla* Ortea & Moro, 2016; *J. davidbowieii* Ortea & Moro, 2016; *J. spazzola* (Er. Marcus, 1955); *J. spongiosa* Alvim & Pimenta, 2013] occur along the coasts of Mexico, Cuba, Costa Rica, and Brazil. In addition, records of *J. coloradilla* from Manzanillo, Mexico, expand its range to the Eastern Pacific. At last, six species [*J. efe* Ortea & Moro, 2014; *J. evansi* (Eliot, 1906); *J. ghanensis* Edmunds, 2011; *J. glandulosa* Edmunds, 2011; *J. onubensis* Cervera, García-Gómez & García, 1986; *J. tomentosa* (Cuvier, 1804)] are distributed along the Eastern Atlantic coast lines, ranging from Norway to South Africa. In addition, *J. spazzola* is recorded from Naples, Italy and may be listed among the Western Atlantic species as well. Overall, the global latitudinal range of *Jorunna* spans from Auckland, New Zealand in the South [*J. ramicola*; *J. pantherina*] (Camacho-García & Gosliner, 2008) to Finnmark, Norway in the North [*J. tomentosa*] (present study).

In Europe, *Jorunna* is represented by the five currently recognized valid species *J. efe* (*e.g.*, Azores, Canary Islands), *J. evansi* (*e.g.*, Italy, Cape Verde Islands), *J. onubensis* (*e.g.*, Spain, Portugal, Canary Islands), *J. spazzola* (*e.g.*, Naples, Italy), and *J. tomentosa* (*e.g.*, Norway, Sweden, British Isles, France, Italy, Canary Islands, Azores) (Hunnam & Brown, 1975; Cervera *et al.*, 2004; Camacho-García & Gosliner, 2008; García & Bertsch, 2009; Ortea *et al.*, 2014; Ballesteros, Madrenas & Pontes, 2016). In addition, the species *Gargamella lemchei* (Ev. Marcus, 1976), former attributed to the genus *Jorunna*, is included among the European species addressed in this revision. Ev. Marcus (1976) described the species *Jorunna lemchei* based on two specimens from Ballyvaughan Bay, Western Ireland, collected by Dr. Henning Lemche in 1975 (Holotype: USNM* 710703; Just & Edmunds, 1985), yet Ortea *et al.* (2014) transferred it to the genus *Gargamella* due to the presence of penial hooks. To test the generic assignment of the species *G. lemchei*, specimens from nearby its type locality are included in this revision. (*USNM = National Museum of Natural History, Smithsonian Institution, Washington DC, USA).

1.3 Study group: The dorid nudibranch *Jorunna tomentosa* (Cuvier, 1804)

Jorunna tomentosa sensu lato is characterized by an oval-elongate body depicting shades of grey-white, cream-yellow, and pale orange. The notum may be plain or blotched with light brown to chocolate brown spots of various sizes, distributed either irregularly, in two longitudinal lines aligned with the rhinophores, or present as a combination of both (Thompson & Brown, 1984; Thompson, 1988; Bergh, 1893; Picton & Morrow, 1994; Malmberg & Lundin, 2015) (Figure 2). The ample mantle is covered with numerous, closely spaced (~ 80 mm^{-2})

caryophyllidia tubercles with four to seven protruding spicules of about 200 µm height, encircling a rounded ciliated central knob. Standing only 50–100 µm apart, the caryophyllidia yield a granular, velvety appearance (Kress, 1981; Foale & Willan, 1987; Wägele, 1998). Spherical mantle glands surround the mantle edge in a single row and are slightly brighter in colour than the mantle itself (Figure 3A, 3B; see also Wägele, 1998). Their rhinophores are slightly brighter in colour than the notum and carry pigmentation. The number of rhinophoral lamellae is reported to vary with size (Ev. Marcus, 1976), being 12–14 in fixed specimens of 13–30 mm length (Camacho-García & Gosliner, 2008; own observations). A cup-shaped rim of bi- to tripinnate gills encircles the speckled anal papilla. Adult individuals may carry up to 17 gills, juvenile specimens usually have fewer (Thompson & Brown, 1984; Hayward & Ryland, 2017). The branchial leaves are slightly brighter than the mantle colour and pigmented with minute brown spots. The muscular foot is coloured as the notum, may be speckled with small brown spots, and is posteriorly visible when in motion, somewhat pointed at the end. Anteriorly, the foot is deeply notched and grooved. Close to the mouth opening, there are two short, digitiform oral tentacles visible from the ventral side (Figure 1). The size spans from about 10 to 55 mm, most specimens being between 20 and 30 mm (Odhner, 1907; Hunnam & Brown, 1975; Thompson & Brown, 1984; Hayward & Ryland, 2017; own observations).

Ecology and life cycle

Jorunna tomentosa sensu lato has a large bathymetric range, being reported from a few meters below surface down to more than 400 m (Grieg, 1912; Hunnam & Brown, 1975; Ev. Marcus, 1976; Camacho-García & Gosliner, 2008; Cordeiro *et al.*, 2015). It feeds on heteroscleromorphan sponges of the species *Halichondria panicea* (Pallas, 1766), *Haliclona oculata* (Linnaeus, 1759), and *Haliclona cinerea* (Grant, 1826) (Millott, 1937; Swennen, 1961; Wolter, 1967; Bloom, 1976; Todd, 1981; Thompson & Brown, 1984; Thompson, 1988; McDonald & Nybakken, 1997). According to Garstang (1893), their circular branchial plume resembles the osculum of a small *Halichondria* sp. and their ovate contour, when at rest, combined with their mantle colour and velvety texture gives the slug a remarkable sponge-like appearance (Figure 3A). This suggests that *J. tomentosa* is highly associated with its prey, feeding and living on it. Posterior to mating, eggs are deposited as light-coloured coiled ribbons (Figure 3B–D; see also Alder & Hancock, 1845, fam. 1, pl. 5, fig. 7; Ev. Marcus, 1976, figs 16, 17) with up to 145.000 eggs of 69–90 µm in diameter in each spiral. In the course of 23 days (T = 10°C), the eggs develop to planktonic veliger larvae of type I (Thompson, 1961, 1976; Thompson & Brown, 1984). According to Miller (1958) and Allen (1962), egg-laying happens

from February to August, with the smallest spawning individual observed being 19 mm. Alder & Hancock (1845) observed specimens laying eggs in May and June. According to Todd (1981), *J. tomentosa s. l.* has a biennial life cycle. These observations are supported by Swennen (1961) and Thompson & Brown (1984) who observed full-grown specimens spawn in September in Biscay Bay, France.

Geographic distribution

In Europe, the species is present from Finnmark, Norway (present study) to the Kattegat, Sweden (Hansson, 1998; Evertsen & Bakken, 2002, 2005, 2013), Helgoland (Ev. Marcus, 1976), the Netherlands (Swennen, 1961), the British Isles and Atlantic French coast (Fisher, 1937; Moore & Sproston, 1940; Pruvot-Fol, 1954; Thompson & Brown, 1984; Picton & Morrow, 1994), and the Iberian Peninsula including the archipelagos of the Azores and Canary Islands (Ros, 1978; García Gómez, 1983; Malaquias & Morenito, 2000; Malaquias, 2001; Valdés & Gosliner, 2001; Calado *et al.*, 2003; Cervera *et al.*, 2004; Domènech, Avila & Ballesteros, 2006; Camacho-García & Gosliner, 2008; Malaquias *et al.*, 2009; Malaquias *et al.*, 2014; Cordeiro *et al.*, 2015; Ortea & Moro, 2016). In the Mediterranean Basin including the Adriatic Sea, its distribution ranges from Spain (Ballesteros, 1984; Sánchez Tocino, 2003; Ballesteros, Madrenas & Pontes, 2016), Italy (Perrone, 1983; Zenetos *et al.*, 2016; Furfaro *et al.*, 2020), Slovenia (Zenetos *et al.*, 2016), and Croatia (Zenetos *et al.*, 2016; Prkić *et al.*, 2018) to the easternmost reported locality in Istanbul, Turkey (Saltik, 2005). In addition, the species has been recorded from South Africa in Cape Province (Camacho-García & Gosliner, 2008) and Eastern False Bay and Knysna Lagoon (present study).

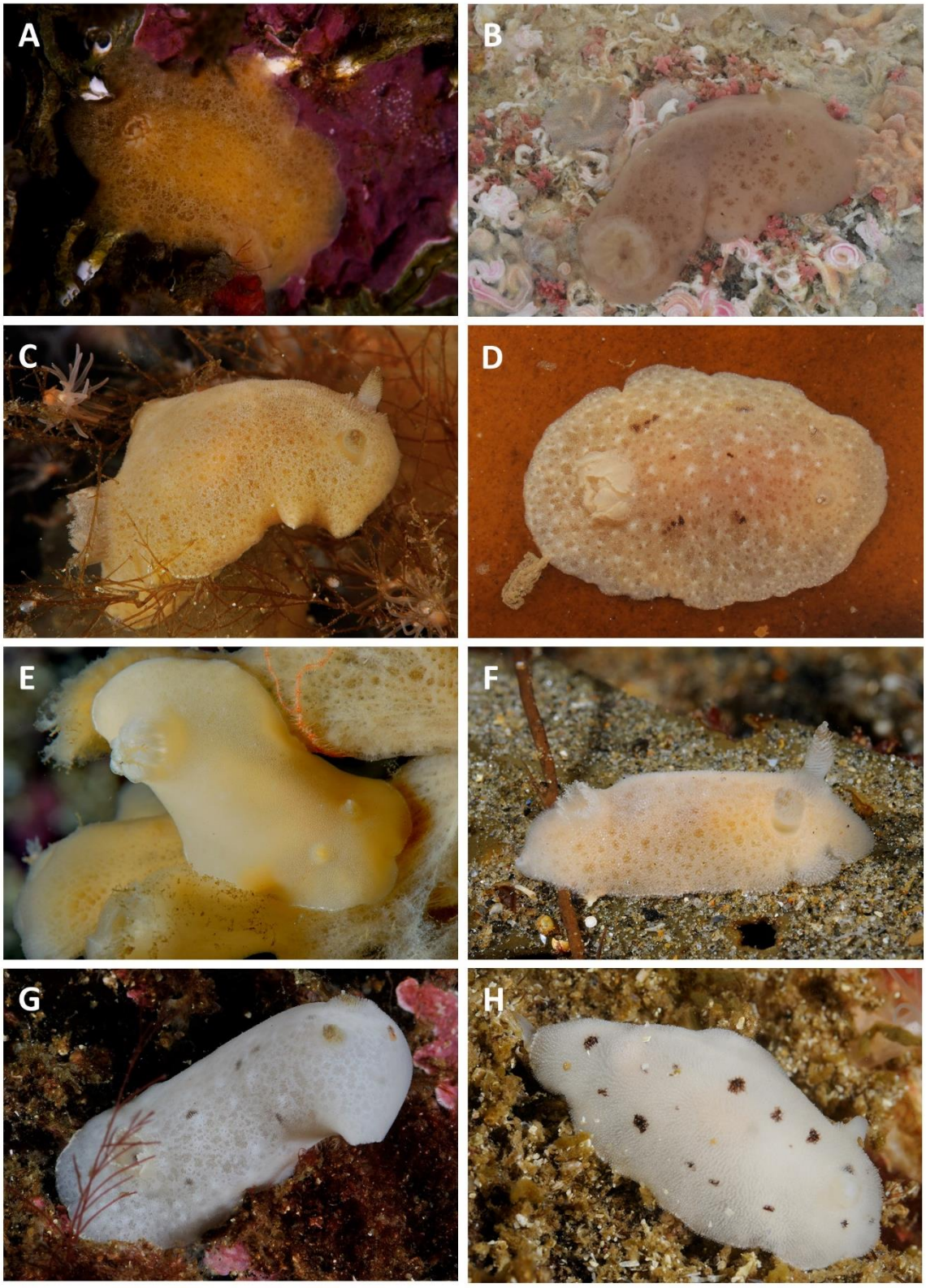

Figure 2. Chromatic variability in *Jorunna tomentosa sensu lato*. **A.** Drøbak, Akershus, Norway, ZMBN 125553, photo by T. Kinn Kvamme, 2018. **B.** Mosteiros, São Miguel Island, Azores, ZMBN 87955, photo by M. A. E. Malaquias, 2011. **C.** Kristiansund, Møre og Romsdal, Norway, ZMBN 125644, photo by N. Aukan, 2017. **D.** Ballyhenry Island, Northern Ireland, CASIZ 193035, photo by T.M. Gosliner, 2013. **E.** Kristiansund, Møre og Romsdal, Norway, ZMBN 125651, photo by N. Aukan, 2018. **F.** Averøy, Møre og Romsdal, Norway, photo by N. Aukan, 2013. **G.** Averøy, Møre og Romsdal, Norway, ZMBN 125591, photo by N. Aukan, 2018. **H**. Tingvoll, Møre og Romsdal, Norway, photo by N. Aukan, 2014. (*J. tomentosa* lineage A: **D**; *J. tomentosa* lineage B: **A**–**C**, **E**, **G**).

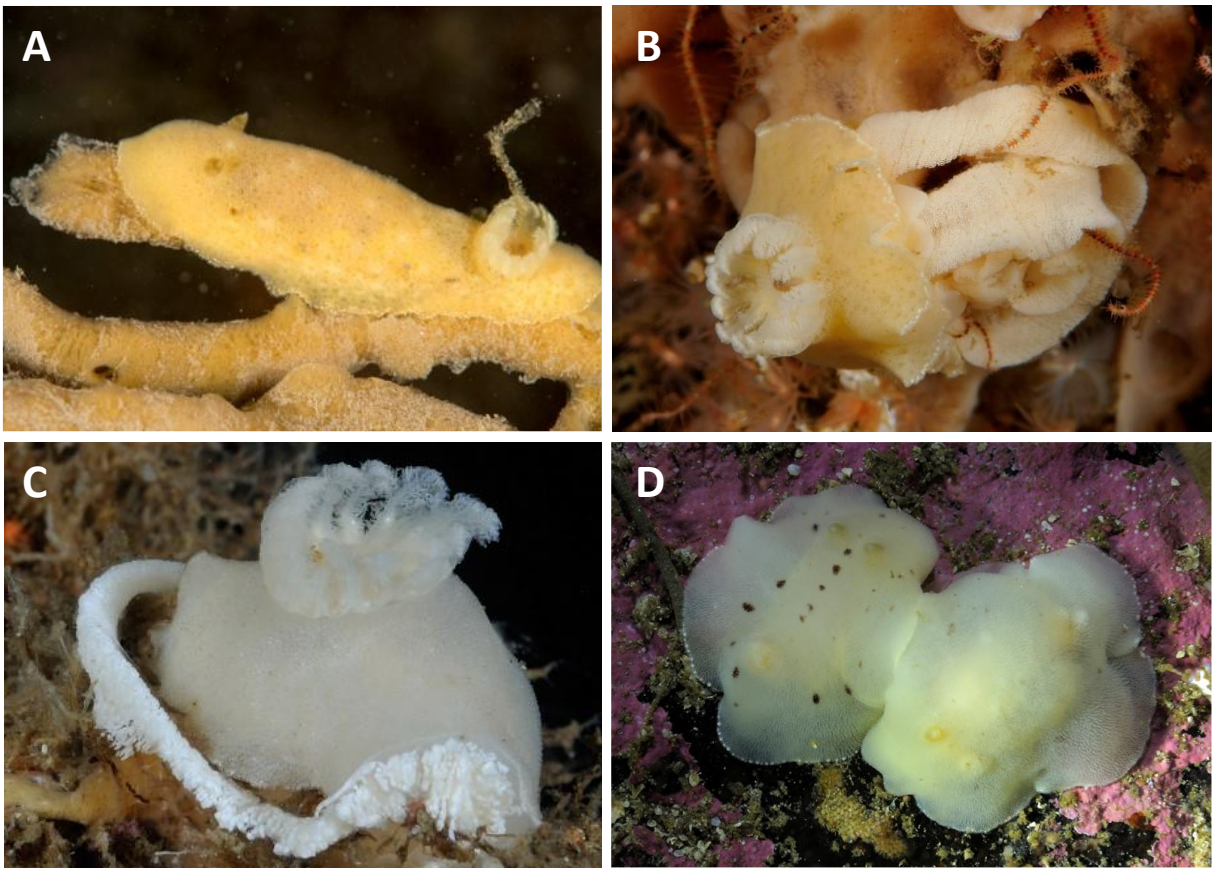

Figure 3. *Jorunna tomentosa sensu lato*. **A**. Well-camouflaged specimen with an erect gill circlet crawling on a *Halichondria* sp., Ballyhenry Island, Northern Ireland, ZMBN 127704, photo by B. Picton, 2015. **B**. Specimen laying eggs on a sponge, Kristiansund, Møre og Romsdal, Norway, photo by N. Aukan, July 2017. **C**. Specimen laying eggs, Kristiansund, Møre og Romsdal, Norway, photo by N. Aukan, August 2015. **D**. Two individuals mating on a rock at 35 m depth, Averøy, Møre og Romsdal, Norway, photo by N. Aukan, May, 2020.

2.Objectives

This thesis presents a comprehensive literature review on the five currently recognized European species of the nudibranch genus *Jorunna* (*J. efe*, *J. evansi*, *J. onubensis*, *J. spazzola*, *J. tomentosa*), and a generic assessment of the species *Gargamella lemchei*, originally described as *Jorunna lemchei*. An integrative approach, combining molecular phylogenetics with morpho-anatomical studies and scanning electron microscopy, is used to investigate:

(1) The taxonomic status of the species *J. tomentosa*, *i.e.*, whether this species, as currently defined, is a single taxon or alternatively comprises a complex of multiple species.
(2) Establish a relation between colour-morphs and putative cryptic lineages and describe their morpho-anatomical differences.
(3) Define the geographical distribution of the putative cryptic lineages.

3. Material and methods

3.1 Taxon sampling

A total of 42 specimens were obtained by snorkeling and SCUBA diving (self-contained underwater breathing apparatus) in collaboration with citizen scientists contributing to the project *Sea Slugs of Southern Norway* (Rauch & Malaquias, 2019) between February 2018 and December 2019. Live specimens were photographed *in situ* or inside a small aquarium with a black background using a digital SLR camera equipped with macro lens and external flashlights. Each animal was individually measured for their total length (mm) with the aid of a standard ruler. Specimens were frozen in seawater for approximately 12–24 h after which they were defrosted and preserved in absolute ethanol (> 96%). This enables the body of the animals to become fully extended easing, if necessary, anatomical work. Specimens were given a voucher number and databased with information on sampling location, depth, habitat, and collector. All samples are deposited in the collections of the University Museum of Bergen (ZMBN) and catalogued according to Darwin Core standards (Wieczorek *et al.*, 2009). In addition, samples were obtained from specimens housed in the collections of the University Museum of Bergen (ZMBN), through donations from colleagues and by loans from the Norwegian University of Science and Technology University Museum, Trondheim (NTNU-VM), the California Academy of Sciences (CAS-IZ), the National Museum of Natural History, Paris (MNHN), and the Zoological Museum, Hamburg (ZMH). One sample (ZMBN 125946) was obtained from a bottom trawl during a research cruise with the University of Bergen in October 2018 on board the research vessel F/F "G.O. Sars". The geographic distribution of the European species of *Jorunna* was inferred based on the studied material and reliable literature records. A map showing the overall distributional pattern of *J. tomentosa* and sampled specimens was generated using the software QGIS v. 3.14 (QGIS Geographic Information System, 2020).

3.2 DNA extraction, amplification, and sequencing

DNA was extracted from a small sample of foot tissue using the Qiagen DNeasy® Blood and Tissue Kit (Qiagen, California, USA, catalogue nr. 69506) following the manufacturer's protocol for "Purification of Total DNA from Animal Tissues", but repeating point 9 with only 100 µl of AE buffer (Appendix I, A). Three gene markers were obtained for this study: the mitochondrial cytochrome *c* oxidase subunit I (COI) and 16S rRNA (16S), and the nuclear histone H3 (H3). Primers used for amplification and sequencing are presented in Table 1.

Amplification was carried out by polymerase chain reaction (PCR) in a BIO-RAD C1000 thermal cycler with a total reaction volume of 50 µl for all three genes. For COI and 16S, PCR solutions contained 17.5 µl Sigma-Aldrich water, 5 µl buffer (Qiagen OneStep RT-PCR Buffer), 5 µl dNTP, 5 µl Q-solution, 7 µl $MgCl_2$, 2 µl of each primer, 0.5 µl TAQ, and 1 µl DNA, whereas for H3, 20.5 µl Sigma-Aldrich water and 4 µl $MgCl_2$ were used instead. PCR thermal cycling conditions were the same for all three genes, but with specific annealing temperatures. Initial denaturation was set at 95°C for three minutes followed by denaturation for 45 s at 94°C with annealing for 45 s at 45°C (COI), 40°C (16S), and 50°C (H3), and an extension for two minutes at 72°C, with a total of 39 cycles.

Table 1. Primers for amplification and sequencing.

	Name	Sequence 5' → 3'	Source
COI	LCO1490 (F)	GGTCAACAAATCATAAAGATATTGG	Folmer *et al.* (1994)
	HCO2198 (R)	TAAACTTCAGGGTGACCAAAAATCA	Folmer *et al.* (1994)
16S	16S ar-L (F)	CGCCTGTTTATCAAAAACAT	Palumbi *et al.* (1991)
	16S br-H (R)	CCGGTCTGAACTCAGATCACGT	Palumbi *et al.* (1991)
H3	H3AD5'3' (F)	ATGGCTCGTACCAAGCAGACVGC	Colgan *et al.* (1998)
	H3BD5'3' (R)	ATA-TCC-TTR-GGC-ATR-ATR-GTG-AC	Colgan *et al.* (1998)

Final extension lasted for 10 minutes at 72°C. Both a positive and negative control were included in each run to check for successful amplification and to rule out contamination. Difficult samples that did not yield successful PCR results with the standard protocols were run adding 2 µl or 4 µl DNA (decreasing the respective volume of Sigma-Aldrich water). For some samples, the volume of $MgCl_2$ was reduced to 1,75 µl (increasing the respective volume of Sigma-Aldrich water). The PCR cycling conditions remained the same as stated above (Appendix I, B).

The quality and quantity of PCR products was assessed using gel electrophoresis. PCR product (4 µl) with Ficoll x5 loading dye (1 µl) was run on a 1.2% agarose gel containing the staining agent GelRed covered in TAE x1 buffer. To quantify and estimate the length of amplified DNA fragments, 5 µl FastRuler was used as a ladder. The gel was run for 20 minutes at 80 V and then analyzed under UV light (Syngene, Cambridge, UK). GeneSnap (v. 7.01) and GeneTools (v. 4.0; Syngene) were used for images and manual band quantification (Appendix I, C & D).

Successful PCR products were purified using the EXO-SAP method with Exonuclease 1 (EXO 10 units/µl) and Shrimp Alkaline Phosphatase (SAP 1 unit/µl, USB©) in 10 µl reactions (EXO 0.1 µl, SAP 1.0 µl, Sigma-Aldrich water 0.9 µl, PCR product 8 µl). Reactions were run on a thermal cycler at 37°C (incubation) for 30 min followed by 15 min at 80°C (enzyme inactivation). Samples that contained high concentrations of DNA were diluted after the manual band quantification, adding 1 µl PCR product and 7 µl Sigma-Aldrich water (Appendix I, E).

To prepare successfully amplified PCRs for sequencing, the BigDye® Terminator v3.1 Cycle Sequencing Kit protocol (Applied Biosystems™) was followed. The total reaction volume for each sample was 10 µl; 1 µl of DNA (10 ng), 1 µl of sequencing buffer, 1 µl BigDye, 1 µl of each primer (3.2 mM), and 7 µl Sigma-Aldrich water. The reactions were run in a thermal cycler at 96°C for 5 min (initial denaturation), followed by 25 cycles at 96°C for 10 seconds (denaturation), 50°C for 5 seconds (annealing) and finally at 60°C for 4 min. After the thermal reactions, 10 µl of Sigma-Aldrich water was added to the samples to obtain a final volume of 20 µl before submitting to the sequencing laboratory facility at the Department of Biological Sciences, University of Bergen. All sequencing reactions were run on the capillary-based Applied Biosystems 3730XL DNA Analyzer (Appendix I, F).

3.3 Sequence editing, alignment, and phylogenetic analysis

A total of 114 novel sequences were obtained from 63 specimens of the genus *Jorunna* for the three gene markers COI, 16S, and H3. Specimens were sampled from Norway (39), Northern Ireland (6), Ireland (5), France (1), Spain (2), Portugal, including the archipelago of the Azores (8), and South Africa (2). In addition, four sequences of *J. tomentosa s. l.*, three sequences of *J. funebris*, and 42 sequences of 14 cryptobranch dorid species were obtained from GenBank. The 14 cryptobranch dorids *Chromodoris striatella, C. willani, Discodoris cebuensis, D. hummelincki, Felimida binza, F. clenchi, Geitodoris heathi, Glossodoris hikuerensis, Halgerda carlsoni, H. dichromis, H. nuarrensis, H. wasinensis, Peltodoris atromaculata,* and *Rostanga elandsia* were used as outgroup taxa. The chromodorid nudibranch *Glossodoris hikuerensis* was chosen to root the phylogenetic trees, based on Valdés (2002) who suggested the family Chromodorididae to be sister to Discodorididae. See Table 2 for list of specimens used for molecular analyses with collection data, voucher information, and GenBank accession numbers. Specimens used for morpho-anatomical studies are listed in the examined material section 4.2.

Table 2. List of specimens used for molecular sequencing. Novel successful sequences obtained for the gene markers COI, 16S, and H3 are marked with an asterisk (*). Sequences obtained from GenBank are marked with GenBank accession numbers. *Jorunna tomentosa* A and *Jorunna tomentosa* B refer to respective lineages retrieved from the phylogenetic analyses.

Species	**Locality**	**Voucher no.**	**COI**	**16S**	**H3**	**Source**
Jorunna funebris	Guam: Mariana Islands	CPIC00633	KP871645	KP871693	KP871669	Mahguib & Valdés (2015)
Jorunna onubensis	Spain: Huelva	ZMBN 125474	*	*	*	Present study
Jorunna sp. nov.	Norway: Trondheim	NTNU-VM-58891	*	*	*	Present study
Jorunna sp. nov.	Norway: Kristiansund	ZMBN 127749	*	*	-	Present study
Jorunna sp. nov.	Norway: North Sea	ZMBN 125946	*	*	*	Present study
Jorunna tomentosa A	Norway: Gulen	ZMBN 127710	*	*	*	Present study
Jorunna tomentosa A	Ireland: Ringhaddy	ZMBN 127707	*	*	*	Present study
Jorunna tomentosa A	Northern Ireland: Ballyhenry Island	ZMBN 127711	*	*	*	Present study
Jorunna tomentosa A	Northern Ireland: Ballyhenry Island	CAS-IZ 193035	*	*	*	Present study
Jorunna tomentosa A	France: La Rochelle	ZMBN 125512	*	*	*	Present study
Jorunna tomentosa A	Portugal: Parque Natural da Arrábida	CAS-IZ 176820	*	-	*	Present study
Jorunna tomentosa B	Spain: Bay of Biscay	–	KU697718	-	-	Miralles *et al.* (2016)
Jorunna tomentosa B	Sweden: Kristineberg	EMBL	AJ223267	AJ225191	-	Thollesson (2000)
Jorunna tomentosa B	Sweden: Kattegatt	Gastr 8965V	MG935216	-	-	Lundin (2018)
Jorunna tomentosa B	South Africa: Eastern False Bay	SAMC-A089801	*	*	-	Stellenbosch University
Jorunna tomentosa B	South Africa: Knysna Lagoon	SAMC-A089803	*	-	-	Stellenbosch University
Jorunna tomentosa B	Norway: Trondheim	NTNU-VM-66871	*	-	-	NTNU University Museum
Jorunna tomentosa B	Norway: Trondheim	NTNU-VM-67968	*	-	-	NTNU University Museum
Jorunna tomentosa B	Norway: Finnmark	NTNU-VM-75953	*	-	-	NTNU University Museum
Jorunna tomentosa B	Norway: Finnmark	NTNU-VM-75975	*	-	-	NTNU University Museum
Jorunna tomentosa B	Norway: Finnmark	NTNU-VM-76040	*	-	-	NTNU University Museum
Jorunna tomentosa B	Norway: Lofoten	NTNU-VM-213	*	-	*	Present study

Species	Locality	Voucher no.	COI	16S	H3	Source
Jorunna tomentosa B	Norway: Trondheim	NTNU-VM-66873	*	-	-	Present study
Jorunna tomentosa B	Norway: Trondheim	NTNU-VM-58888	*	*	*	Present study
Jorunna tomentosa B	Norway: Trondheim	NTNU-VM-66872	*	*	*	Present study
Jorunna tomentosa B	Norway: Gulen	NTNU-VM-66876	*	-	-	Present study
Jorunna tomentosa B	Norway: Gulen	NTNU-VM-66874	*	-	-	Present study
Jorunna tomentosa B	Norway: Gulen	NTNU-VM-68525	*	-	-	Present study
Jorunna tomentosa B	Norway: Gulen	NTNU-VM-66875	*	-	-	Present study
Jorunna tomentosa B	Norway: Gulen	ZMBN 127712	*	-	-	Present study
Jorunna tomentosa B	Norway: Drøbak	ZMBN 125057	*	-	-	Present study
Jorunna tomentosa B	Norway: Drøbak	ZMBN 125563	*	-	-	Present study
Jorunna tomentosa B	Norway: Drøbak	ZMBN 125581	*	-	-	Present study
Jorunna tomentosa B	Norway: Drøbak	ZMBN 127577	*	-	-	Present study
Jorunna tomentosa B	Norway: Drøbak	ZMBN 127593	*	-	-	Present study
Jorunna tomentosa B	Norway: Drøbak	ZMBN 125038	*	*	*	Present study
Jorunna tomentosa B	Norway: Drøbak	ZMBN 125553	*	*	*	Present study
Jorunna tomentosa B	Norway: Drøbak	ZMBN 127603	*	*	*	Present study
Jorunna tomentosa B	Norway: Kristiansund	ZMBN 125644	*	-	-	Present study
Jorunna tomentosa B	Norway: Kristiansund	ZMBN 125651	*	-	-	Present study
Jorunna tomentosa B	Norway: Kristiansund	ZMBN 125632	*	-	-	Present study
Jorunna tomentosa B	Norway: Kristiansund	ZMBN 127775	*	-	-	Present study
Jorunna tomentosa B	Norway: Gjemnes	ZMBN 127730	*	-	-	Present study
Jorunna tomentosa B	Norway: Haugesund	ZMBN 125878	*	-	-	Present study
Jorunna tomentosa B	Norway: Egersund	ZMBN 127553	*	-	-	Present study
Jorunna tomentosa B	Norway: Egersund	ZMBN 127567	*	-	-	Present study
Jorunna tomentosa B	Norway: Egersund	ZMBN 127568	*	-	-	Present study
Jorunna tomentosa B	Norway: Averøy	ZMBN 125591	*	-	-	Present study

Species	Locality	Voucher no.	COI	16S	H3	Source
Jorunna tomentosa B	Ireland: Connemara	ZMBN 127715	*	-	-	Present study
Jorunna tomentosa B	Ireland: Connemara	ZMBN 127713	*	-	-	Present study
Jorunna tomentosa B	Ireland: Connemara	ZMBN 127714	*	*	*	Present study
Jorunna tomentosa B	Ireland: Connemara	ZMBN 127705	*	*	*	Present study
Jorunna tomentosa B	Northern Ireland: Ballyhenry Island	ZMBN 127704	*	-	-	Present study
Jorunna tomentosa B	Northern Ireland: Stangford	ZMBN 127706	*	-	-	Present study
Jorunna tomentosa B	Northern Ireland: Ballyhenry Island	ZMBN 127709	*	*	*	Present study
Jorunna tomentosa B	Northern Ireland: Rathlin Island	ZMBN 127708	*	*	*	Present study
Jorunna tomentosa B	Spain: Pontevedra, Galicia	ZMBN 132446	*	*	*	Present study
Jorunna tomentosa B	Portugal: Parque Natural da Arrábida	CAS-IZ 176819	*	-	-	Present study
Jorunna tomentosa B	Azores: Faial Island	CAS-IZ 175753	*	*	*	Present study
Jorunna tomentosa B	Azores: Faial Island	CAS-IZ 175752	*	*	*	Present study
Jorunna tomentosa B	Azores: Faial Island	CAS-IZ 175757	*	*	*	Present study
Jorunna tomentosa B	Azores: Faial Island	CAS-IZ 175761	*	*	*	Present study
Jorunna tomentosa B	Azores: Faial Island	ZMBN 81683	*	*	*	Present study
Jorunna tomentosa B	Azores: São Miguel Island	ZMBN 87955	*	*	*	Present study
Outgroup species						
Chromodoris striatella	Australia: Shoalwater Bay	AM C415149D	MG883327	MG883021	MG873227	Layton *et al*. (2018)
Chromodoris willani	Japan: Ie Island	UF352011A	MG883374	MG883069	MG873242	Layton *et al.* (2018)
Discodoris cebuensis	Hawaii: Maalea Bay	CAS-IZ 185141	KP871639	KP871687	KP871663	Mahguib & Valdés (2015)
Discodoris hummelincki	Jamaica: St. James	CPIC00654	KU950019	KU949949	KU950062	Lindsay *et al.* (2016)
Felimida binza	Portugal: Madeira Island	MMFHN29959	KX262409	KX262442	KX279317	Padula *et al.* (2016)
Felimida clenchi	Brazil: Cabo Frio	MZSP97531	KX262390	KX262429	KX279311	Padula et al. (2016)
Geitodoris heathi	United States: California	CAS-IZ 181314	KP871642	KP871690	KP871666	Mahguib & Valdés (2015)
Glossodoris hikuerensis	Mozambique: Vamizi Island	MB28-0050001	MK994107	MK994159	MK994133	Tibiriçá et al. (2020)

Species	Locality	Voucher no.	COI	16S	H3	Source
Halgerda carlsoni	Philippines: Batangas	CAS-IZ 177575	KP871643	KP871691	KP871667	Mahguib & Valdés (2015)
Halgerda dichromis	South Africa: KwaZulu-Natal	MHN-VFI	MH578088	MH578116	MH578152	Tibiriçá et al. (2018)
Halgerda nuarrensis	Mozambique: Nuarro	MB28-004874	MH578102	MH578115	MH578132	Tibiriçá et al. (2018)
Halgerda wasinensis	Mozambique: Pomene	MB28-004918	MH578091	MH578129	MH578140	Tibiriçá et al. (2018)
Peltodoris atromaculata	–	GB	AF120637	DQ280054	DQ280013	Giribet et al. (2006)
Rostanga elandsia	South Africa: Olifantsbos Bay	CAS-IZ 176110	KP871651	KP871699	KP871674	Mahguib & Valdés (2015)

Chromatograms of forward and reverse DNA strands were edited and aligned using the software Geneious R11 v. 11.0.5 (Biomatters, Auckland, New Zealand) (Kearse *et al.*, 2012). To test for potential contamination, all sequences were individually checked using Basic Local Alignment Searchtool (*BLAST)* implemented in Geneious. Sequences of protein-coding genes were translated using the Geneious translation tool and the invertebrate mitochondrial genetic code to disclose the presence of stop codons. A multiple sequence alignment was generated using the software MUSCLE (Edgar, 2004) implemented in Geneious using default settings (*i.e.*, a maximum of eight iterations). Single gene alignments were trimmed to a position at which at least half of the sequences contained nucleotide information. Remaining gaps were filled with missing data (N). Blocks of ambiguous data were identified using Gblocks Server 0.91b (Castresana, 2000) with both stringent and relaxed settings (Table 3). Saturation was tested for the first, second, and third codon positions for protein coding genes by plotting the total number of transitions and transversions against uncorrected pairwise (*p*) distances between sequences (Appendix III, A, Figure VII). Uncorrected *p*-distances for the COI gene were estimated using MEGA-X (Kumar *et al.*, 2018). Intra-specific and inter-specific minimum and maximum COI genetic *p*-distances of all species of *Jorunna* were calculated (Table 4).

Best-fit models of evolution were estimated using the Akaike information criterion (AIC) (Sakamoto, Ishiguro & Kitagawa, 1986) implemented in jModelTest v. 2.1.10 (Guindon & Gascuel, 2003; Darriba *et al.*, 2012). The selected models were GTR+I+G for COI, TVM+I+G for 16S, TPM1uf+I+G for 16S stringent (S16S), TIM1+I+G for 16S relaxed (R16S), and GTR+I for H3. Single-gene phylogenetic analyses for COI, H3, 16S, S16S, and R16S alignments (Figures 4–6; Appendix III, B, Figures IX–X) were performed in MrBayes v. 3.2.1 (Huelsenbeck & Ronquist, 2001) run through the portal CIPRES (Miller, Pfeiffer & Schwartz, 2010), using three parallel runs of five million generations, sampling every 100 generations (Appendix III, B, Figure VIII). Convergence of independent runs was examined in Tracer v. 1.7 (Rambaut *et al.*, 2018) with a burn-in of 25%. The R16S dataset yielded the best resolved tree among the three 16S datasets analyzed and was therefore used for combined gene analyses (COI + R16S and COI + R16S + H3) using Bayesian inference (BI) and maximum likelihood (ML) methods (Figures 7–8). Concatenated analyses were performed only with taxa with sequences available for at least two gene markers ($n = 44$). For BI, the concatenated alignments were performed in MrBayes using three parallel runs of 15 million generations, sampling every 100 generations. For ML, analyses were conducted using RAxML v. 8.2.12 (Stamatakis, 2014) run through the portal CIPRES, with random starting trees and 1000 bootstrap replicates. Nodal

support was assessed by posterior probabilities (PP) for BI and with nonparametric bootstrap (BS) for ML. Only nodes with PP values ≥ 0.95 and BS ≥ 75 were considered supported. Consensus phylograms were converted into graphical trees using FigTree v. 1.4.4 (Rambaut, 2009) and edited with the software Gravit Designer (Corel Corporation, 2020).

3.4 Species delimitation analysis

The Automatic Barcode Gap Discovery (ABGD) method (Puillandre et al. 2012) was conducted via the ABGD interphase website to perform molecular species delimitation. The COI alignment both with and without outgroups was used as the input file and analyzed with the three evolutionary models implemented, namely Jukes-Cantor (J69), Kimura (K80), and Simple Distance, using default settings (Appendix II, Figures I–VI). ABGD is an exploratory method that partitions alignments into candidate species and detects the barcode gap in the distribution of pairwise distances. The barcode gap, *i.e.*, where intraspecific divergence is smaller than interspecific divergence, is detected by means of a model-based confidence limit for intraspecific divergence (*P*). By default, *P* is reported from 0.001 to 0.1, yielding higher and lower numbers of partitions, respectively. Here, initial partitions are recursively applied to previously obtained species groups, yielding a recursive hypothesis with more groups compared to the initial ones. Two parameters are crucial for ABGD to perform soundly. First, the dataset should contain at least three specimens per species and secondly, if speciation events have occurred too recent relative to population ancestry, the method may not be sensitive enough (Puillandre *et al.*, 2012).

3.5 Examination of morpho-anatomical characters

Morpho-anatomical characters of 12 specimens of *J. tomentosa s. l.*, representing the three lineages recognized by the molecular phylogenetic hypotheses and ABGD method, were examined in collaboration with Prof. Marta Pola at the Universidad Autónoma de Madrid, Spain. Dissections were performed using a Nikon SMZ 1500 stereo microscope equipped with a Nikon D5100 digital camera and a *camera lucida*. Oral tentacles, rhinophoral lamellae, branchial leaves, and mantle structures such as the caryophyllidia were studied prior to dissections. The animals were dissected by dorsal incision and the digestive parts were separated from the buccal mass by cutting the esophagus and parted from the reproductive system cutting the hermaphroditic duct. The buccal mass was dissolved in a 10 % sodium hydroxide solution until the labial cuticle and radula had been cleansed from their surrounding tissue (*ca.* 24 h). The structures were then rinsed with distilled water and examined with the aid

of an Olympus CX31 light microscope using the Life Science Imaging software *cellSens* (v.1.18, Olympus Cooperation). Each reproductive system was studied in detail and drawn using a *camera lucida.* Penial structures and the copulatory spines were isolated for further examination by light microscopy and SEM. Caryophyllidia, labial cuticles, penises, and copulatory spines were critical point dried transferring the structures from absolute ethanol to a dry dish and adding one drop of hexamethyldisilazane. After approximately 30 minutes the dried structures, together with the radulae, were mounted on stubs, sputter coated with gold or gold-palladium and studied by the aid of SEM (Hitachi S-3000N and FEI Quanta^{TM} FEG 450).

4. Results

4.1 Molecular phylogenetic analysis

DNA was successfully amplified for 62 of 78 specimens of *Jorunna tomentosa s. l*., yielding 111 novel sequences for the three gene markers COI (581–658 bp; 61 sequences), 16S (464–483 bp; 25 sequences), and H3 (252–339 bp; 25 sequences). In addition, sequences for each of the three gene markers were obtained for a specimen of *J. onubensis*. In total, 114 novel sequences and 49 GenBank sequences were included in the final phylogenetic analyses (Table 2). The single-locus COI (658 bp; 80 sequences) and R16S (464 bp; 42 sequences) alignments yielded the best-resolved phylograms compared to the H3 (350 bp; 41 sequences), S16S (382 bp; 42 sequences), and 16S (497 bp; 42 sequences) datasets (Figures 4–6; Appendix III, B, Figures IX–X). Two concatenated alignments (COI + R16S; COI + R16S + H3) were generated containing sequences that covered at least two of the genetic markers. The molecular phylogenetic analyses partially recovered the three clades *Jorunna* sp. nov., *J. tomentosa* lineage A, and *J. tomentosa* lineage B, revealing the existence of a cryptic species complex in the European *J. tomentosa*. Whereas *Jorunna* sp. nov. was resolved as a single clade in all analyses, *J. tomentosa* A and *J. tomentosa* B were either resolved as single clades or depicted as a cluster of sequences (Figures 4–8; Appendix III, B, Figures IX–X). The COI phylogram (658 bp; 80 sequences) revealed fully supported clades for *Jorunna* sp. nov. (PP/BS = 1/100) and *J. tomentosa* A (PP/BS = 0.98/98), whereas *J. tomentosa* B gained strong support in the Bayesian analysis only (PP/BS = 0.90/48) (Figure 4). A similar result was obtained with the concatenated dataset COI + R16S where *Jorunna* sp. nov. and *J. tomentosa* A received high statistical support with PP/BS = 1/100 and PP/BS = 1/99, respectively, whereas *J. tomentosa* B was not supported (PP/BS = 0.70/59) (Figure 7). The R16S analysis (464 bp; 42 sequences) yielded *Jorunna* sp. nov. with PP/BS = 0.91/71 and a well-supported cluster of the lineages A

and B (PP/BS = 0.95/57) where *J. tomentosa* A was resolved as a supported clade nested within (PP/BS = 0.99/94) (Figure 5). A comparable result was obtained with the 16S dataset (497 bp; 42 sequences), revealing *Jorunna* sp. nov. as a single clade (PP = 0.94) and clustering the sequences of lineage A and B (PP = 0.92), supporting the clade of lineage A nested within lineage B (PP = 0.99) (Appendix III, B, Figure IX). This clustering was again revealed in the concatenated COI + R16S + H3 dataset (Figure 8), fully resolving *Jorunna* sp. nov. with PP/BS = 1/100 and the clade *J. tomentosa* A (PP/BS = 1/99) within the cluster of sequences of lineage A and B (PP/BS = 1/47). At last, the H3 phylogram (350 bp; 41 sequences) recovered *Jorunna* sp. nov. as a single clade with nearly full support (PP = 0.99) and depicted lineage A and B as a non-supported cluster of sequences (PP = 0.58) (Figure 6). The S16S phylogram (382 bp; 42 sequences) recovered *Jorunna* sp. nov. with a lower support (PP = 0.76) but instead yielded a supported cluster of lineage A and B (PP = 0.97) (Appendix III, B, Figure X).

The COI uncorrected genetic *p*-distances within all sequenced *Jorunna* spp. are depicted in Table 4. The genetic distances between *J. funebris* and *J. onubensis* were estimated to 16.9%. The same genetic distance was estimated between *J. funebris* and *Jorunna* sp. nov.. Generally, the three lineages *Jorunna* sp. nov, *J. tomentosa* A, and *J. tomentosa* B are 10–20% genetically different from *J. funebris* and *J. onubensis*. Between *Jorunna* sp. nov. and *Jorunna tomentosa* A, the estimated genetic distance is 10.3–10.8%. *Jorunna* sp. nov. and *Jorunna tomentosa* B depict an even greater range of *p*-distances, laying between 9.0–12.3%. Between *J. tomentosa* A and *Jorunna tomentosa* B, the estimated genetic distance varied between 3.2–5.0%. All other intraspecific differences were estimated to be less than 1%, with the highest variation of 0.68% among specimens of *J. tomentosa* A.

The ABGD analyses of the COI alignment both including and excluding outgroup species were run with a prior maximum divergence of intraspecific diversity (*P*) between 0.001 and 0.1 for each of the evolutionary models and resulted in up to 10 partitions, ranging from 2 to 35 groups (Appendix II, Figures I–VI). The partitions that yielded four and five groups (outgroup species excluded) were both considered putatively congruent with the results rendered by the phylogenetic analyses. Between *P* values of 0.02–0.06, the analyses with all three evolutionary models recovered four lineages, namely *J. funebris*, *J. onubensis*, *Jorunna* sp. nov., and *J. tomentosa* A + *J. tomentosa* B. Between *P* values of 0.005–0.01, the analyses rendered *J. tomentosa* A and *J. tomentosa* B as two valid lineages, as well as *J. funebris*, *J. onubensis*, and *Jorunna* sp. nov.. Partitions which retrieved less than four or five groups ($P > 0.06$) were considered unreliable as all species except *J. funebris* were lumped as a single taxonomic unit,

even though morphological and molecular evidence clearly separate these species. On the other hand, partitions exceeding four or five groups ($P < 0.003$) likely result from splitting artifacts caused by lower P values (Puillandre *et al.*, 2012), and were not consistent with the phylogenetic hypotheses (Figures 4–8) and morphological partitions (see Systematic descriptions).

Overall, the molecular phylogenetic analysis is consistent with the presence of an undescribed species, here called *Jorunna* sp. nov., which prior to this study had been "hidden" under the species name *J. tomentosa* as a cryptic species and is described here for the first time. Character differentiations of *J. tomentosa* lineage A and *J. tomentosa* lineage B are remarked in the systematic description of *J. tomentosa* (see section 4.2).

Table 3. Gblocks masking parameters for the 16S relaxed and the 16S stringent alignments.

	16S relaxed	**16S stringent**
Min. nr. seq. for conserved position	22	22
Max. nr. seq. for a flanking position	22	35
Max. nr. contig. non-conserved positions	8	4
Min. length of block	5	10
Allowed gap position	Half	None
Gblocks alignment	**464 (93 % of original 497)**	**382 (76% of original 497)**

Table 4. Interspecific and intraspecific COI uncorrected genetic *p*-distances (%) between species of *Jorunna*. Intraspecific *p*-distances are written in bold. Abbreviation n/a = not applicable.

		1	2	3	4	5
1	*J. onubensis*	**n/a**				
2	*J. funebris*	16.9	**n/a**			
3	*Jorunna* sp. nov.	12.6 – 12.7	16.9	**0.15**		
4	*J. tomentosa* A	10.0 – 10.3	18.0 – 19.1	10.3 – 10.8	**0.0 – 0.68**	
5	*J. tomentosa* B	10.0 – 12.0	18.0 – 20.0	9.0 – 12.3	3.2 – 5.0	**0.0 – 0.26**

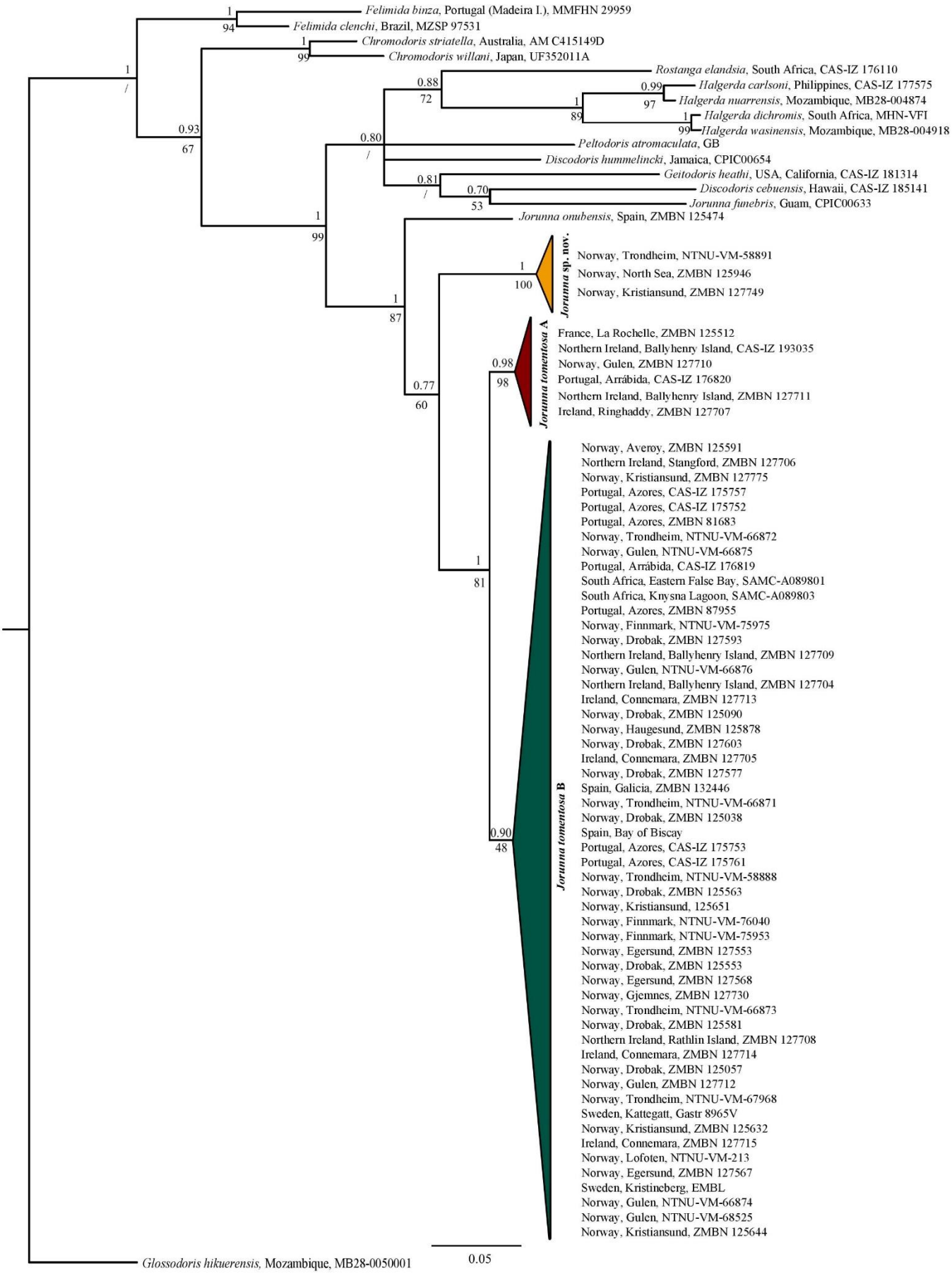

Figure 4. Phylogenetic hypothesis resulting from the COI dataset based on Bayesian analysis. Numbers above branches refer to posterior probabilities while numbers below branches refer to bootstrap values. Tree rooted with *Glossodoris hikuerensis*.

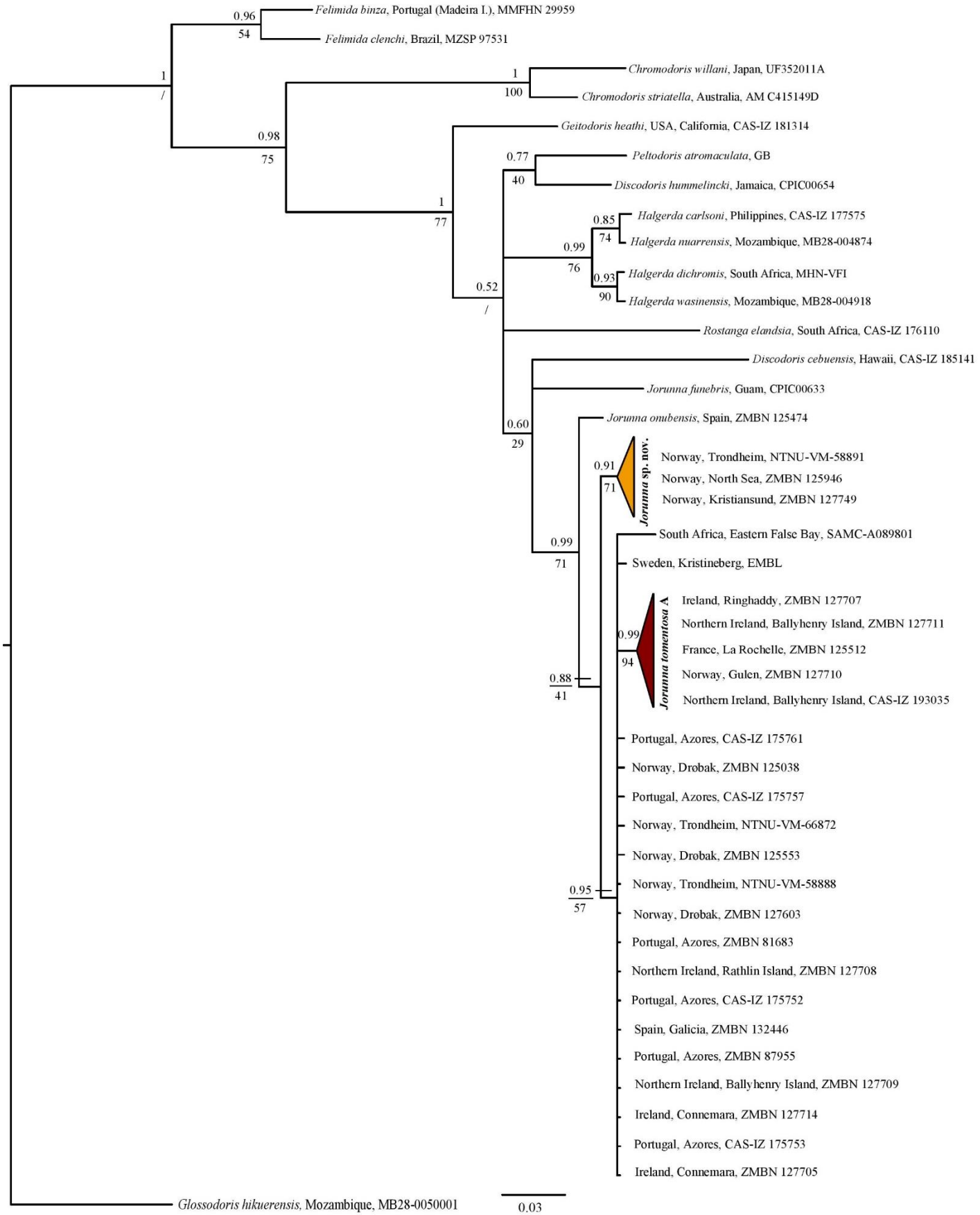

Figure 5. Phylogenetic hypothesis resulting from the relaxed 16S dataset based on Bayesian analysis. Numbers above branches refer to posterior probabilities while numbers below branches refer to bootstrap values. Tree rooted with *Glossodoris hikuerensis*.

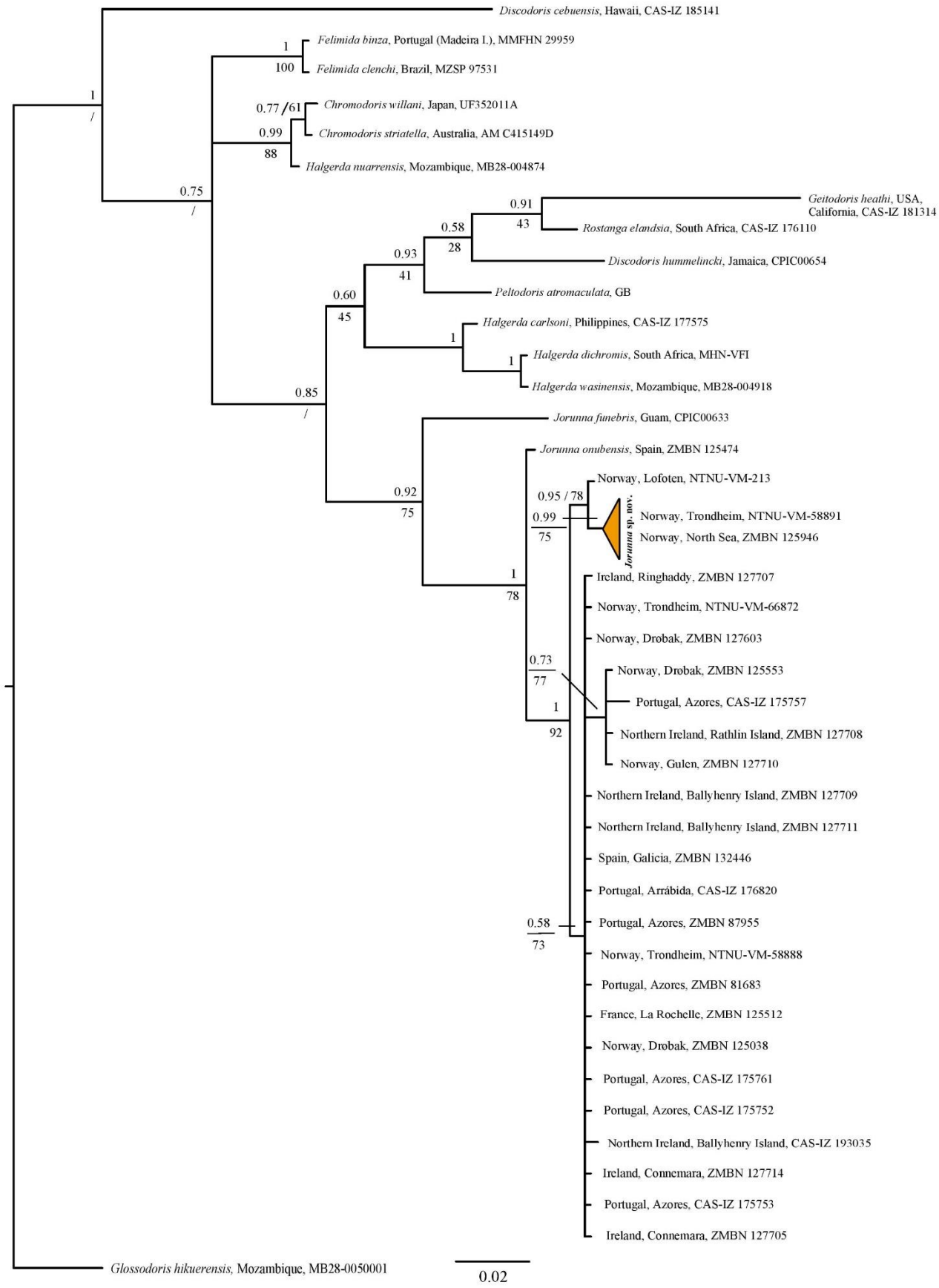

Figure 6. Phylogenetic hypothesis resulting from the H3 dataset based on Bayesian analysis. Numbers above branches refer to posterior probabilities while numbers below branches refer to bootstrap values. Tree rooted with *Glossodoris hikuerensis*.

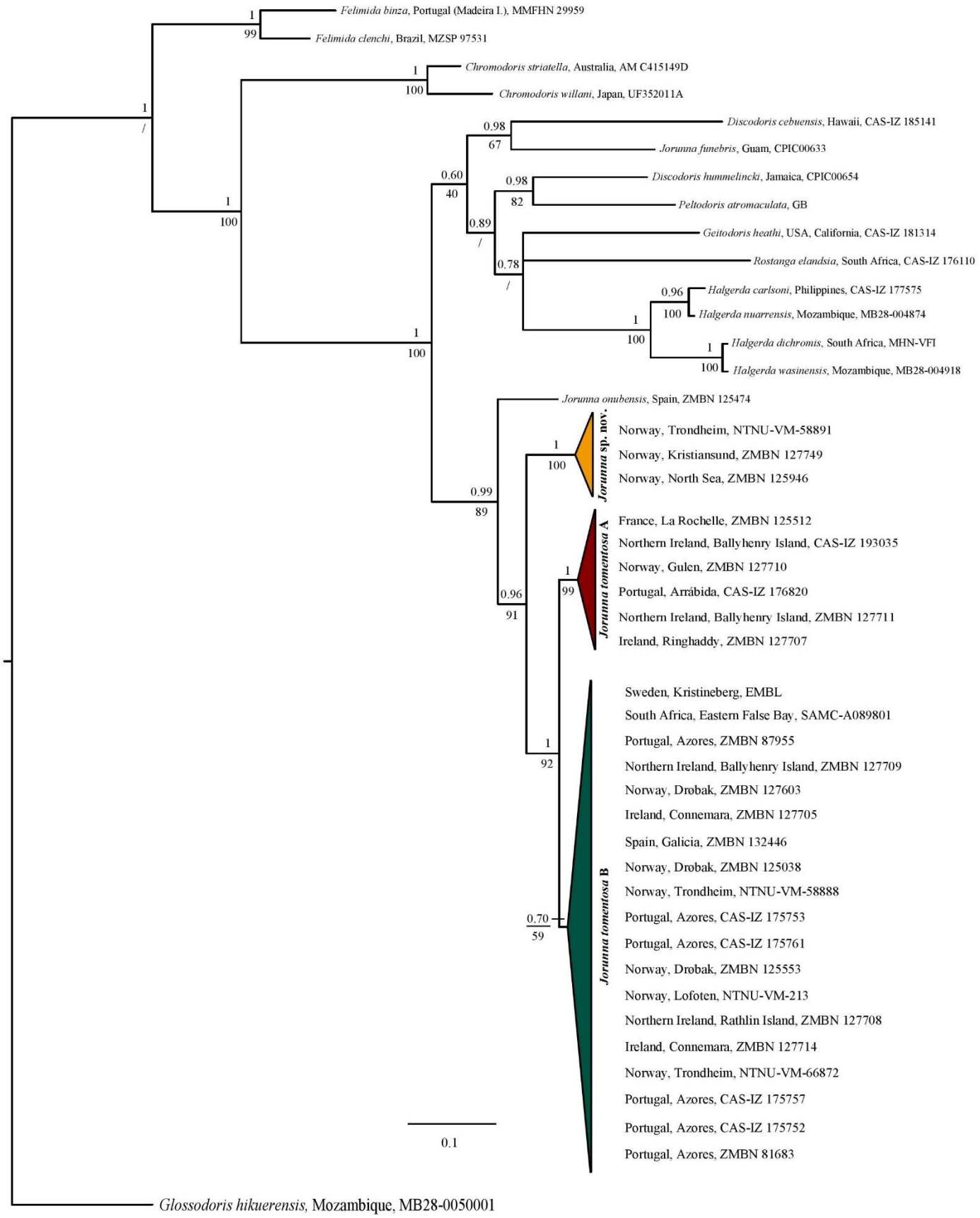

Figure 7. Phylogenetic hypothesis resulting from the COI + R16S dataset based on Bayesian analysis. Numbers above branches refer to posterior probabilities while numbers below branches refer to bootstrap values. Tree rooted with *Glossodoris hikuerensis*.

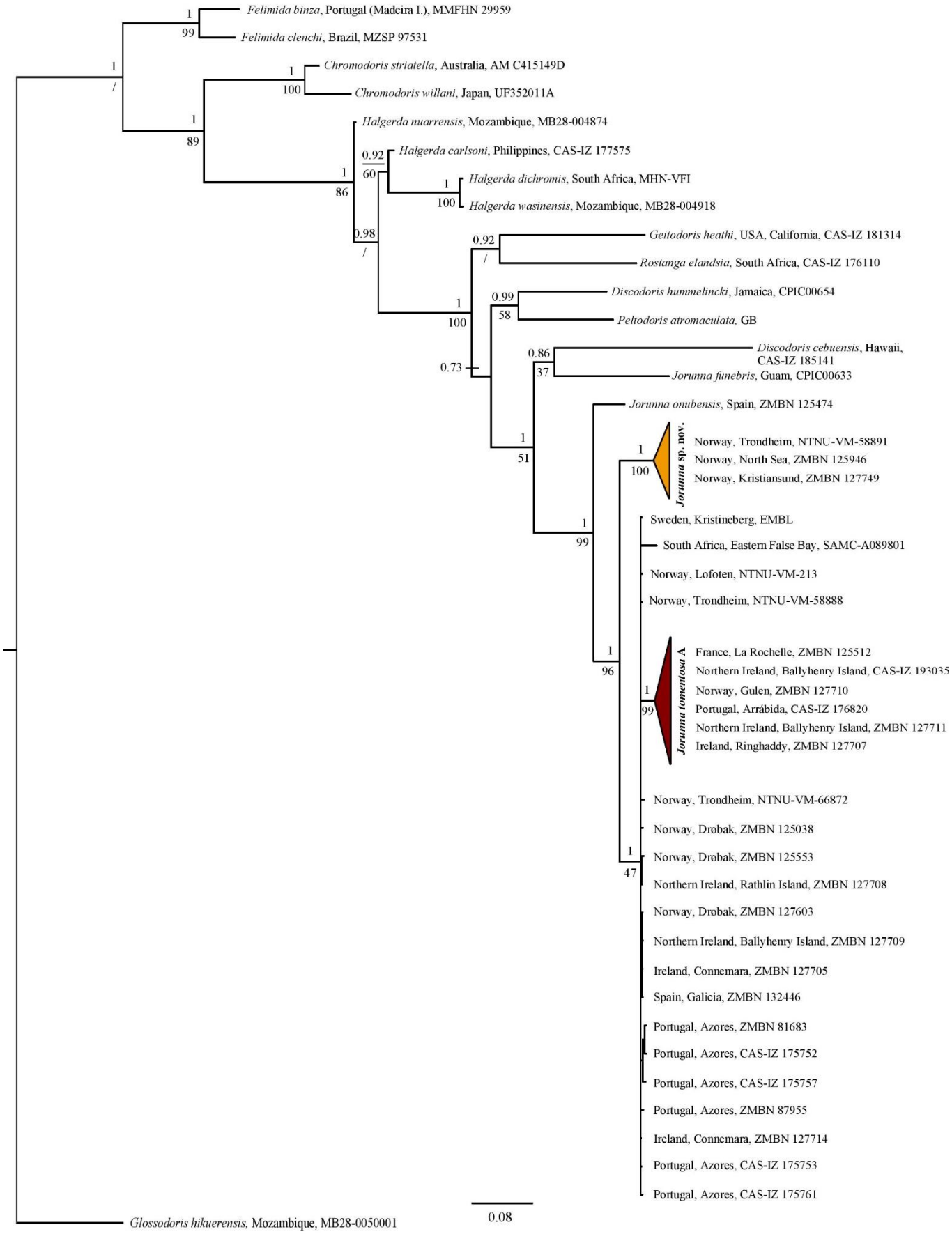

Figure 8. Phylogenetic hypothesis resulting from the COI + R16S + H3 dataset based on Bayesian analysis. Numbers above branches refer to posterior probabilities while numbers below branches refer to bootstrap values. Tree rooted with *Glossodoris hikuerensis.*

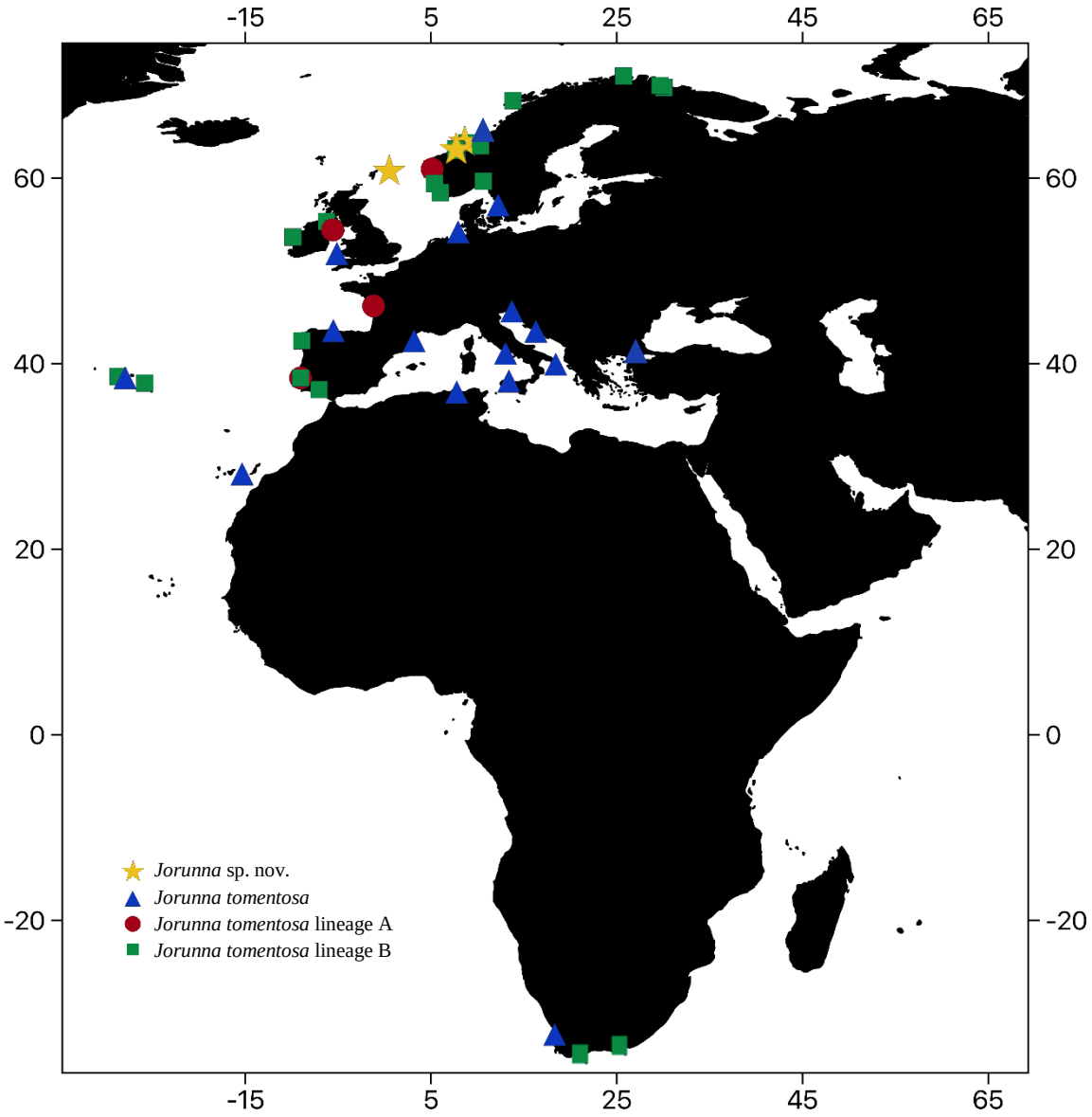

Figure 9. Geographic distribution of *Jorunna* sp. nov. (yellow stars) and *Jorunna tomentosa* (blue triangles = literature records; red circles = lineage A; green squares = lineage B).

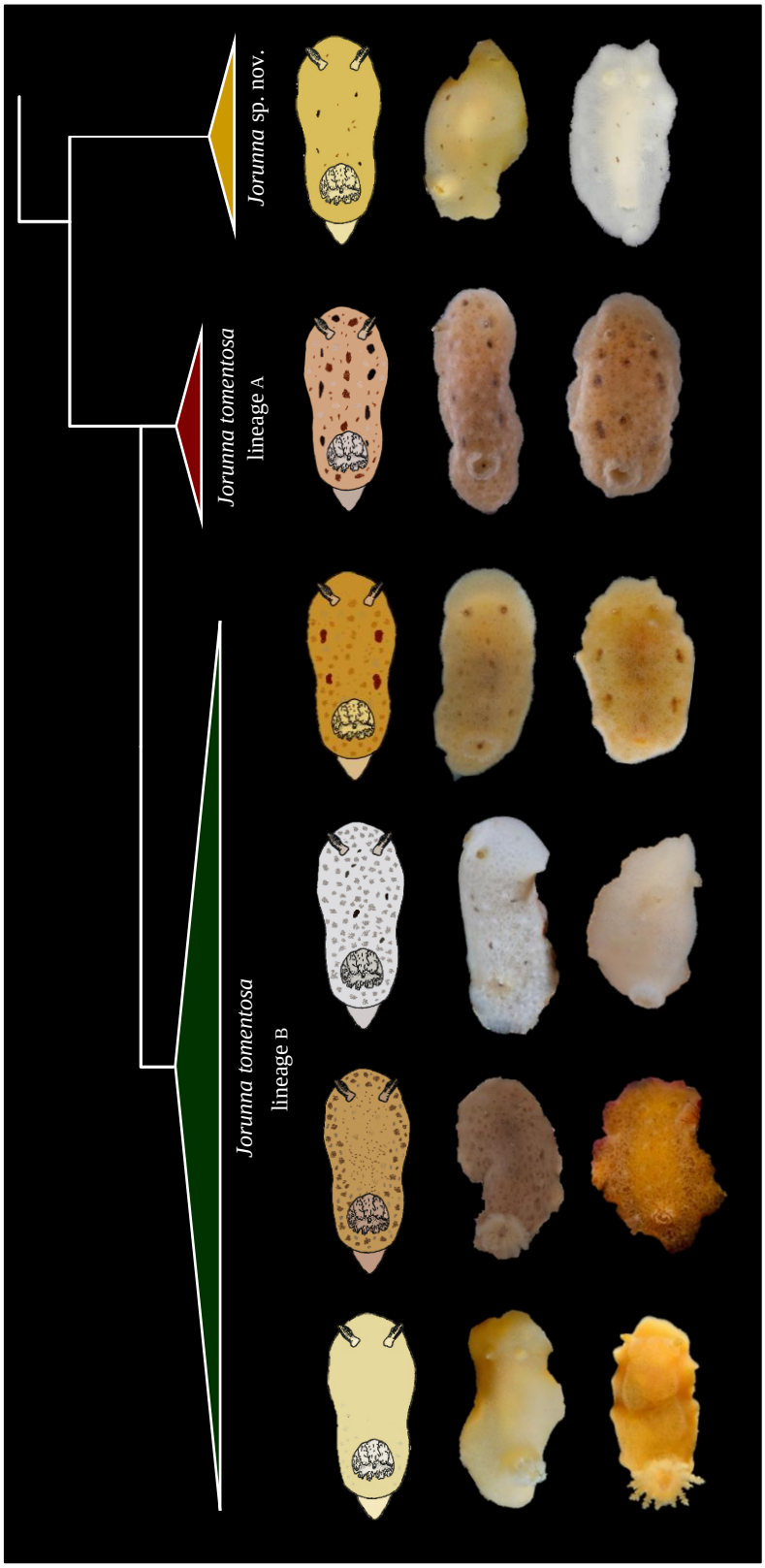

Figure 10. Drawings and live images of the main morphotypes found in the three clades. Information on depicted specimens given from left to right for each row. Row 1: *Jorunna* sp. nov. (ZMBN 127749; NTNU-VM-58891). Row 2: *Jorunna tomentosa* A (ZMBN 127711; ZMBN 127707). Row 3–6: *Jorunna tomentosa* B (Row 3: ZMBN 127712; ZMBN 127567) (Row 4: ZMBN 125591; ZMBN 125632) (Row 5: ZMBN 87955; ZMBN 125553) (Row 6: ZMBN 125651; ZMBN 125038).

4.2 Systematic descriptions

Abbreviations: CAS-IZ = California Academy of Sciences; MNHN = National Museum of Natural History, Paris; NTNU = Norwegian University of Science and Technology University Museum, Trondheim; USNM = National Museum of Natural History, Smithsonian Institution, Washington DC, USA; ZMBN = Department of Natural History, University Museum of Bergen, University of Bergen; TL = total length.

Family **Discodorididae** Bergh, 1891

Genus ***Jorunna*** Bergh, 1876

Synonyms

Jorunna Bergh, 1876: 414. Type species *Doris johnstoni* Alder & Hancock, 1845 [= *Jorunna tomentosa* (Cuvier, 1804), by monotypy].

Kentrodoris Bergh, 1876: 413. Type species *Kentrodoris rubescens* Bergh, 1876 [= *Jorunna rubescens* (Bergh, 1876) by subsequent designation (Ev. Marcus, 1976)].

Audura Bergh, 1878: 567–568. Type species *Audura maima* Bergh, 1878 [= *Jorunna maima* (Bergh, 1878), by monotypy].

Centrodoris P. Fischer, 1883: 522. Unjustified emendation of *Kentrodoris* Bergh, 1876.

Awuka Er. Marcus, 1955: 155–156. Type species *Awuka spazzola* Er. Marcus, 1955 [= *Jorunna spazzola* (Er. Marcus, 1955), by subsequent designation (Ev. Marcus, 1976)].

Taxonomic history

Bergh (1876) established the genus *Kentrodoris* Bergh, 1876 for the species *Kentrodoris gigas* Bergh, 1876, *K. annuligera* Bergh 1876, and *K. rubescens* Bergh 1876, all characterized by a smooth labial cuticle, a penis armed with a long spine and a large accessory gland. In the same work in a footnote, he introduced the genus *Jorunna* based on the description of *Doris johnstoni* Alder & Hancock, 1845, and proposed the new combination name *Jorunna johnstoni* (Bergh, 1876: 414). He considered both genera to be valid, yet closely related to each other, because of the presence of a spine in the penis in *Kentrodoris*, compared to a spine in the accessory gland in *Jorunna*. Later, Bergh (1878) described the genus *Audura* Bergh, 1878 based on the species *A. maima* Bergh, 1878, which could be differentiated from *Kentrodoris* by the presence of jaw elements.

Er. Marcus (1955) established the genus *Awuka* Er. Marcus, 1955, represented by the species *A. spazzola* Er. Marcus 1955, based on the presence of jaw elements, one denticle on the innermost radular teeth, and a spine considered to be situated in the penis. Later, Ev. Marcus (1976) published a revision of the genera *Kentrodoris* and *Jorunna* and found the copulatory spine of *A. spazzola* to be situated in the accessory gland, and not in the penis as considered earlier (Er. Marcus, 1955). Hence, Ev. Marcus (1976) reassigned the species to the genus *Jorunna* as *J. spazzola*. She also found that the penial spine in *Kentrodoris* described by Bergh (1876), was situated in the large accessory gland, exactly as for species of *Jorunna*. However, Ev. Marcus (1976) decided to keep *Kentrodoris* separate from *Jorunna* due to slight differences in the notum, prostate, and the sheathed male organ. She designated *K. rubescens* as the type species and regarded *K. gigas* and *K. annuligera* as members of *Jorunna*.

Valdés & Gosliner (2001) synonymized *Kentrodoris* with *Jorunna*, selecting *Jorunna* as the valid, less nomenclatural disruptive name due to its common use over *Kentrodoris* (ICZN, 1999: Art. 24). *Centrodoris* Fischer, 1883 is an unjustified emendation for *Kentrodoris* and therefore a junior objective synonym of *Kentrodoris* (ICZN, 1999: Art. 33b). Valdés & Gosliner (2001) examined the holotype of *Audura maima* and suggested that the anatomical features described by Bergh (1878), such as the presence of elongated caryophyllidia on the notum and a spine in the accessory gland, were not enough to support its validity and considered it a synonymy of *Jorunna*. However, other characteristics drawn by Bergh (1878) differ from the diagnosis of the genus *Jorunna*. The species *J. maima* carries radular teeth with a wide base in the outermost laterals, compared to slender outermost teeth with a thin base present in the other species of *Jorunna*. Also, the copulatory spine seems to be shorter, compared to the otherwise long spine found in other *Jorunna*. According to Camacho-García & Gosliner (2008), these characters resemble those present in the genus *Sclerodoris* Eliot, 1904, leaving the generic assignment of *J. maima* unclear (MolluscaBase, 2020e).

Diagnosis

Adult size 10–200 mm. Body depressed, oval-elongate. Background colour white, grey-white, yellow-orange, reddish-brown or purple. Notum with larger brown blotches, dark rings, or brownish speckles. Notum of velvety appearance; densely covered with caryophyllidia with long conical base, long spicules and rounded, ciliated tubercle. When present, mantle glands white, distributed around mantle edge. Rhinophores up to 20 lamellae, fully retractile into low sheaths, with apical knob. Gills retractile into low sheath, up to 17 uni- to tripinnate branchial

leaves encircling anal papilla. Rhinophores and gills may be speckled with white, brown, or black spots. Foot narrow, anteriorly notched, grooved. Oral tentacles either slender digitiform, bulbous, or triangular flattened. Labial cuticle smooth or armed with jaw elements. Radula formula 14–35 x 33–13.0.13–33, except for *J. pardus* which depicts a much higher number of lateral teeth (41 x 80.0.80 for a specimen with TL = 20 mm). Lateral teeth hook-shaped, larger in middle of half-row, outermost laterals slender, sometimes denticulated; rachidian tooth absent. Reproductive system triaulic; ampulla large; prostate massive, differentiated; penis and vagina unarmed. Large accessory gland with copulatory spine. Distributed worldwide, mostly in shallow waters, from boreal waters to the tropics (Ev. Marcus, 1976; Valdés & Gosliner, 2001; Camacho-García & Gosliner, 2008; Edmunds, 2011; Alvim & Pimenta, 2013; Ortea *et al.*, 2014; Ortea & Moro, 2016; Zenetos *et al.*, 2016; Tibiriçá, Pola & Cervera, 2017; Furfaro *et al.*, 2020).

Anatomy (Figures 11–14)

Digestive gland large, covered by pigmented peritoneum. Intestine emerging anteriorly from oval stomach, terminating in anal opening situated within center of gill circlet. Melon-shaped renal syrinx situated near anal opening. Pericardial cavity situated distally of anal pore, comprising ventricle with two posteriorly emerging auricular veins; aorta runs along intestine towards anterior side, connecting with blood gland and reproductive system. Blood gland separated into two portions. Oral tube wide, about same length as buccal bulb; buccal bulb muscular. Pair of elongate, thin salivary glands attached on both sides of buccal bulb at point where esophagus connects to buccal mass; thin glands embedded in porose tissue collar wrapped around digestive gland and parts of reproductive apparatus.

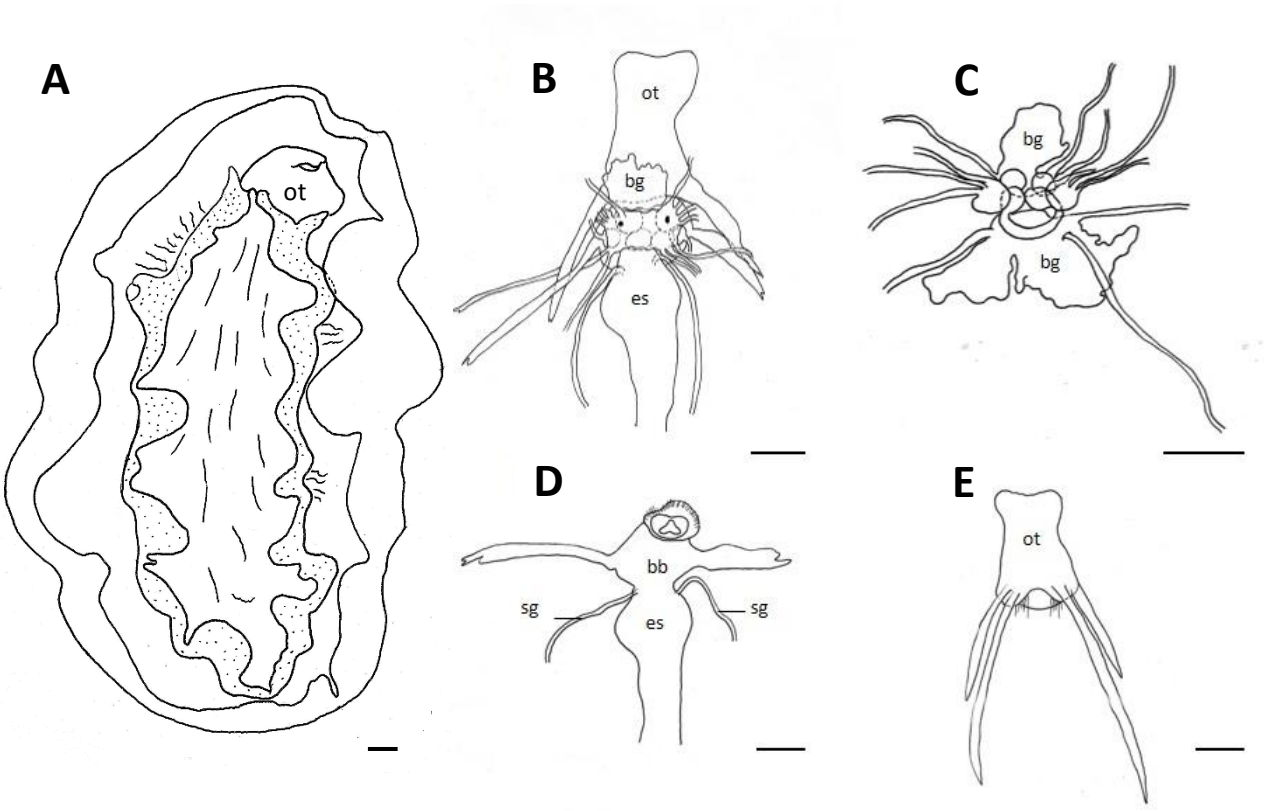

Figure 11. Drawings of internal anatomy structures of *J. tomentosa* (lineage B; ZMBN 87955, TL = 30 mm) representing the general internal anatomy of the genus (ZMBN 87955). **A**. Ventral view of intact specimen with everted oral tube. **B**. Dorsal view of blood glands with attached nerves. **C**. Ventral view of blood gland and the nerve ring. **D**. Buccal bulb detached from oral tube which was situated dorsally. **E**. Oral tube detached from buccal bulb depicted in D. Abbreviations: ot = oral tube; bb = buccal bulb; bg = blood gland; e = eye spot; es = esophagus; st = stomach; i = intestine; a = aorta; pe = pericardium; au = auricula; v = ventriculum; r = renal syrinx; mg = mucus gland; g = gonopore. Scale bars = 1 mm.

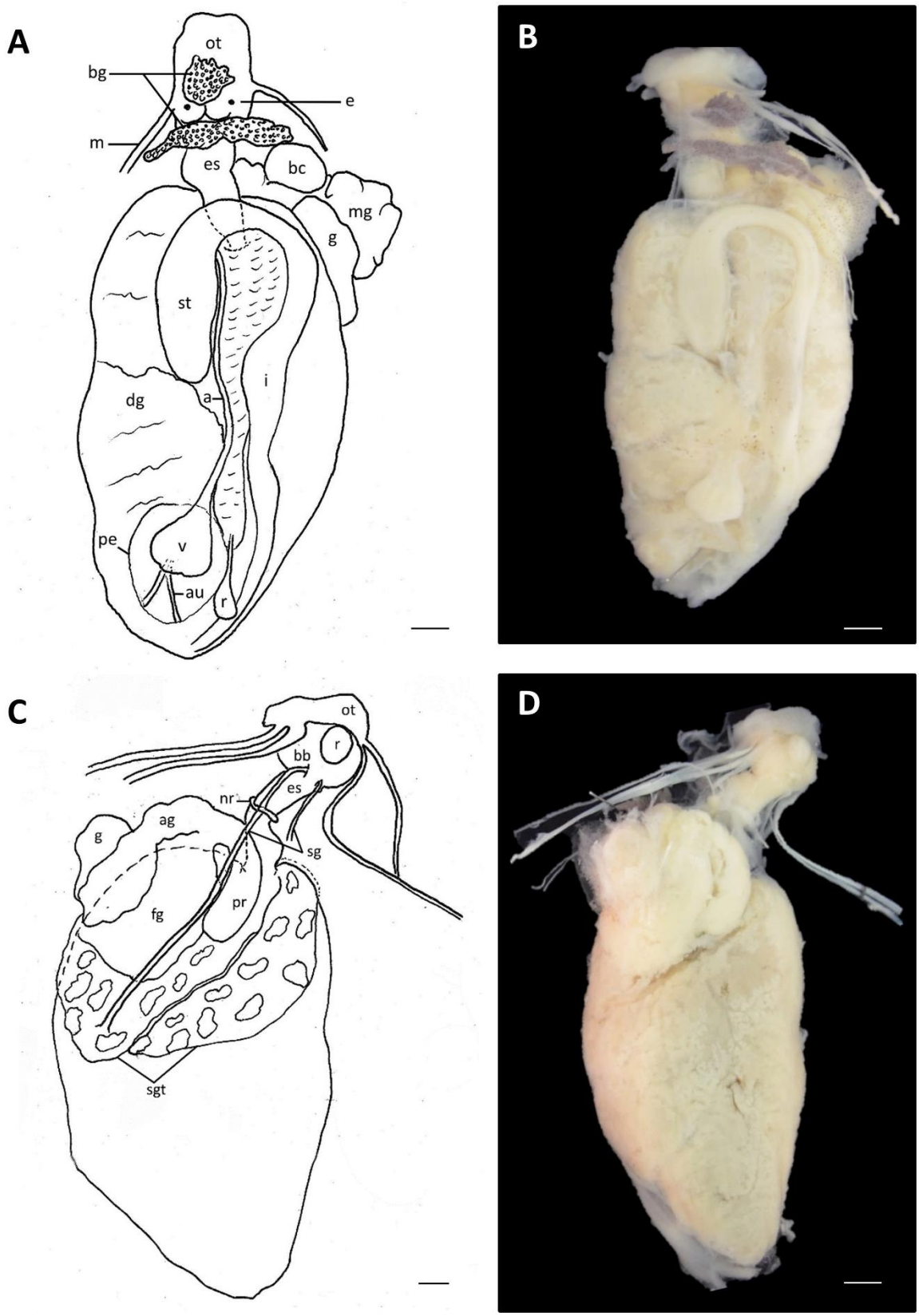

Figure 12. Drawings and images of *J. tomentosa* (lineage B; ZMBN 87955, TL = 30 mm) representing the general internal anatomy of the genus. **A, B**. Dorsal views. **C, D**. Ventral views. Abbreviations: ot = oral tube; bg = blood gland; e = eye spot; r = radular sac; m = muscle; bb = buccal bulb; es = esophagus; nr = nerve ring; sg = salivary glands; sgt = salivary gland tissue; st = stomach; i = intestine; a = aorta; pe = pericardium; au = auricula; v = ventriculum; r = renal syrinx; dg = digestive gland; mg = mucus gland; g = gonopore; bc = bursa copulatrix; pr = prostate; fg = female gland; ag = accessory gland. Scale bars = 1 mm.

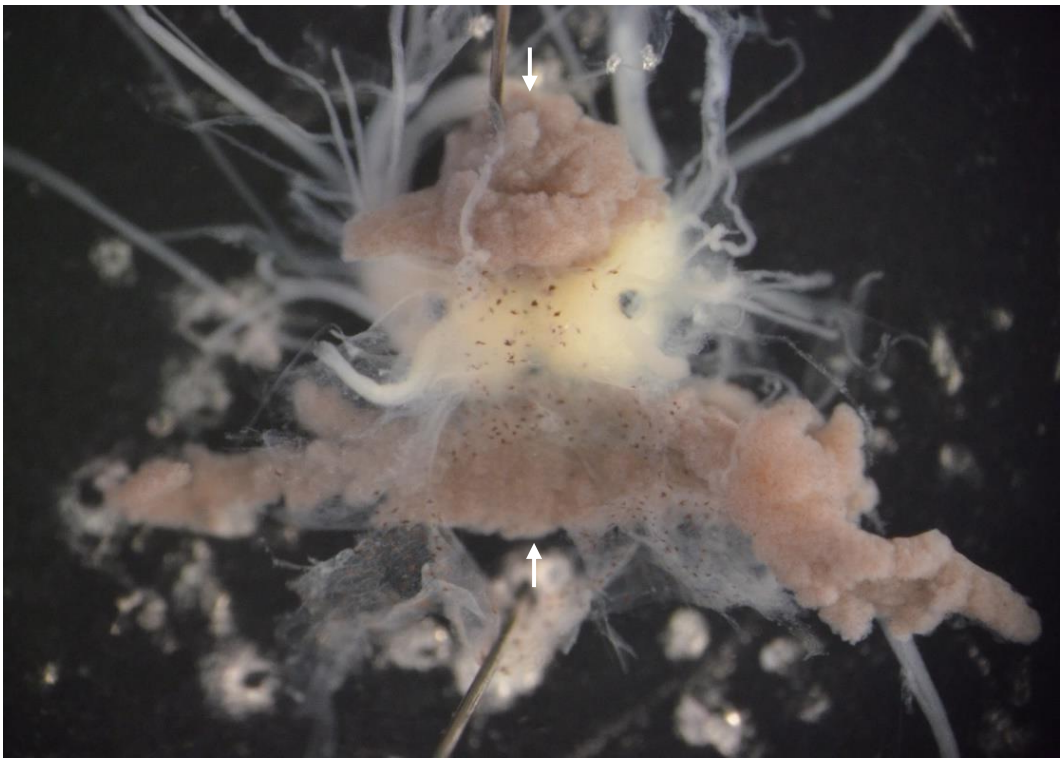

Figure 13. Blood gland in *J. tomentosa* (lineage B; ZMBN 87955, TL = 30 mm). Arrows pointing to the two separated blood glands. The pigmented peritoneal tissue can be seen between the glands. Note: scale bar absent.

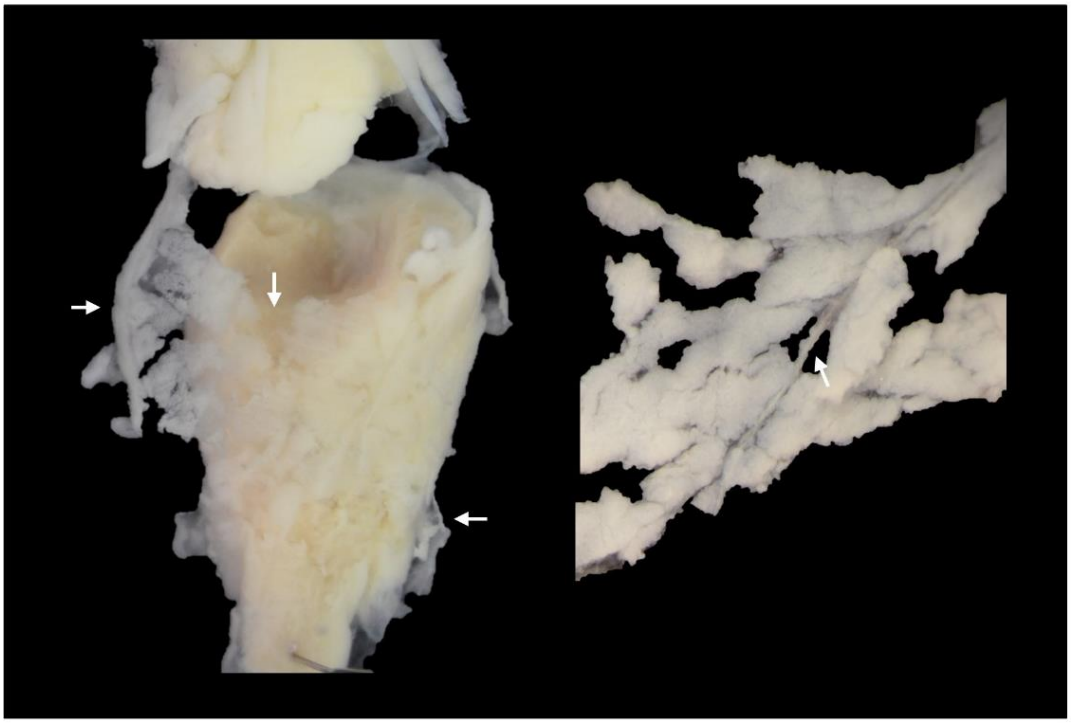

Figure 14. Left: Detailed view of salivary gland tissue in *J. tomentosa* (lineage B; ZMBN 127705, TL = 25 mm) wrapped around the digestive gland, seen from the ventral side. Arrow (left) highlights the thin salivary gland running through the salivary gland tissue. Arrows (center, right) indicate tissue contour. Right: Detailed view of thin salivary gland (indicated with arrow) embedded in the salivary gland tissue. Note: scale bar absent.

Jorunna tomentosa (Cuvier, 1804)

(Figures 2–3; 9–25)

Synonyms

Doris tomentosa Cuvier, 1804: 470–472 [type locality: La Rochelle, France based on neotype designated by Camacho-García & Gosliner (2008), MNHN-IM-2000-35690].

Jorunna tomentosa – Iredale & O'Donoghue, 1923: 227; Odhner, 1939: 35–36, fig. 18; Pruvot-Fol, 1954: 274, figs 109–110; Swennen, 1961: 196–197; Ev. Marcus, 1976: 20–26, figs 9–19; García Gómez, 1983: 43; Cervera *et al.*, 2004: 44, 82; Camacho-García & Gosliner, 2008: 144–148, figs 1a, 1b, 2, 3; Moen & Svensen, 2014: 413; Malmberg & Lundin, 2015: 38; Prkić *et al.*, 2018: 222–223.

Doris obvelata Johnston, 1838: 52, pl. 2, figs 4–7.

Doris johnstoni Alder & Hancock, 1845: fam. 1, pl. 5, figs 1–8. Alder & Hancock, 1851: fam. 1, pl. 2, figs 8–10. Hancock & Embleton, 1852: 215–220, pl. XII, figs 2, 10, pl. XIV, fig. 10, pl. XV, fig. 1, pl. XVII, fig. 2. Alder & Hancock, 1855: pl. 46, fig. 4.

Jorunna johnstoni – Bergh, 1876: 414 (new combination name). Bergh, 1880: 47–52, 117, pl. 8, fig. 19; pl. 9, figs 1–11. Bergh, 1881: 114, pl. K, figs 20–28. Bergh, 1884: 683, pl. 70, figs 21–23. Cuénot 1904: 17. Hoffmann, 1926: 10. Odhner, 1926: 23. Labbé, 1933: 214, figs 2, 3. Nobre, 1938: 51.

Jorunna johnstoni var. *alba* Bergh, 1881: 119, pl. J, figs 17–21, pl. K, figs 29–36. Bergh, 1884: 683–685, pl. 70, fig. 20.

Jorunna atypha Bergh, 1881: 145, pl. J, figs 22–25.

Material examined

Norway: Kråka, Borgvær, Vestvågøy, Nordland (68.334701, 13.813291), 1 spc., sequenced and dissected, TL = 20 mm (fixed), NTNU-VM-213. Aursøya Brygge, Frøya, Trøndelag (63.792438, 8.89163), 1 spc., sequenced, TL = 10 mm (fixed), NTNU-VM-58888. NTNU Biological station, Trondheim, Trøndelag (63.441109, 10.348831), 1 spc., sequenced, TL = 13 mm (fixed), NTNU-VM-66873. 1 spc., sequenced, TL = 14 mm (fixed), NTNU-VM-66872. Brattøya, Kristiansund, Møre og Romsdal (63.062076, 7.695494), 1 spc., sequenced, TL = 26 mm (fixed), ZMBN 125651. 1 spc., sequenced, TL = 15 mm (fixed), ZMBN 125644. 1 spc., sequenced, TL = 25 mm (fixed), ZMBN 125632. 1 spc., sequenced, TL = 35 mm (fixed), ZMBN 127775. Stavnes, Averøy, Møre og Romsdal (63.114832, 7.662235), 1 spc., sequenced, TL = 28 mm (fixed), ZMBN 125591. Krifast, Bergsøya, Gjemnes, Møre og Romsdal

(62.973522, 7.784554), 1 spc., sequenced, TL = 12 mm (fixed) ZMBN 127730. Glossvika, Gulen, Vestland (60.960225, 5.128899), 1 spc., sequenced and dissected, TL = 23 mm (fixed), ZMBN 127710. 1 spc., sequenced, TL = 12 mm (fixed), NTNU-VM-66874. 1 spc., sequenced, TL = 12 mm (fixed), NTNU-VM-66876. 1 spc., sequenced, TL = 13 mm (fixed), NTNU-VM-68601. 1 spc., sequenced, TL = 17 mm (fixed), NTNU-VM-68525. 1 spc., sequenced, TL = 12 mm (fixed), NTNU-VM-66875. Gylte Brygge, Drøbak, Viken (59.682436, 10.623525), 1 spc., sequenced and dissected, TL = 25 mm (fixed), ZMBN 125553. 1 spc., sequenced and dissected, TL = 25 mm (fixed), ZMBN 127603. 1 spc., sequenced and dissected, TL = 30 mm (fixed), ZMBN 125038. 1 spc., sequenced, TL = 23 mm (fixed), ZMBN 125563. 1 spc., sequenced, TL = 18 mm (fixed), ZMBN 125581. 1 spc., sequenced, TL = 17 mm (fixed), ZMBN 127577. 1 spc., sequenced, TL = 12 mm (fixed), ZMBN 127593. Færgestad, Hurum, Viken (59.664458, 10.600886), 1 spc., sequenced, TL = 26 mm (fixed), ZMBN 125057. Sandholmen, Haugesund, Rogaland (59.408210, 5.377251), 1 spc., sequenced, TL = 13 mm (fixed), ZMBN 125878. Tingelsædet, Egersund, Rogaland (58.417110, 5.998327), 1 spc., sequenced, TL = 15 mm (fixed), ZMBN 127553. 1 spc., sequenced, TL = 18 mm (fixed), ZMBN 127567. 1 spc., sequenced, TL = 12 mm (fixed), ZMBN 127568. **Northern Ireland:** Ballyhenry Island, Strangford Lough (54.393969, -5.578313), 1 spc., sequenced, TL = 32 mm (fixed), ZMBN 127704. 1 spc., sequenced, TL = 29 mm (fixed), ZMBN 127709. 1 spc., sequenced and dissected, TL = 30 mm (fixed), ZMBN 127711. 1 spc., sequenced, CAS-IZ 193035. Rathlin Island (55.31138, -6.256670), 1 spc., sequenced, TL = 17 mm (fixed), ZMBN 127708. Ringhaddy, Strangford Lough (54.451046, -5.631184), 1 spc., sequenced and dissected, TL = 30 mm (fixed), ZMBN 127707. **Ireland:** Strangford Lough (54.537024, -5.615899), 1 spc., sequenced, TL = 21 mm (fixed), ZMBN 127706. Inishdegil More, Connemara (53.636815, -9.919531), 1 spc., sequenced, TL = 13 mm (fixed), ZMBN 127715. 1 spc., sequenced, TL = 13 mm (fixed), ZMBN 127713. 1 spc., sequenced, TL = 14 mm (fixed), ZMBN 127714. 1 spc., sequenced and dissected, TL = 25 mm (fixed), ZMBN 127705. **France:** Vieux Passage, Plouhinec, (47.671968, -3.209786), 1 spc., sequenced, ZMBN 125512. **Portugal:** Faial Island, Azores (38.590668, -28.697813), 1 spc., sequenced, TL = 9 mm (fixed), ZMBN 81683. 1 spc., sequenced, TL = 9 mm (fixed), CAS-IZ 175753. 1 spc., sequenced, CAS-IZ 175752. 1 spc., sequenced, TL = 12 mm (fixed), CAS-IZ 175757. 1 spc., sequenced, TL = 9 mm (fixed), CAS-IZ 175761. São Miguel Island, Mosteiros, Azores (37.898156, -25.821991), 1 spc., sequenced and dissected, TL = 30 mm (fixed), ZMBN 87955. Parque Natural da Arrábida, Arflor (38.439806, -9.053361), 1 spc., sequenced, CAS-IZ 176820. 1 spc., sequenced, CAS-IZ

176819. **South Africa:** Eastern False Bay (-34.182600, 18.821896), 1 spc., sequenced, SAMC-A089801. Knysna Lagoon (-34.049100, 23.048600), 1 spc., sequenced, SAMC-A089803.

Diagnosis

Background colour varies between grey-white, yellow-cream, dark-yellow, pale-orange and orange-brown; caryophyllidia uniform, dense, sometimes tilted towards each other forming slightly elevated whitish patches; notum may be plain or mottled with small, pale-brown spots, often combined with four to nine large, dark-brown blotches placed along lateral and median line. Mantle glands present. Rhinophores with 9–12 lamellae, uppermost with brown pigmentation. Nine to 14 gills, slightly brighter than background colour, with brown pigmentation on some leaves, cup-shaped. Foot visible when animal in motion. Oral tentacles digitiform. Radular formula 19–25 x 28–19.0.19–28. Up to eight slender, sickle-shaped outermost lateral teeth. Outermost laterals predominantly denticulated (up to eight denticles), sometimes smooth. Labial cuticle smooth.

Taxonomic history

Cuvier (1804) established the species *Doris tomentosa* based on material received from the naturalist Louis Benjamin Fleuriau de Bellevue, collected in La Rochelle, France. He described the species having a curved body, with a white to grey semi-translucent background colour and a mantle exceeding the foot, "*a little woolly to the touch, […] covered by small rounded tubercles in elongated cones*" (Cuvier, 1804: 472). Cuvier (1804) associated the *woolly touch* with what botanists refer to as coverd in hairs [latin: *tomentosa*]. Johnston (1838) identified a small specimen from Berwick Bay, U. K. with an ovate depressed body and broad, granulated mantle with uniform yellowish-white background, covered by few dark spots, 15 bipinnate cup-shaped gills, and a white foot, as *Doris obvelata* O. F. Müller, 1776 (today considered a synonym of *Cadlina laevis* (Linnaeus, 1767); see MolluscaBase, 2020f). Alder & Hancock (1845) studied this same specimen and considered it to be an undescribed species which the authors named after George Johnston as *Doris johnstoni* Alder & Hancock, 1845. According to Alder & Hancock (1845), *D. johnstoni* has an ovate body, capable of great extension, with a yellowish-white or pale cream background colour blotched with chocolate-brown spots arranged in two or three longitudinal rows, and a mantle covered with dense spiculose tubercles with a granular appearance. Fischer (1869) regarded *D. johnstoni* as a synonym of *D. tomentosa* for the first time. Since then, this synonymy has been generally accepted.

Bergh (1876), based on the original description of *D. johnstoni*, proposed the new combination name *Jorunna johnstoni* which was adopted and referred to by Cuénot (1904). Later, Bergh (1881) described three white specimens from Trieste, Italy as *Jorunna johnstoni* var. *alba*. This variety was considered a synonym of *J. tomentosa* by Ev. Marcus (1976), but at the same time the author pointed to the possibility that these specimens could belong to a distinct species. Camacho-García & Gosliner (2008) adopted the synonymy proposed by Ev. Marcus (1976) without further remarks.

Iredale & O'Donoghue (1923), based on Fischer (1869) and Bergh (1876), established the new combination name *Jorunna tomentosa*, yet several authors continued referring to the species as *J. johnstoni* (*e.g.*, Hoffmann, 1926; Odhner, 1926; Labbé, 1933; Nobre, 1938). Works after 1938, such as Odhner (1939), Pruvot-Fol (1954), Swennen (1961), Ev. Marcus (1976), and García Gómez (1983), applied the established combination name correctly. Kay & Young (1969) and Edmunds (1971) considered *J. tomentosa* to be distributed worldwide. Subsequently, Ev. Marcus (1976) ascribed the specimens studied from Hawaii by Kay & Young (1969), and from Tanzania by Edmunds (1971), to the species *J. alisonae* Ev. Marcus, 1976 and *J. malcolmi* Ev. Marcus, 1976, respectively, revoking the cosmopolitan distribution of *J. tomentosa*.

External morphology (Figures 2A; 3A–C, E, G; 10, row 2–6; 15)

TL = 20–30 mm. Coloration of notum orange-brown (lineage A; Figure 3D; Figure 10, row 2) or varying from grey-white to yellow, yellow-orange, and orange-brown (lineage B; Figure 3A–C, E, G; Figure 10, rows 3–6); notum with four to nine dark-brown blotches placed along lateral and median line (lineage A; Figure 10, row 2) or mottled with small, pale-brown spots, sometimes in combination with dark-brown blotches, or lacking spots and blotches (lineage B; Figure 10, rows 3–6). Caryophyllidia densely spaced, some tilted towards each other forming white patches. Rhinophores with 9–12 lamellae, slightly brighter than dorsum, pigmented in the tips. Nine to 14 bi- to tripinnate gills, slightly brighter than dorsum, encircling pigmented anal pore. Foot of same colour as dorsum, posteriorly visible when gliding, somewhat pointed at end. Oral tentacles pale-yellow, slender.

Labial cuticle (Figure 16)

Labial cuticle smooth.

Radula (Figures 17–20)

Radular formula of smallest studied specimens 21–22 x 23.0.23 (TL = 23 mm, ZMBN 125038; ZMBN 127710) and largest studied specimens 19–25 x 28–25.0.25–28 (TL = 30 mm, ZMBN 87955; ZMBN 127707; ZMBN 127711). Radula broad. Rachidian tooth absent; lateral teeth simple, hook-shaped with broad base and rounded cusp; mid lateral teeth larger than inner laterals; innermost laterals smooth or with one denticle or round swelling; three to eight slender, sickle-shaped outermost lateral teeth; outermost lateral teeth smooth or bearing up to eight denticles.

Reproductive system (Figures 21–25)

Hermaphroditic duct slender, emerging from digestive gland. Ampulla long, curved, divided into short oviduct entering upper mass of female gland and connective duct entering prostate. Prostate large, tubular, differentiated into two portions; narrows into coiled deferent duct leading to penial bulb situated within common atrium. Penis cylindrical, smooth. Vagina wider than deferent duct, without hooks, enters common atrium. Bursa copulatrix rounded, twice as large as oval seminal receptacle, connected by a short duct to bursa. Uterine duct thin, coiled, connecting distally with female gland mass entering common atrium. In mature specimens, hardened female gland mass is surrounded by large mucous gland; immature specimens possess small, soft female gland and lack mucus gland. Accessory gland large, convoluted; emerges into long, coiled duct connecting to heart-shaped ovate sac bearing a straight copulatory spine with rounded base; ovate sac embedded in muscular pouch emptying into common atrium; copulatory spine placed within a lining membrane forming a protective sheath, protruding from posterior end of ovate sac beyond tip of spine.

Ecology (Figure 3)

Commonly distributed in the lower part of the littoral zone down to approximately 400 m depth (Grieg, 1912; Moen & Svensen, 2014; Cordeiro *et al.*, 2015). Found on rocky-shores on or near sponges upon which it feeds, such as *Halichondria panicea*, *Haliclona oculata*, and *Haliclona cinerea* (Swennen, 1961; Wolter, 1967; Bloom, 1976; McDonald & Nybakken, 1997; Moen & Svensen, 2014). Sometimes found crawling upon ascidians and other rock-associated fauna (own observations).

Distribution (Figure 9)

From its northernmost records in Bøkfjorden, Troms og Finnmark and Borgvær, Vestvågøy, Nordland (present study; lineage B) the distributional range extends southwards to Trøndelag, Møre og Romsdal, Vestland, Viken, and Rogaland in Norway, the Kattegat in Sweden (Hansson, 1998; Evertsen & Bakken, 2002, 2005, 2013), Helgoland, Germany (Ev. Marcus, 1976), and the Netherlands (Swennen, 1961). Furthermore, *J. tomentosa* is common all around the British coasts (Thompson & Brown, 1984; Picton & Morrow, 1994; Moen & Svensen, 2014) (lineage A & B) and is found along the Atlantic French coast where it has its type locality (La Rochelle, France; Cuvier, 1804) (lineage A; Moore & Sproston, 1940; Pruvot-Fol, 1954) to the Iberian Peninsula including the archipelagos of the Azores and Canary Islands, being its westernmost distribution (Ros, 1978; Malaquias, 2001; Cordeiro *et al.*, 2015; Ortea & Moro, 2016) (lineage B). In the Mediterranean Basin and the Adriatic Sea, the species is distributed along the coasts of Algeria (Camacho-García & Gosliner, 2008), Spain (Ballesteros, Madrenas & Pontes, 2016), Italy (Furfaro *et al.*, 2020), Slovenia (Zenetos *et al.*, 2016), Croatia (Prkić *et al.*, 2018), and its easternmost reported locality in Turkey (Saltik, 2005). In the south, the species is additionally reported to occur in South Africa at Cape Province (Camacho-García & Gosliner, 2008), the Eastern False Bay, and the Knysna Lagoon (lineage B; own observations).

Remarks

The systematic revisions by Ev. Marcus (1976) and Camacho-García & Gosliner (2008) included comprehensive morpho-anatomical data on *J. tomentosa*. However, this study recognized for the first time the existence of two putative lineages within *J. tomentosa* (here designated A and B) suggesting a possible case of incipient speciation. Specimens of lineage A correspond to the morphotype originally described for *J. tomentosa* (Cuvier, 1804; Alder & Hancock, 1845; Pruvot-Fol, 1954; Ev. Marcus, 1976), having an orange-brown notum covered with dark-brown blotches (Figure 10, row 2). Specimens of lineage B are more variable both in notal coloration and blotchy patterns (Figure 10, rows 3–6). Genetically, the single-gene alignment COI (Figure 4) supports the existence of the two lineages *J. tomentosa* A (PP = 0.98) and *J. tomentosa* B (PP = 0.90), as well as the concatenated alignment COI + R16S (Figure 7) which fully resolved lineage A (PP = 1) and yielded lineage B with a posterior probability of 0.70. The R16S analysis yielded a cluster of both lineages (PP = 0.95) within which all representatives of lineage A are placed as an almost fully supported sub-cluster (PP = 0.99) (Figure 5). A comparable phylogeny was retrieved for the single-gene alignment 16S (Appendix III, Figure IX) and the concatenated alignment COI + R16S + H3 (Figure 8) where

a fully supported cluster of lineage A (16S: PP = 0.99; COI + R16S + H3: PP = 1) is nested within a comb of unresolved sequences attributed to lineage B (16S: PP = 0.92; COI + R16S + H3: PP = 1). For the single genes H3 (Figure 6) and S16S (Appendix III, Figure X), on the other hand, specimens of lineage A and B are resolved as one cluster of sequences, being non-supported in H3 (PP = 0.58) and well supported in S16S (PP = 0.97). These findings, in addition to the COI uncorrected genetic pairwise distances of 3.2–5.0 % between lineage A and B, support the possibility of an ongoing process of incipient speciation, but are not yet consistent with complete lineage sorting and the occurrence of two valid species within *J. tomentosa*. Furthermore, the estimated intra-specific distances of lineage A (0.0–0.68 %) and lineage B (0.0–0.26 %) show a greater range compared to *Jorunna* sp. nov. (0.15 %), providing another line of evidence for a possible ongoing process of speciation between lineages A and B (Table 4). Yet, discrete anatomical characters between both lineages remain to be unraveled (Figures 17–25).

There are discrepant observations regarding the number of gills in *J. tomentosa*. For example, Thompson & Brown (1984, p. 219, pl. 21) and Hayward & Ryland (2017, Fig. 10.26), reported 17 branchial leaves in specimens of 40 and 55 mm, yet on their illustrations only nine and 11 leaves are visible. Among the material examined here, a maximum of 14 branchial leaves were counted and assumed to correspond to the maximum number of gills in this species (see Table 5). According to Ev. Marcus (1976) and Camacho-García & Gosliner (2008), the number of denticles on the outermost lateral teeth are a variable character both among and within species of *Jorunna*. This observation was confirmed for both lineages of *J. tomentosa* examined here, either bearing up to eight denticles or having entirely smooth outermost lateral radular teeth.

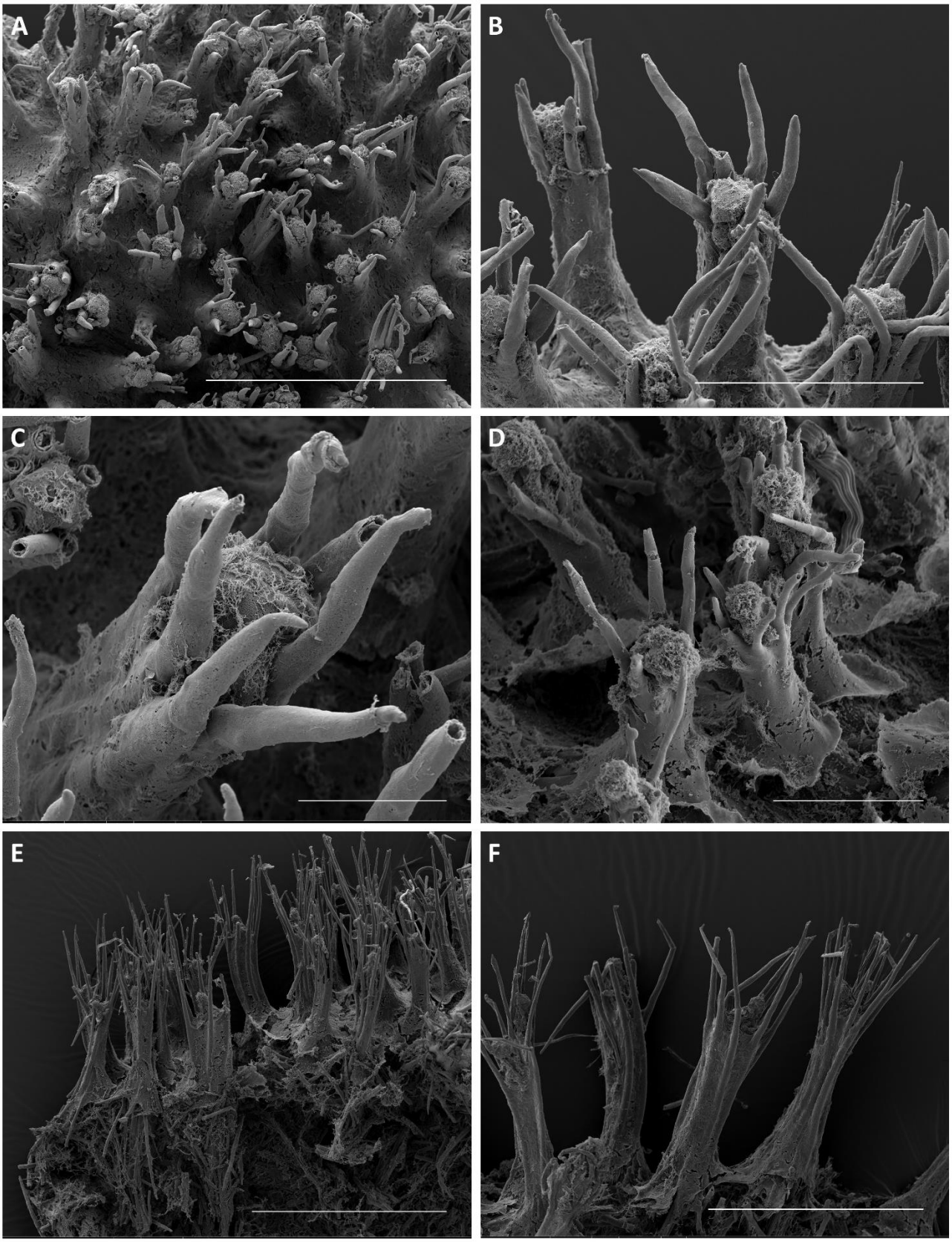

Figure 15. General and detailed views of the caryophyllidia of three specimens of *J. tomentosa* from lineage A and B. **A–C**. Lineage B; Dense caryophyllidia with up to seven spicules surrounding the ciliated knob (NTNU-VM-213). **D**. Lineage B; Detailed view of caryophyllidia (ZMBN 127705). **E+F**. Lineage A; Dense caryophyllidia with long, slender spicules (ZMBN 127711). Scale bars: A = 500 µm, B = 200 µm, C = 50 µm, D = 100 µm, E = 500 µm, F = 300 µm.

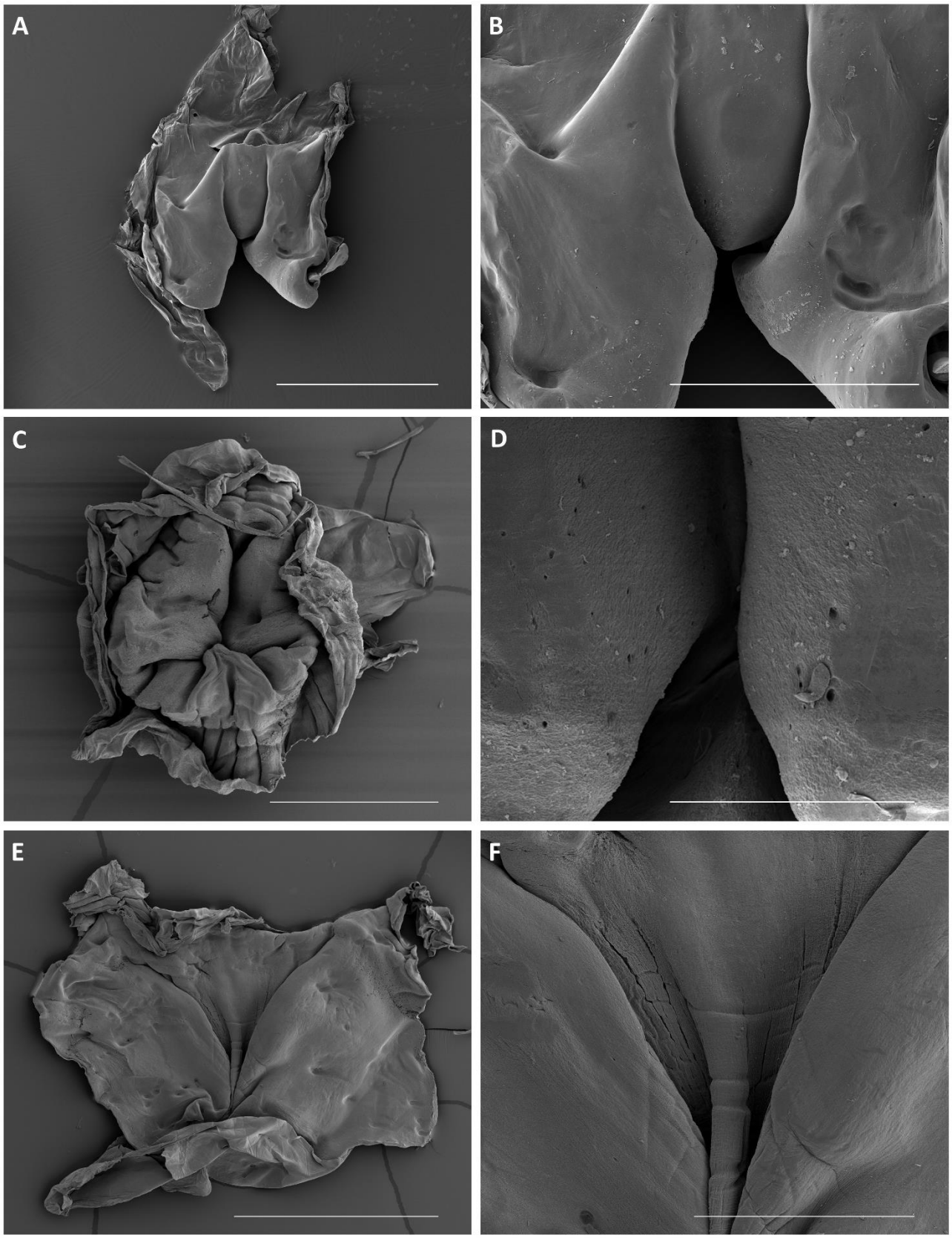

Figure 16. Scanning electron micrographs of labial cuticles of three specimens of *J.tomentosa* from lineage A and B. **A+B**. Lineage A; Opened labial cuticle (ZMBN 127707). **C+D**. Lineage B; Non-opened labial cuticle (ZMBN 87955). **E+F**. Lineage B; Opened labial cuticle (ZMBN 125553). Scale bars: A = 500 µm, B = 100 µm, C = 1 mm, D = 500 µm, E = 1 mm, F = 300 µm.

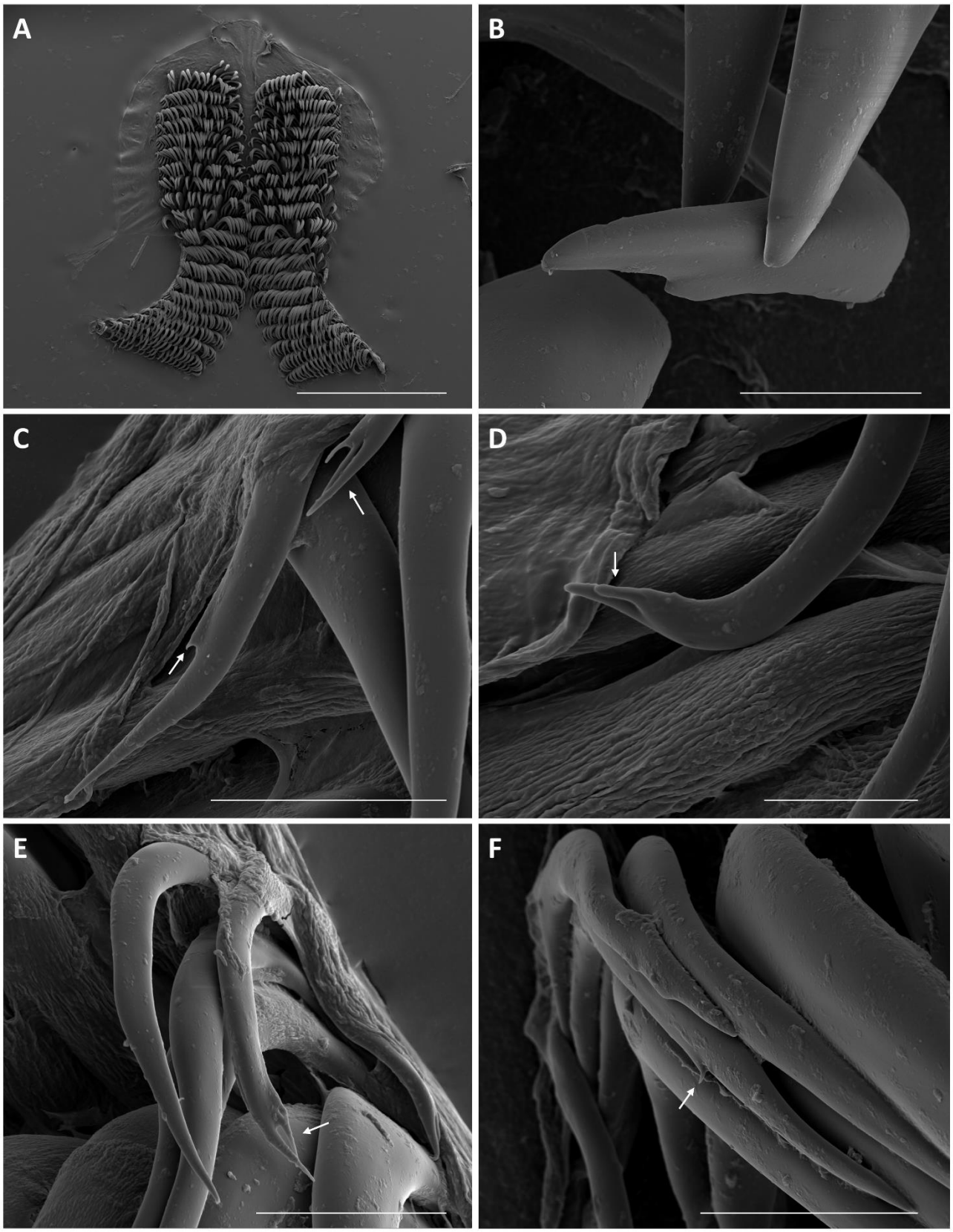

Figure 17. Scanning electron micrographs of *J. tomentosa* A (ZMBN 127710). **A**. General view of the radula (21 x 23.0.23). **B**. Detail of innermost lateral carrying one denticle. **C–F**. Detailed view of outermost sickle-shaped laterals with denticles, being either serrated or bifurcate (indicated with arrows). Scale bars: A = 1 mm, B = 20 µm, C = 20 µm, D = 10 µm, E = 20 µm, F = 20 µm.

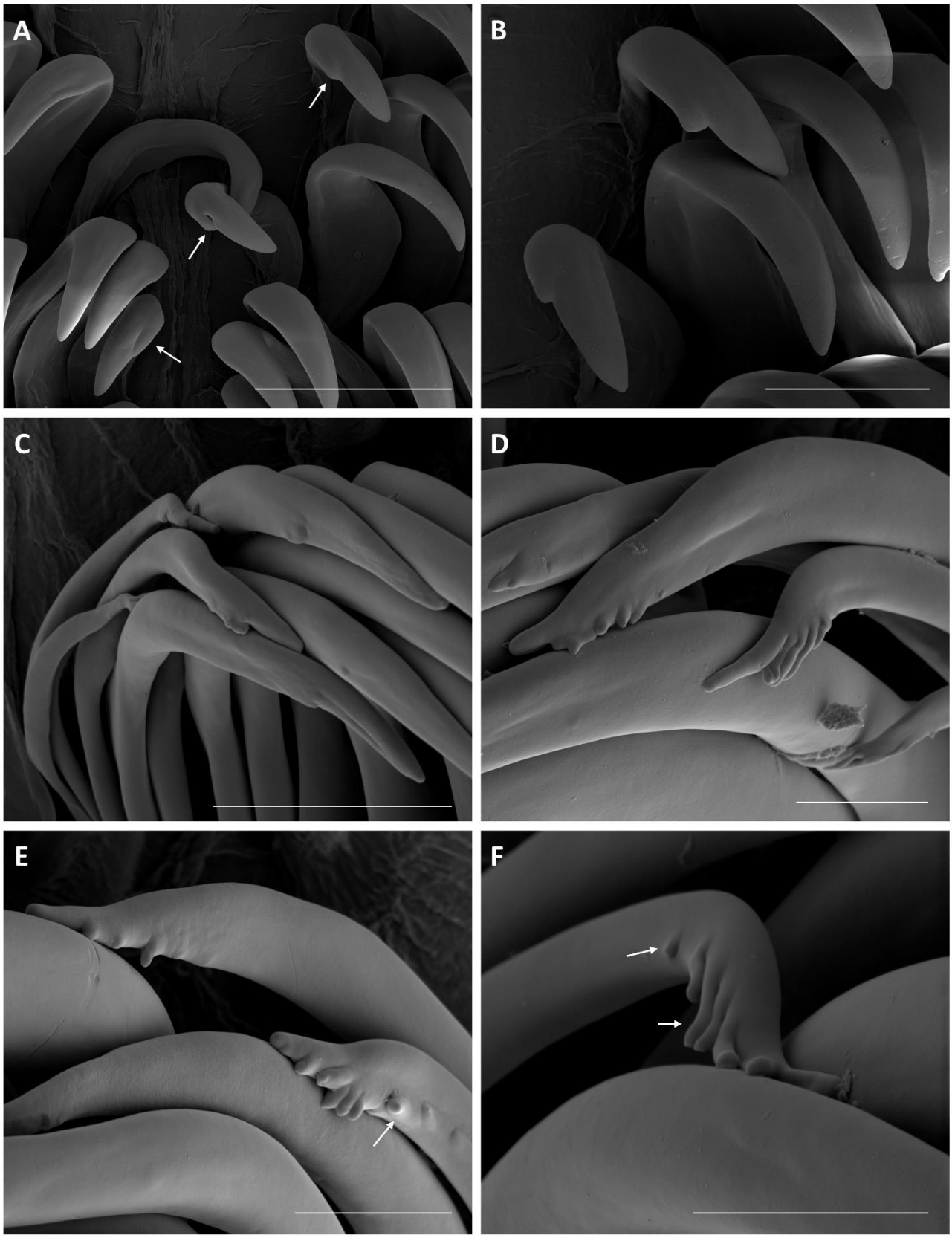

Figure 18. Scanning electron micrographs of *J. tomentosa* B (ZMBN 125038). **A+B**. Detailed view of innermost laterals carrying one denticle (indicated with arrows). **C–F**. Detailed view of outermost lateral teeth with up to eight denticles, being either knob-shaped or fingerlike (indicated with arrows). Scale bars: A = 100 µm, B = 50 µm, C = 30 µm, D = 10 µm, E = 10 µm, F = 10 µm.

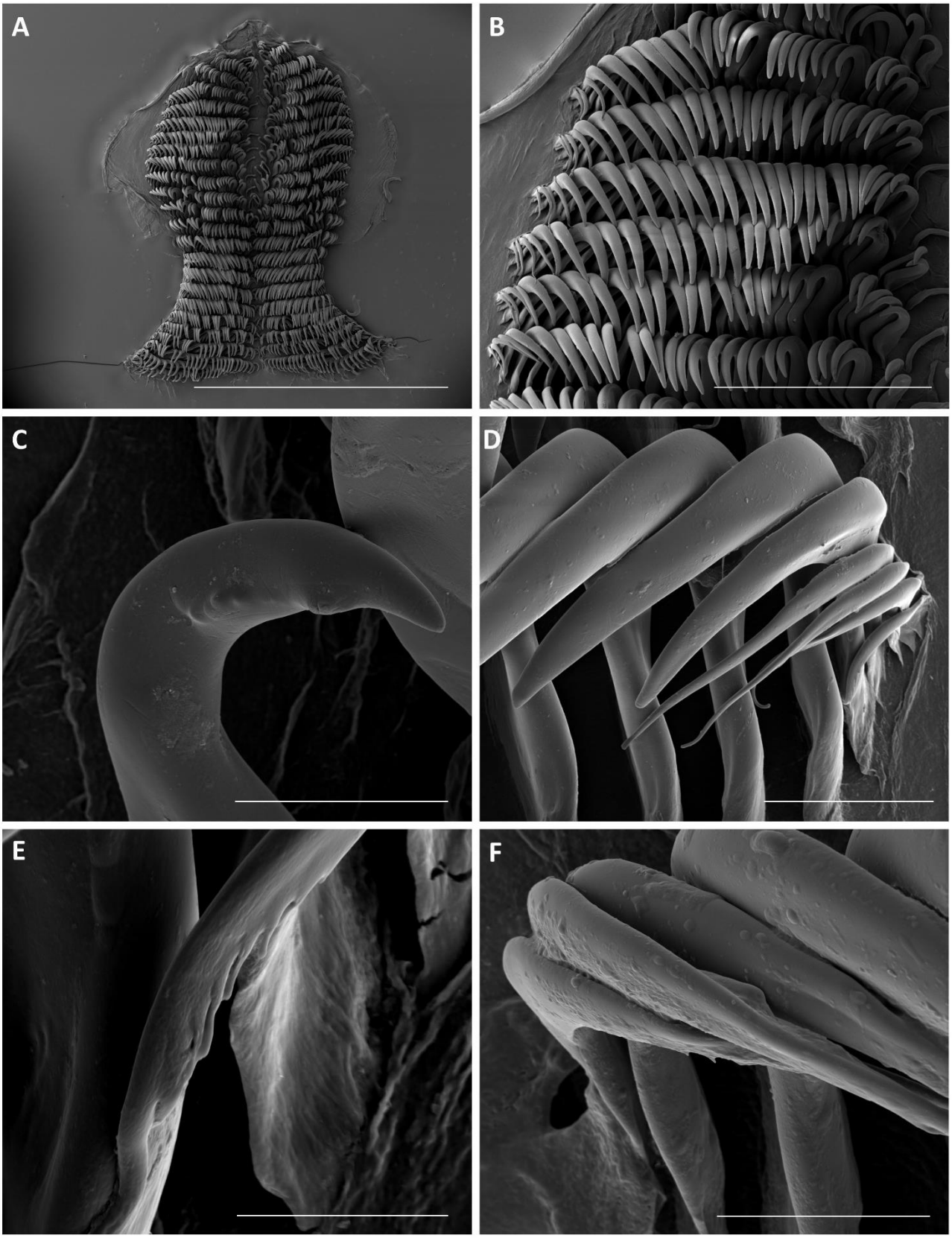

Figure 19. Scanning electron micrographs of *J. tomentosa* B (ZMBN 87955). **A**. General view of the radula (23 x 28.0.28). **B**. General view of the left side with slender outermost and large middle and innermost lateral teeth. **C**. Detailed view of innermost lateral with five knob-shaped denticles. **D**. Detailed view of outermost sickle-shaped laterals. **E**. Outermost lateral with four fingerlike denticles. **F**. Outermost lateral with two small denticles. Scale bars: A = 2 mm, B = 400 µm, C = 20 µm, D = 50 µm, E = 10 µm, F = 10 µm.

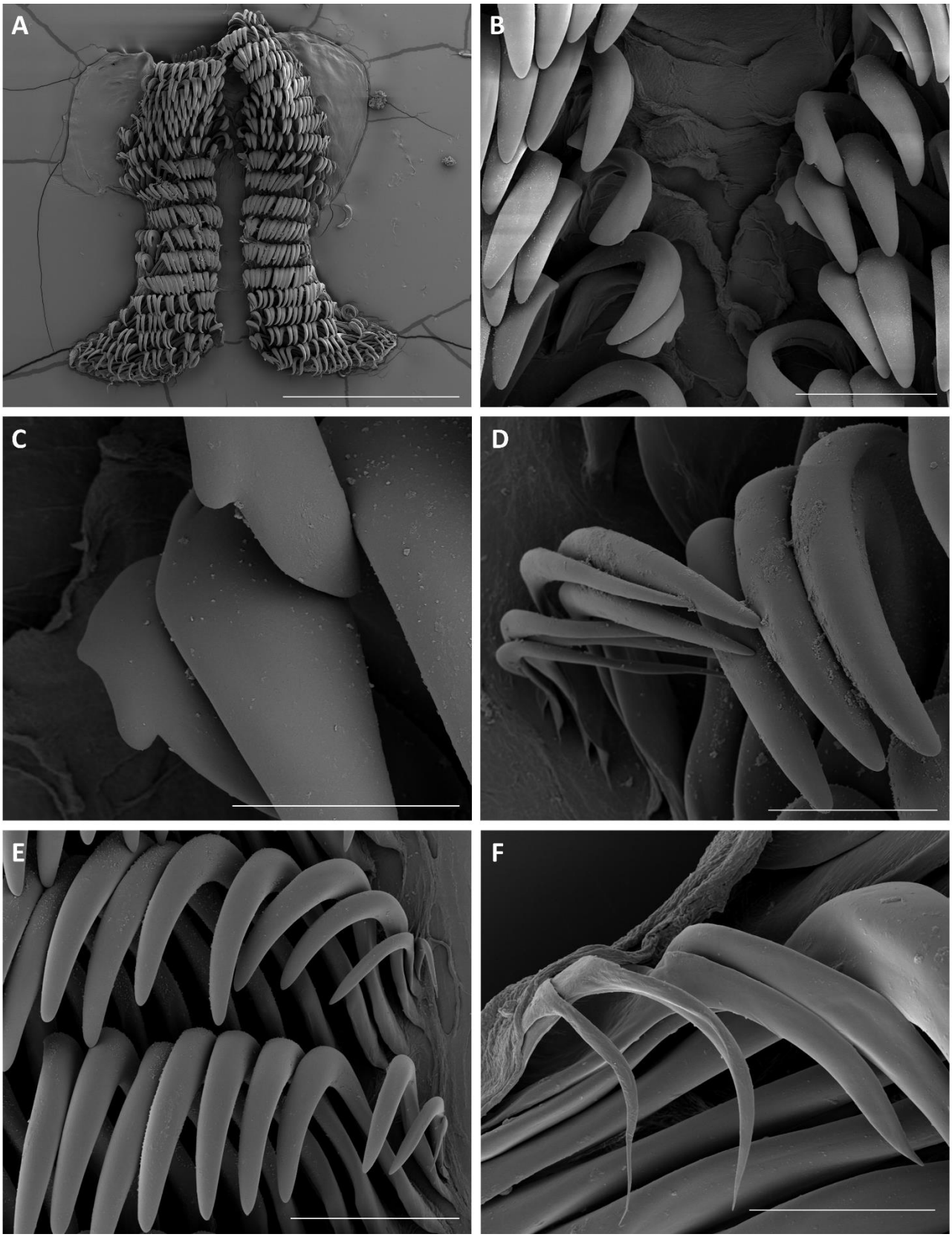

Figure 20. Scanning electron micrographs of *J. tomentosa* B (ZMBN 127603). **A**. General view of the radula (20 x 19.0.19). **B**. Absence of rachidian teeth. Some of the innermost laterals carry one denticle. **C**. Detailed view of innermost laterals with each one denticle **D–F**. Detailed view of outermost sickle-shaped laterals lacking denticles. Scale bars: A = 1 mm, B = 100 µm, C = 40 µm, D = 50 µm, E = 100 µm, F = 30 µm.

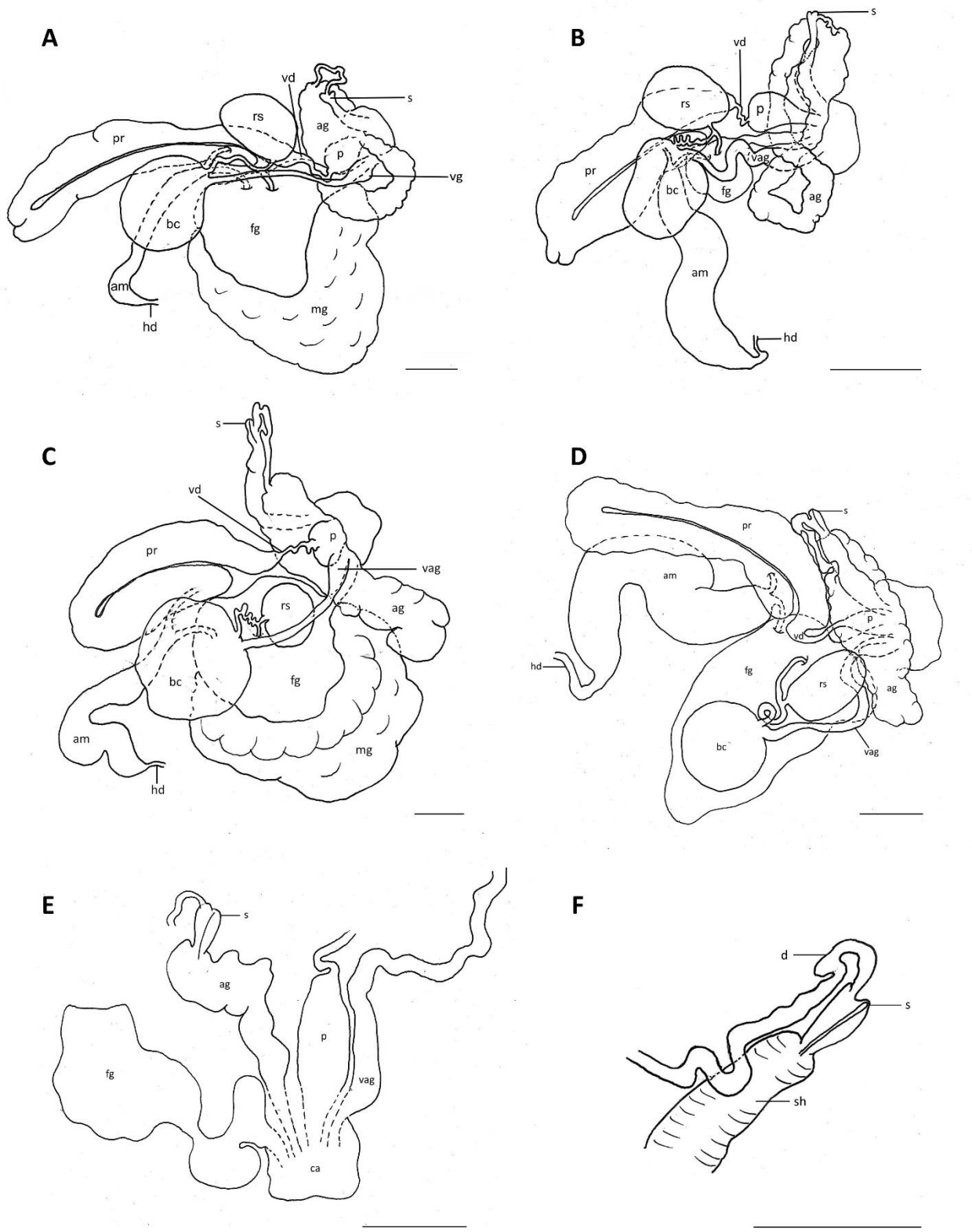

Figure 21. Drawings of the reproductive organs of four specimens of *J. tomentosa* from lineages A and B. **A**. Lineage B; Reproductive system with large mucous gland (ZMBN 87955). **B**. Lineage B; Reproductive system without mucous gland and small female gland (ZMBN 127705). **C**. Lineage A; Reproductive system with large female and mucous glands (ZMBN 127710). **D**. Lineage A; Reproductive system where mucous gland was removed (ZMBN 127711). **E**. Lineage A; Female gland, accessory gland, penis, and vagina converging in the common atrium (ZMBN 127707). **F**. Lineage A; Detailed drawing of muscular spine sheath with attached duct connecting to the accessory gland (ZMBN 127711). Abbreviations: hd = hermaphroditic duct, am = ampulla, bc = bursa copulatrix, rs = seminal receptacle, pr = prostate, fg = female gland, mg = mucous gland, vd = vas deferens, vag = vagina, p = penis, ag = accessory gland, s = copulatory spine, ca = common atrium, sh = spine sheath, d = duct connecting ag with spine sheath. Scale bars = 1 mm.

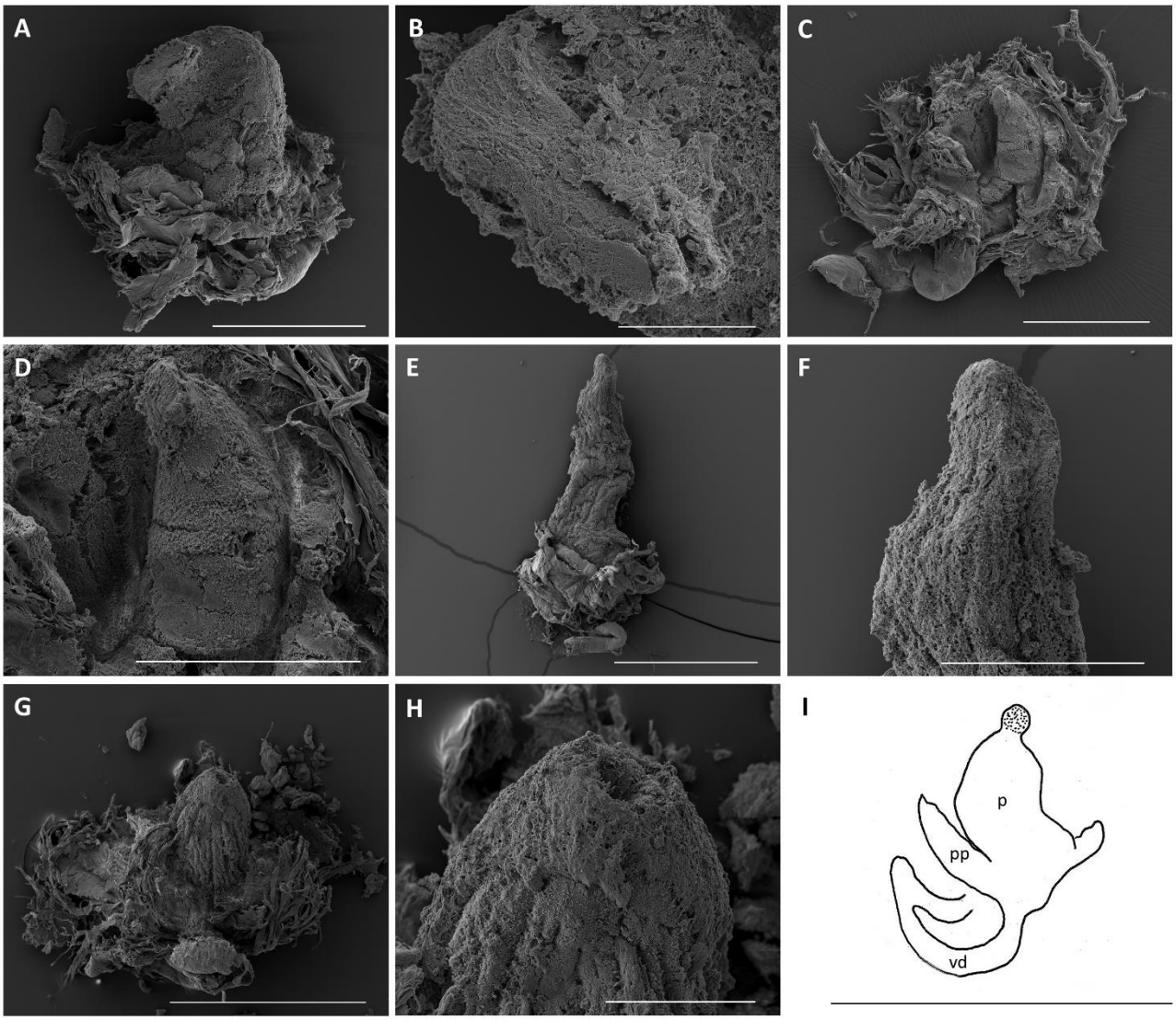

Figure 22. Scanning electron micrographs of penises of four specimens of *J. tomentosa* from lineages A and B. **A+B**. Lineage A; General and detailed view of the penis and the penial tip (ZMBN 127710). **C**. Lineage A; General view of the penis embedded in the penial bulb (ZMBN 127711). **D**. Lineage A; Detailed view of the penis (ZMBN 127711). **E+F**. Lineage B; General and detailed view of the penis and the penial tip (ZMBN 125553). **G+H**. Lineage B; General and detailed view of the penis and the penial tip (ZMBN 87955). **I**. Lineage B; Drawing of the penis (ZMBN 87955) prior to preparation. Here, the penial tip ends in a circular knob which got lost in the process of preparation. Abbreviations: vd = vas deferens, p = penis, pp = tissue of penial bulb. Scale bars: A = 500 µm, B = 100 µm, C = 500 µm, D = 300 µm, E = 1 mm, F = 300 µm, G = 500 µm, H = 100 µm, I = 1 mm.

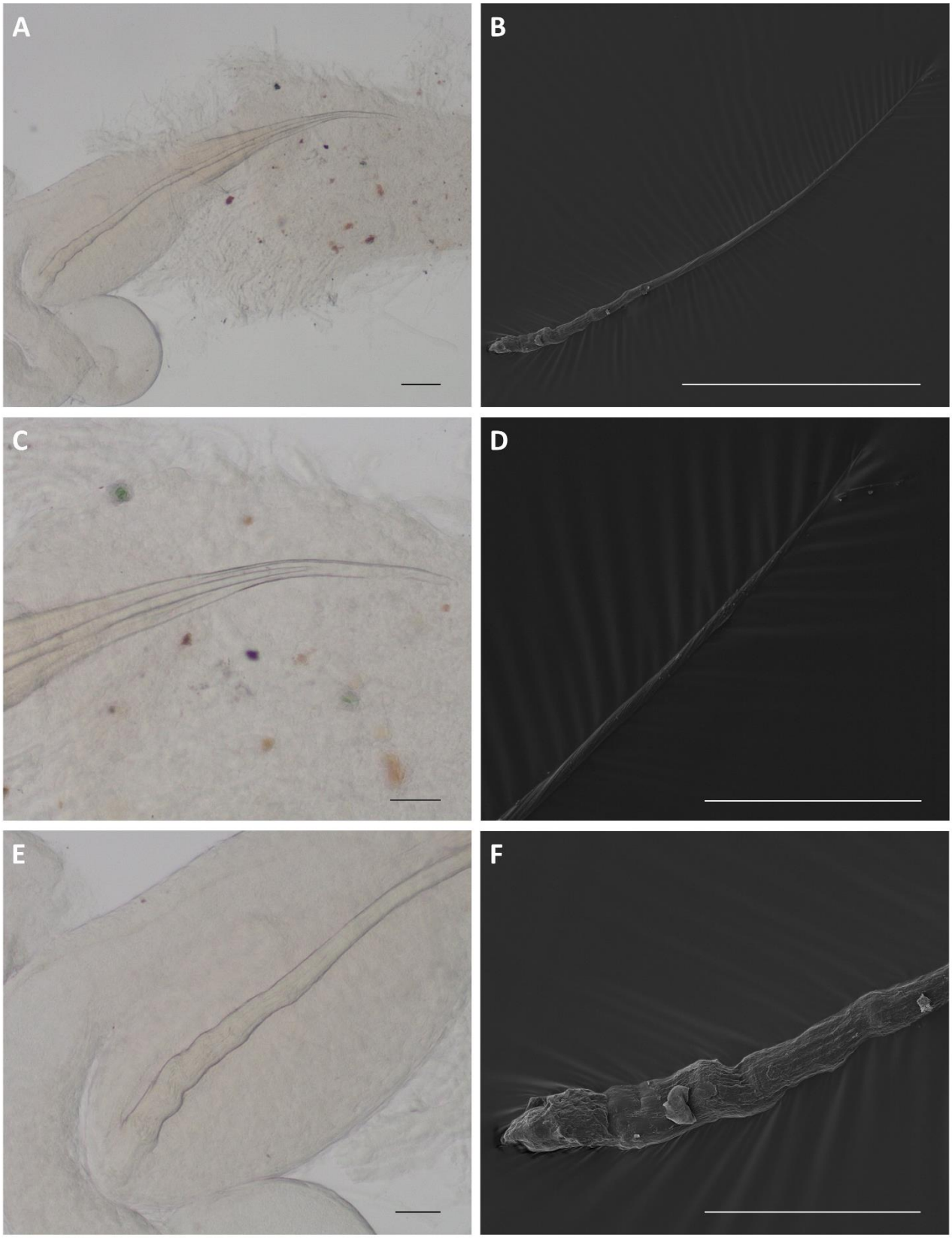

Figure 23. Light microscope images and scanning electron micrographs of the copulatory spine of *J. tomentosa* B (ZMBN 87955). **A+B**. Entire copulatory spine. **C**. Spine tip. Entire spine is embedded within a duct. **D**. Pointed tip of spine. **E+F**. Spine base. Scale bars: A = 100 µm, B = 400 µm, C = 50 µm, D = 100 µm, E = 50 µm, F = 100 µm.

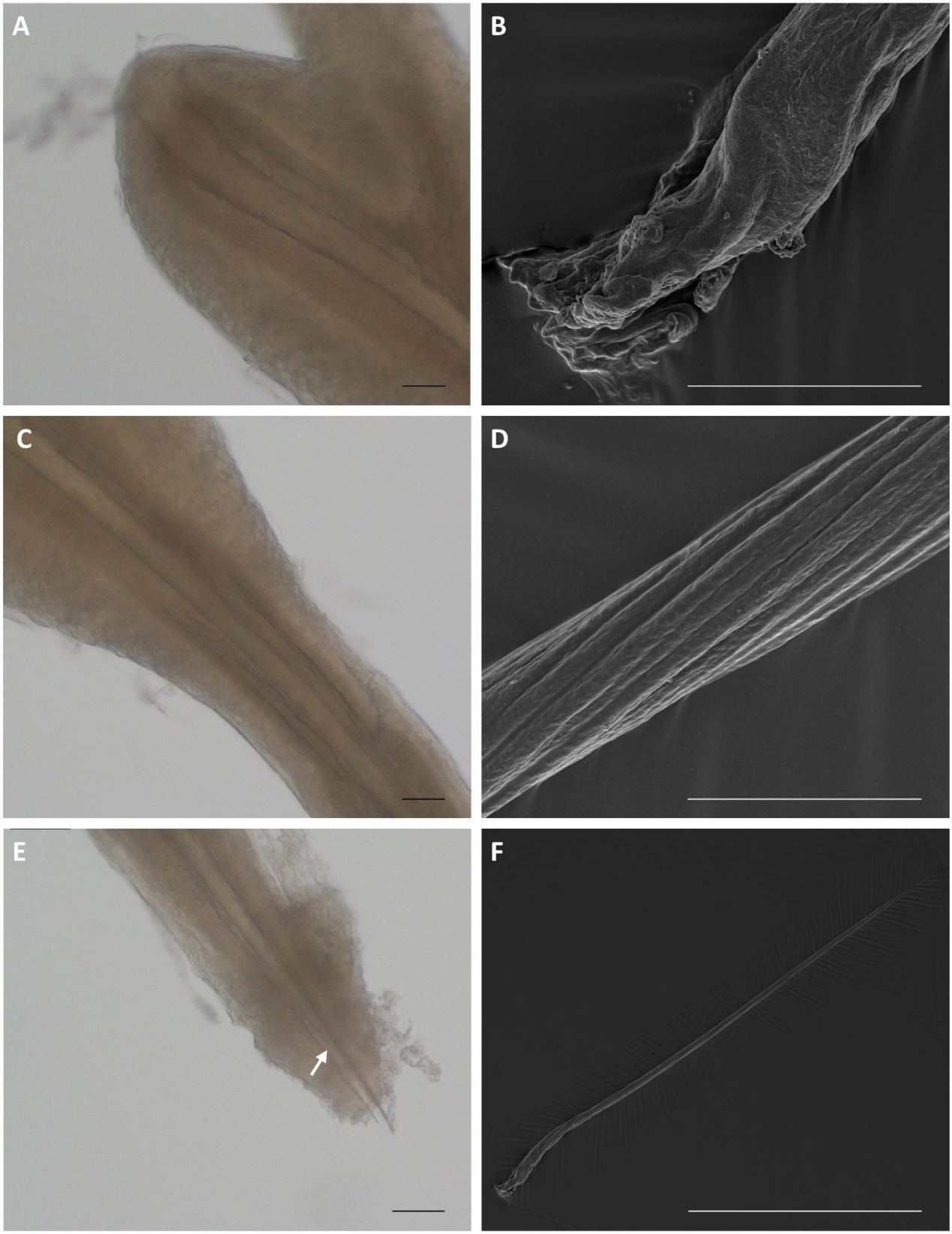

Figure 24. Light microscope images and scanning electron micrographs of the copulatory spine of *J. tomentosa* A (ZMBN 127710). **A**. Base of copulatory spine embedded in tissue. **B**. Detailed view of spine base. **C**. Copulatory spine within the protective spine tunnel, embedded in tissue. **D**. Detailed view of the spine texture. **E**. Tip of the spine tunnel penetrating the tissue embedding the copulatory spine (spine tip indicated with arrow). **F**. Entire copulatory spine. Scale bars: A = 50 µm, B = 50 µm, C = 50 µm, D = 30 µm, E = 50 µm, F = 500 µm.

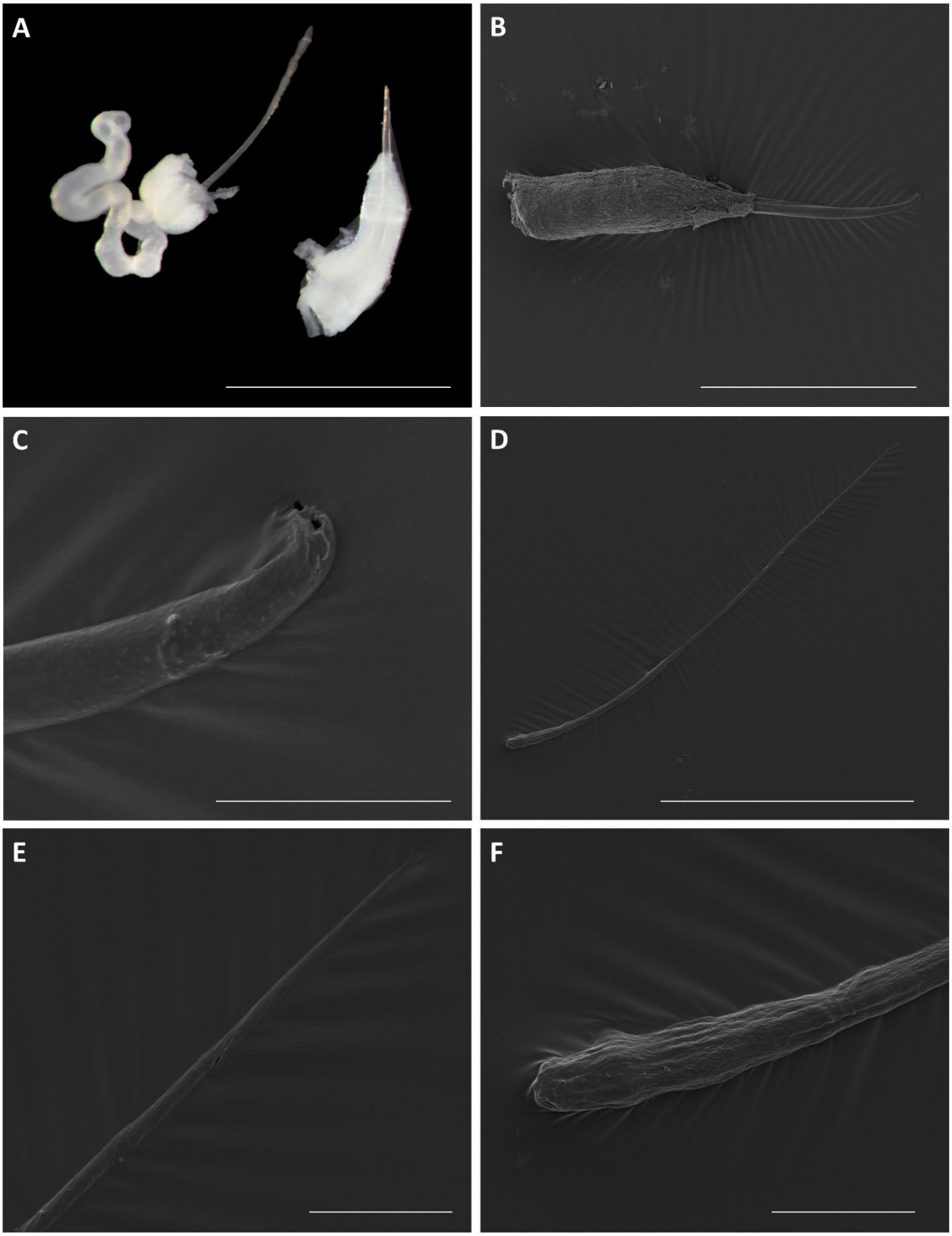

Figure 25. Light microscope image and scanning electron micrographs of the copulatory spine structures of *J. tomentosa* B (ZMBN 127705). **A**. Left: Copulatory spine with tissue from spine sheath connected to duct leading to the accessory gland. Right: Protective spine tunnel within which spine is situated. **B**. General view of spine tunnel. **C**. Detailed view of spine tunnel tip with opening for the copulatory spine to be ejected through. **D**. Entire copulatory spine. **E**. Pointed tip of copulatory spine. **F**. Rounded base of copulatory spine. Scale bars: A = 300 µm, B = 300 µm, C = 30 µm, D = 500 µm, E = 50 µm, F = 50 µm.

Jorunna sp. nov.

(Figures 9–10; 26–33)

Material examined

Norway: Skogsøya, Frøya, Trøndelag (63.845076, 8.631778), 1 spc., sequenced and dissected, TL = 15 mm (fixed), NTNU-VM-58891. Brattøya, Kristiansund, Møre og Romsdal (63.062076, 7.695494), 1 spc., sequenced and dissected, TL = 40 mm (fixed), ZMBN 127749. North Sea (60.726944, 0.505371), 1 spc., sequenced and dissected, TL = 30 mm (fixed), ZMBN 125946.

Diagnosis

Background colour yellow to white; caryophyllidia uniform, densely arranged; notum speckled with irregularly distributed brown spots of various size and number. Mantle glands present. Rhinophores with 9–12 lamellae, lacking pigmentation. Nine to 14 gills slightly brighter than background colour, lacking pigmentation. Oral tentacles digitiform. Radular formula 19–25 x 21–18.0.18–21. Three to six slender, sickle-shaped outermost smooth lateral teeth. Labial cuticle smooth.

External morphology (Figures 10, row 1; 26–27)

TL = 15–40 mm. Dorsum yellow to white speckled with irregularly distributed brown spots; Rhinophores with 9–12 lamellae, slightly brighter than dorsum, lacking pigmentation. Nine to 14 bi- to tripinnate gills, slightly brighter than dorsum, encircling anal pore. Foot of same colour as dorsum, somewhat pointed at end. Oral tentacles of same colour as foot, digitiform.

Labial cuticle (Figure 28)

Labial cuticle smooth.

Radula (Figures 29–30)

Radular formula of smallest studied specimen 19 x 18.0.18 (TL = 15 mm, NTNU-VM-58891), medium-sized specimen 25 x 20.0.20 (TL = 30 mm, ZMBN 125946), and largest specimen 23 x 21.0.21 (TL = 40 mm, ZMBN 127749). Radula broad. Rachidian tooth absent; lateral teeth simple, hook-shaped with broad base and rounded cusp; mid lateral teeth larger than inner laterals; inner laterals lacking denticles; Three to six slender, smooth, sickle-shaped outermost laterals.

Reproductive system (Figures 31–33)

Hermaphroditic duct slender. Ampulla long, curved, varying in shape; divided into short oviduct entering upper mass of female gland and connective duct entering prostate. Prostate large, tubular, differentiated into two portions; narrows into long deferent duct leading to penial bulb situated within common atrium. Penis smooth, with rounded base and elongated tip. Vagina long, wider than deferent duct, without hooks; entering common atrium. Bursa copulatrix rounded, slightly larger than seminal receptacle. Seminal receptacle connected to bursa copulatrix by short duct. Uterine duct thin, connecting distally with female gland mass. Female gland mass enters common atrium. Accessory gland large, convoluted; emerges into long, coiled duct connecting to heart-shaped ovate sac bearing a long copulatory spine with rounded base; ovate sac embedded in muscular pouch emptying into common atrium; copulatory spine held in a lining membrane forming a protective sheath, protruding from posterior end of ovate sac beyond tip of spine.

Ecology (Figure 26A)

Little is known about the ecology of this new species. The *in-situ* image depicts one specimen crawling on a sponge growing in between tubes of the Family Sabellidae Latreille, 1825 and small ascidians. The sponge resembles *Halichondria* sp., which would suggest a dietary overlap with *J. tomentosa*, however, the poriferan species is not confirmed. The depth range is recorded from 27 m to about 350 m (present study), overlapping with the depth range of *J. tomentosa* (Grieg, 1912; Cordeiro *et al.*, 2015).

Distribution (Figure 9)

The species is confirmed from three localities along the western coast Norway; from Frøya in Trøndelag, Kristiansund in Møre og Romsdal, and North Sea offshore grounds (60.726944; 0.505371).

Remarks

Externally, *Jorunna* sp. nov. differs from the two lineages *J. tomentosa* A and *J. tomentosa* B by having a plain notal background colour accompanied by small, irregularly placed brown spots (Figure 10, row 1; Figure 26). The examined radulae carried less teeth per row compared to specimens of equal body length from *J. tomentosa* lineage A and B (Figures 17–20, 29–30). None of the examined specimens of *Jorunna* sp. nov. carried denticles on the outermost lateral teeth. Denticulation on either innermost or outermost lateral teeth was detected in six of eight

studied radulae of *J. tomentosa* A and B. In two specimens from lineage B, however, denticles on the outermost teeth were absent (Figure 20). The vagina and the deferent duct of *Jorunna* sp. nov. were found to be longer compared to *J. tomentosa* A and B (Figs. 21, 31). The copulatory spines in *Jorunna* sp. nov. were measured to 1.6 mm and 1.7 mm in specimens of 3 cm and 4 cm length, respectively. In lineage A and B, individuals ranging from 2 cm to 3 cm were carrying spines of 550 µm to 1.1 mm, being 600 µm shorter compared to those in *Jorunna* sp. nov. (Appendix IV, Table B). Given the genetic difference of 9.0–12.3% to *J. tomentosa* (Table 4), the new species can be categorized as being pseudo-cryptic by depicting subtle but detectable morphological differences (Korshunova *et al.*, 2017). Besides the distinct notal coloration pattern that is detected so far, the differences in the reproductive system are considered good characters for species delimitation. This is implicit in the Phylogenetic Species Concept for sympatric species where the phylogenetic structure is assumed to be attained by lack of interbreeding, followed by lineage sorting over time.

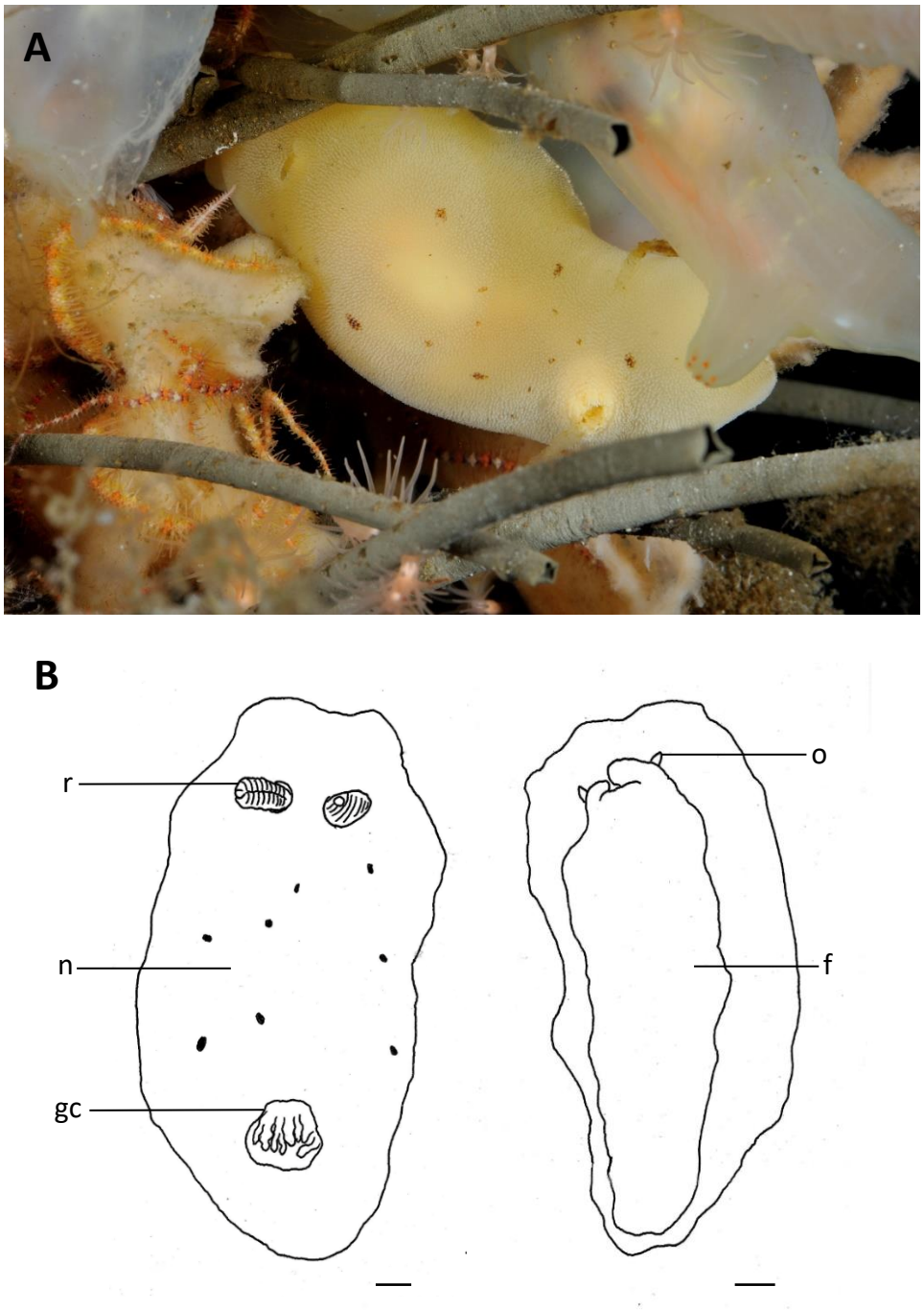

Figure 26. A. *In-situ* photograph of *Jorunna* sp. nov. from Brattøy, Kristiansund, Møre og Romsdal, Norway, ZMBN 127749, photo by N. Aukan, 2018. **B.** Drawing of external morphology of *Jorunna* sp. nov., NTNU-VM-58891. Abbreviations: r = rhinophore; n = notum; gc = gill circlet; o = oral tentacle; f = foot. Scale bars = 1 mm.

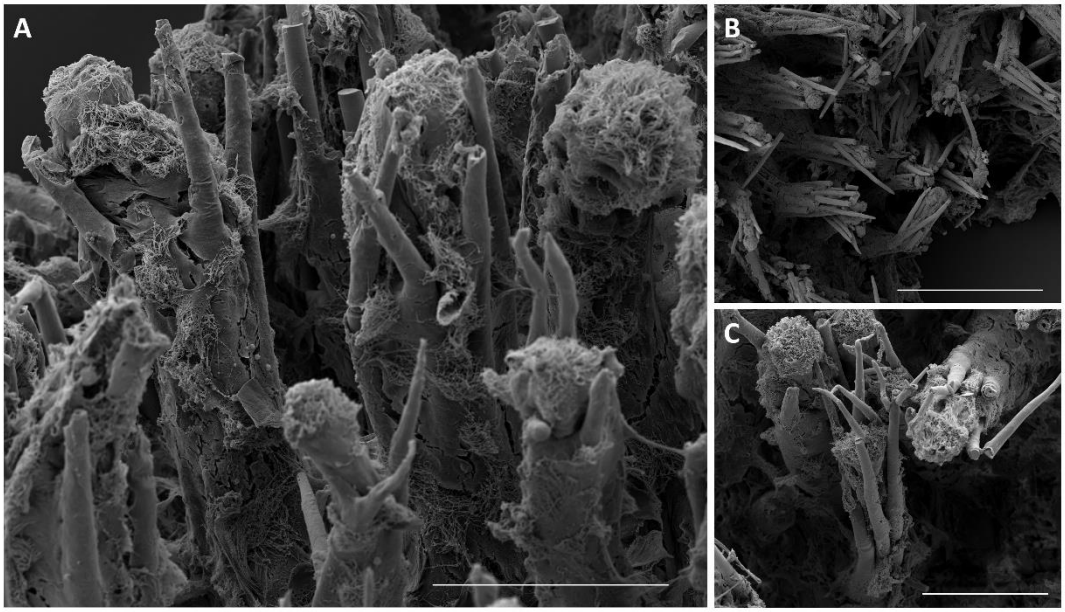

Figure 27. Scanning electron micrographs of caryophyllidia of *Jorunna* sp. nov.. **A**. Detailed view of densely spaced caryophyllidia (NTNU-VM-58891). **B**. General view of slightly damaged caryophyllidia (ZMBN 127749). **C**. Detailed view of spicules surrounding the ciliated tubercle (NTNU-VM-58891). Scale bars: A = 500 µm, B = 100 µm, C = 100 µm.

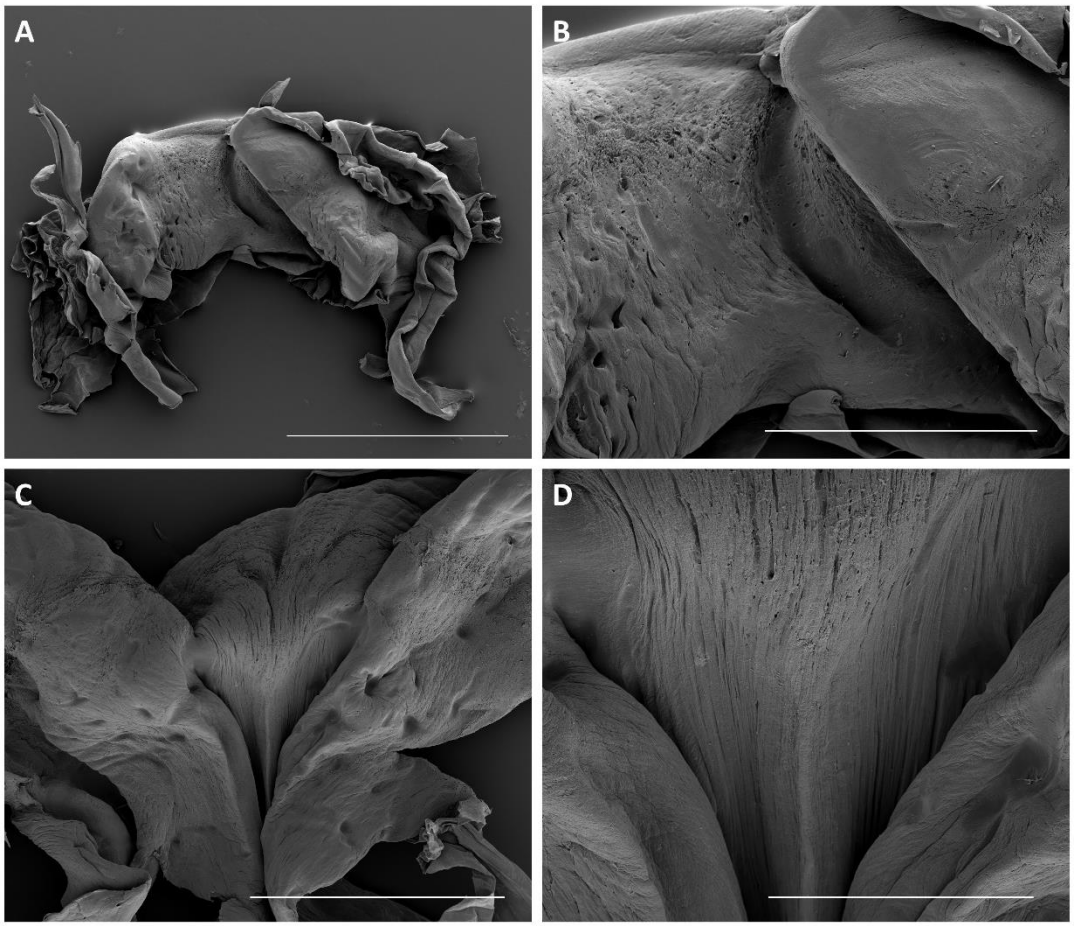

Figure 28. Scanning electron micrographs of labial cuticles of *Joruna* sp. nov.. **A+B**. General and detailed view of labial cuticle (ZMBN 125946). **C+D**. General and detailed view of labial cuticle (ZMBN 127749). Small indentations caused by forceps. Scale bars: A = 1 mm, B = 400 µm, C = 1 mm, D = 300 µm.

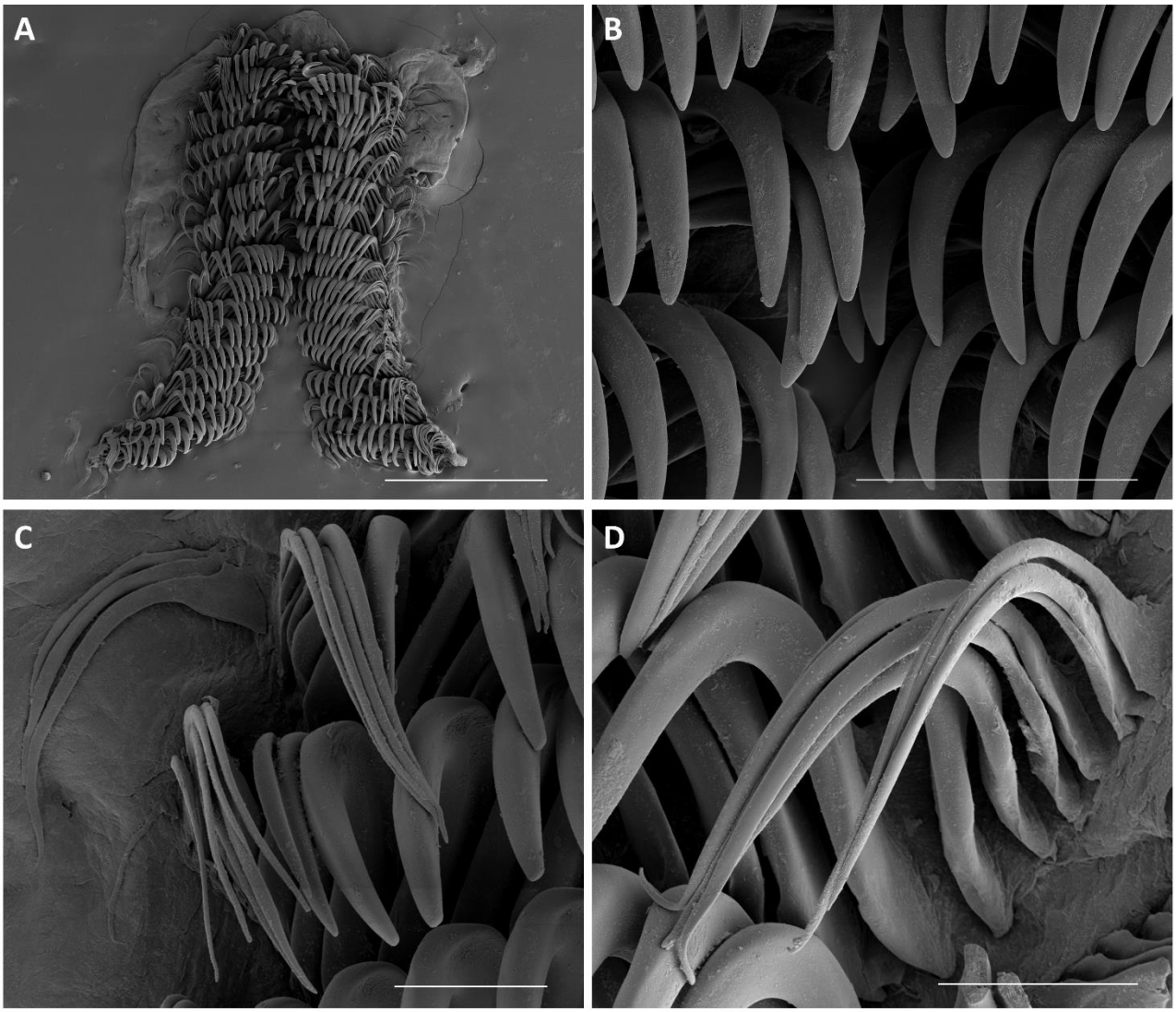

Figure 29. Scanning electron micrographs of *Jorunna* sp. nov. (NTNU-VM-58891). **A**. General view of radula (19 x 18.0.18). **B**. Homogenous innermost lateral teeth without denticles. **C+D**. Detailed view of outermost sickle-shaped laterals lacking denticles. Scale bars: A = 500 µm, B = 100 µm, C = 50 µm, D = 50 µm.

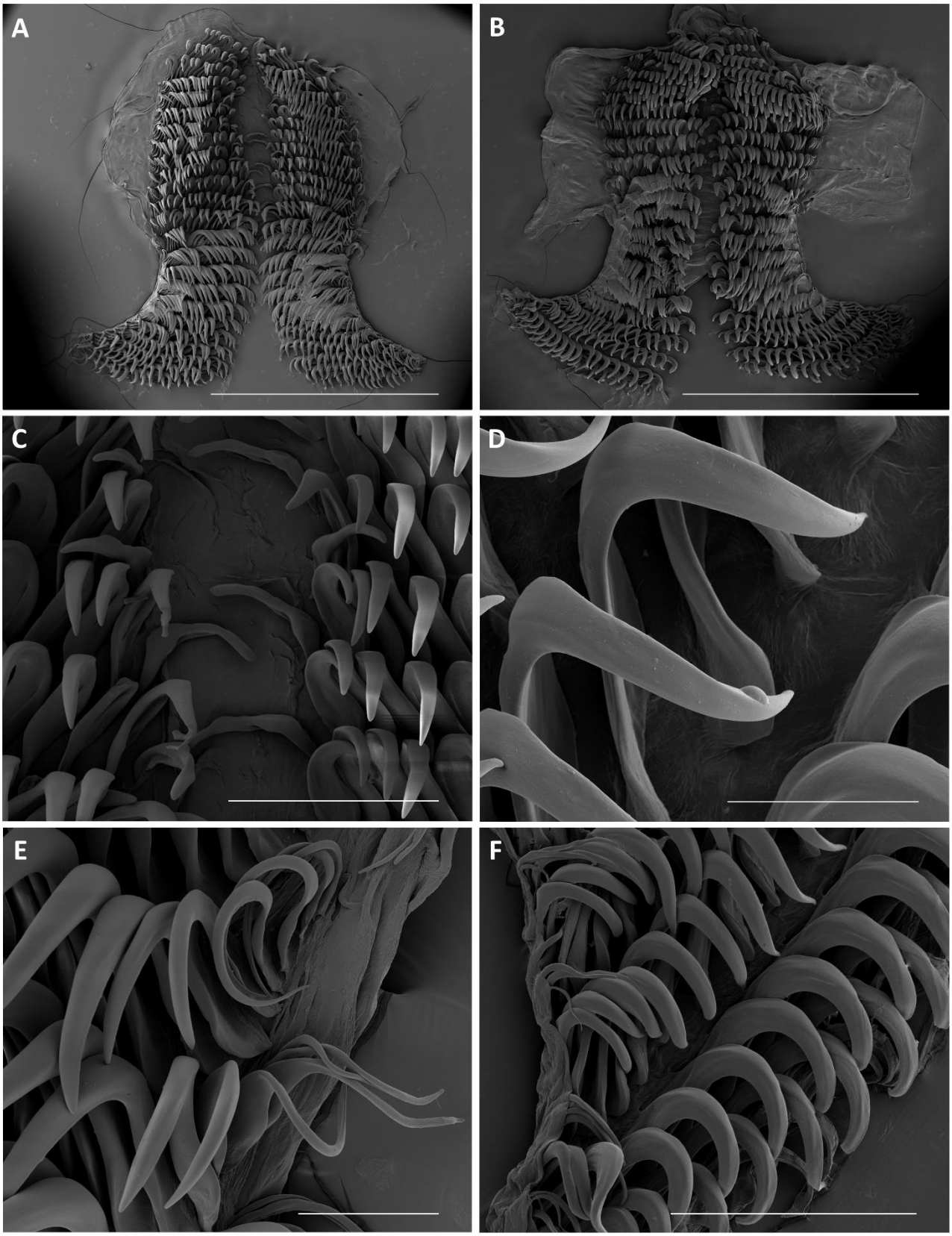

Figure 30. Scanning electron micrographs of *Jorunna* sp. nov.. **A**. General view of radula (25 x 20.0.20) (ZMBN 125946). **B**. General view of radula (23 x 21.0.21) (ZMBN 127749). **C**. Detailed view of innermost lateral teeth without denticles. Rachidian tooth absent (ZMBN 125946). **D**. Detailed view of single case of innermost lateral with swelling (ZMBN 127749). **E**. Detailed view of outermost lateral teeth without denticles (ZMBN 125946). **F**. Outermost lateral teeth without denticles (ZMBN 127749). Scale bars: A = 2 mm, B = 2 mm, C = 300 µm, D = 100 µm, E = 100 µm, F = 300 µm.

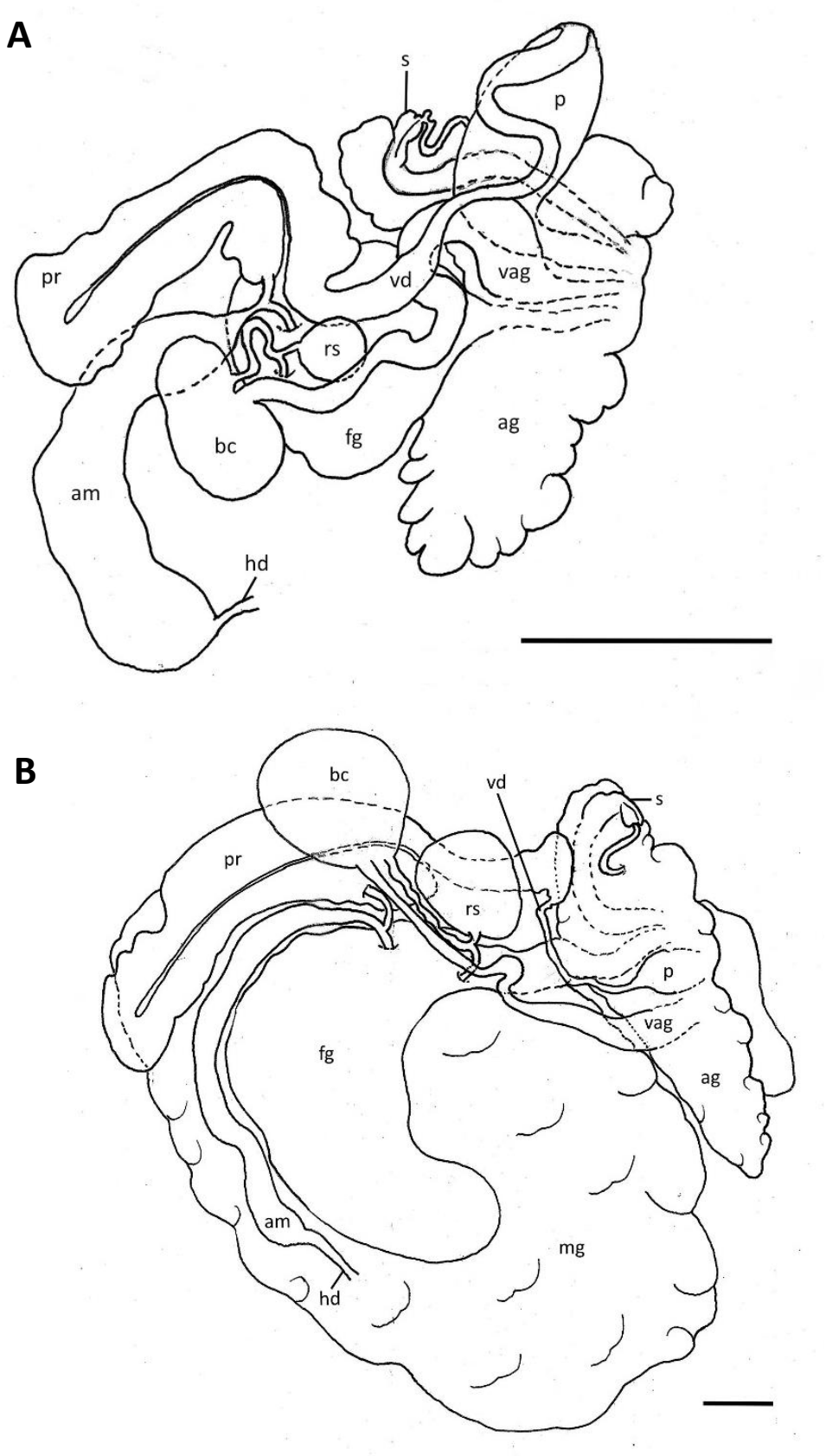

Figure 31. Drawings of the reproductive systems of *Jorunna* sp. nov.. **A**. Reproductive system without mucous gland (NTNU-VM-58891). **B**. Reproductive system with mucous gland (ZMBN 127749). Abbreviations: hd = hermaphroditic duct; am = ampulla; bc = bursa copulatrix; rs = seminal receptacle; pr = prostate; fg = female gland; mg = mucous gland; vd = vas deferens; vag = vagina; p = penis; ag = accessory gland; s = copulatory spine. Scale bars = 1 mm.

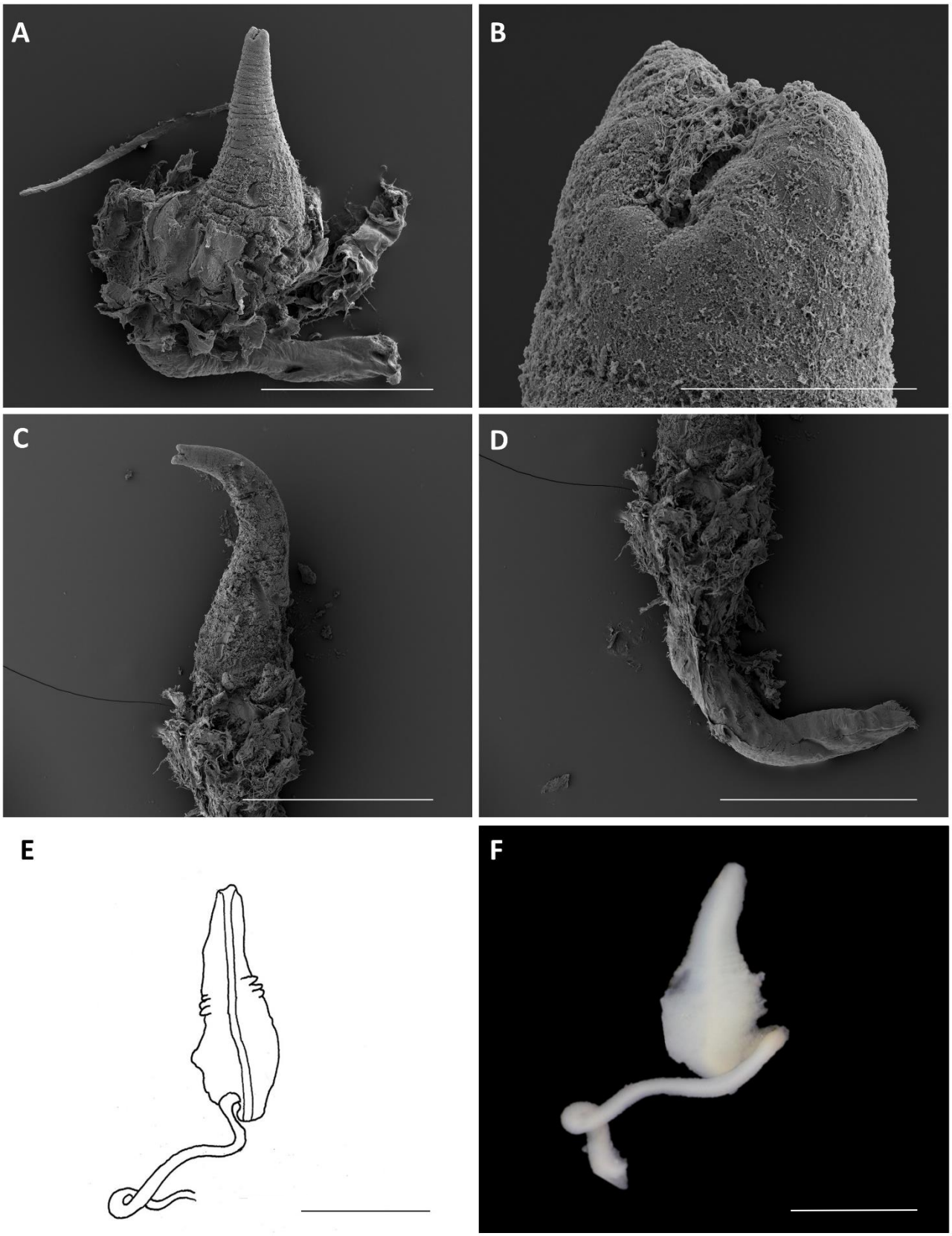

Figure 32. Scanning electron micrographs of penial structures of *Jorunna* sp. nov.. **A**. General view of penis (NTNU-VM-58891). **B**. Detailed view of penial tip (NTNU-VM-58891). **C**. General view of penis (ZMBN 127749). **D**. Detailed view of penial bulb tissue and deferent duct. **E**. Drawing of penis with deferent duct (ZMBN 125946). **F**. Light microscope image of penis with deferent duct (ZMBN 125946). Scale bars: A = 500 µm, B = 50 µm, C = 1 mm, D = 1 mm, E = 1 mm, F = 1 mm.

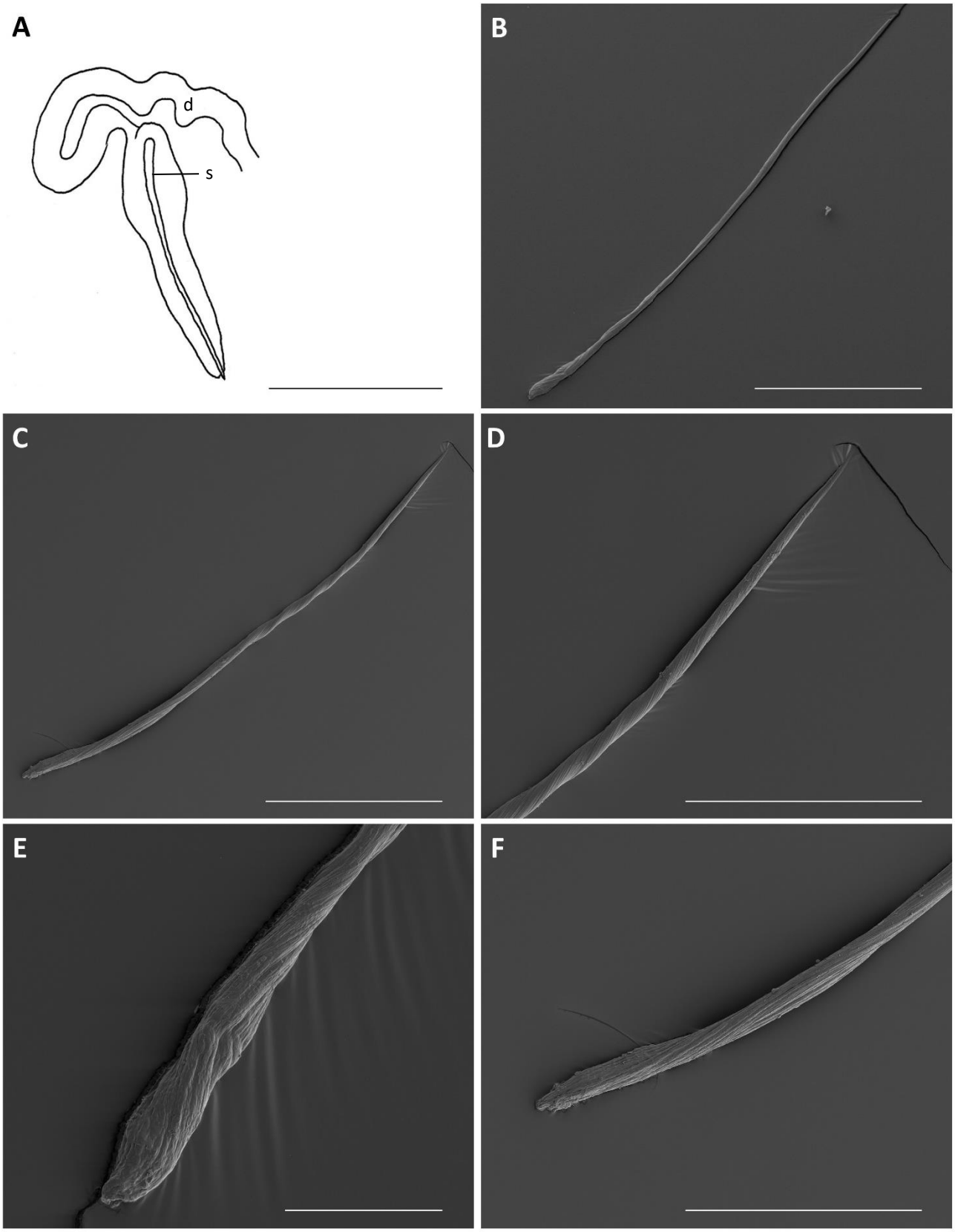

Figure 33. Scanning electron micrographs of copulatory spines of *Jorunna* sp. nov.. **A**. Drawing of spine embedded in tissue with attached duct connecting with the accessory gland (ZMBN 125946). **B**. Entire copulatory spine (ZMBN 127749). **C**. Entire copulatory spine (ZMBN 125946). **D**. Upper part of copulatory spine (ZMBN 125946). **E**. Base of copulatory spine (ZMBN 127749). **F**. Base of copulatory spine (ZMBN 125946). Abbreviations: d = duct connecting with the accessory gland; s = copulatory spine. Scale bars: A = 1 mm, B = 500 µm, C = 500 µm, D = 300 µm, E = 100 µm, F = 300 µm.

4.3 Generic assessment of *Gargamella lemchei*

Ev. Marcus (1976) justified the separation of *J. tomentosa* and *J. lemchei* as different species due to the presence of spines in the male atrium and on the penial papilla. Lemche (see Ev. Marcus, 1976: 53) pointed out differences in the shape of the caryophyllidia between these two species; conical in *J. lemchei* and cylindrical in *J. tomentosa*. However, Ev. Marcus (1976) was unable to recognize such differences and stated that *J. lemchei* is externally indistinguishable from *J. tomentosa* despite the lack of notal spots on a cream-coloured mantle which she mentioned in the species description. In addition, Ev. Marcus (1976) referred to the absence of denticulation on the outermost lateral teeth in *J. lemchei* but at the same time mentioned the irregular occurrence of this character in *J. tomentosa*.

Thompson & Brown (1984) considered *J. lemchei* a synonym of *J. tomentosa*, stating that their studied specimens from Western Ireland are indistinguishable in habits, external morphology, and internal anatomy. However, they acknowledged the absence of dorsal spots which are characteristic for *J. tomentosa*. In their work it is not clear whether their studied specimens are the same as those studied by Ev. Marcus (1976) and the authors did not discuss the presence of penial hooks. Just & Edmunds (1985) presented their findings on a new specimen of *J. lemchei*, in addition to two specimens previously studied by Ev. Marcus (1976), and justified its separation from *J. tomentosa* based on the different coloration pattern without notal spots and the differences in the reproductive system. Based on literature data, Valdés & Gosliner (2001) and Camacho-García & Gosliner (2008) accepted the valid taxonomic status of *J. lemchei* because of the presence of large penial hooks and absence of denticulation on the outermost lateral teeth.

Due to the fact that no other species of *Jorunna* carry penial hooks, Ortea *et al.* (2014) proposed the generic reassignment of *J. lemchei* to the genus *Gargamella*, which remains as the accepted combination name (MolluscaBase, 2020g). Overall, the genera *Jorunna* and *Gargamella* share morpho-anatomical characters such as a dorsum covered with dense caryophyllidia, fully retractable rhinophores and gills, a grooved and notched anterior part of the foot, simple radular teeth, and the absence of rachidian teeth. Their prostate is large and clearly differentiated and their accessory gland is lobate (Table 5) (Bergh, 1894; Perrone, 1986; Garovoy, Valdés & Gosliner, 1999; Moro & Ortea, 2015). In fact, the morpho-anatomical characters shared between these genera are so similar that this over time lead to species being reassigned back and forth. For example, not only *J. lemchei* was moved to *Gargamella* (Ortea *et al.*, 2014), but also *Gargamella novozealandica* Eliot, 1907 was synonymized with *J. pantherina*

(MolluscaBase, 2020h). Despite the shared morpho-anatomical features, all considered valid species of *Gargamella* [*G. immaculata* Bergh, 1894 (type species); *G. blokoverdensis* Moro & Ortea, 2015; *G. bovina* Garovoy, Valdés & Gosliner, 1999; *G. gravastella* Garovoy, Valdés & Gosliner, 1999; *G. perezi* (Llera & Ortea, 1982); *G. wareni* Valdés & Gosliner, 2001] differ from *Jorunna* by possessing either penial or vaginal hooks, or a combination of both. The species *G. lemchei* carries penial hooks (Table 5).

To test the generic position of *G. lemchei* (type locality: Ballyvaughan Bay, Western coast of Ireland), four specimens from Connemara, located near the type locality, were included in this study (Table 2). The phylogenetic analysis showed that all four grouped with specimens of lineage B (Figures 4–8). Their coloration pattern varies from pale yellow to grey-white and all but one carry 2–5 larger brown blotches (Figure 34B–D). In comparison to the morphotype of *G. lemchei*, which lacks these blotches (Figure 35, Table 5) (Ev. Marcus, 1976; Thompson & Brown, 1984; Just & Edmunds, 1985), only one specimen in this study (ZMBN 127714; Figure 34A) depicts a comparable external morphology. In the dissected specimen from Connemara (ZMBN 127705; Figure 34D) no penial hooks were found. This finding is concordant with all other examined specimens in this study and suggests the absence of *G. lemchei* among the studied dataset, considering the presence of penial hooks as a distinctive anatomical character for this species.

A structure present in all examined specimens was the copulatory spine (Figures 23–25). According to Ev. Marcus (1976), *J. lemchei* is equipped with a copulatory spine, too (referred to as vestibular stylet of 500 µm length; Ev. Marcus, 1976, p. 52, fig. 47). In *Gargamella*, however, none of the recognized valid species carry a copulatory spine (Ortea, Pérez & Llera, 1982; Bergh, 1894; Garovoy, Valdés & Gosliner, 1999; Valdés & Gosliner, 2001; Moro & Ortea, 2015). Accordingly, *G. lemchei* represents the first species of *Gargamella* bearing a copulatory spine. Only a future phylogenetic study including specimens of the rare *G. lemchei* can eventually shed light on the correct generic assignment of this enigmatic dorid nudibranch.

Figure 34. Live images of the general morphology of *J. tomentosa* lineage B from Connemara, Western Ireland. **A**. ZMBN 127714. **B**. ZMBN 127713. **C**. ZMBN 127715. **D**. ZMBN 127705.

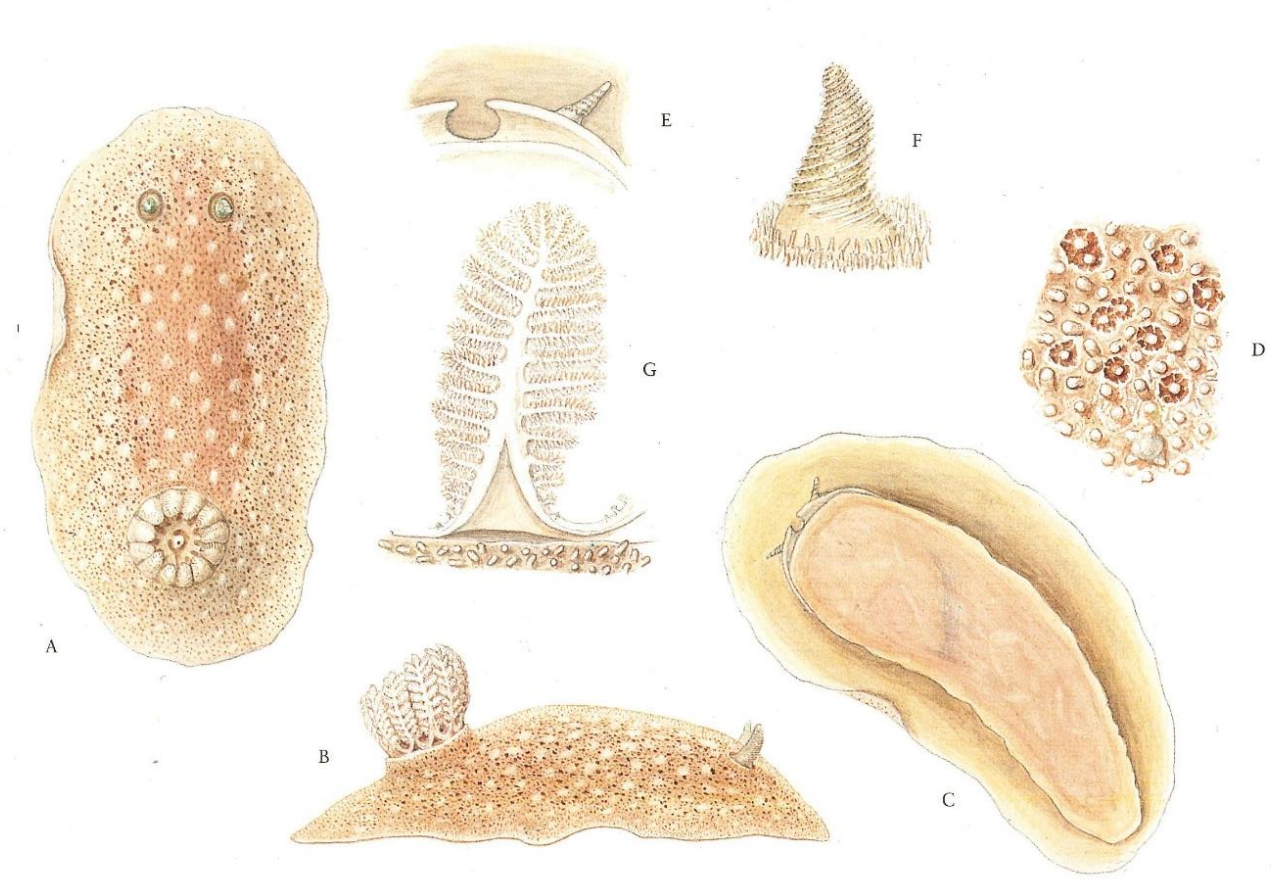

Figure 35. Illustrated specimen of *Jorunna lemchei* by Just & Edmunds, 1975, p. 53, pl. 22. Specimen of 12.6 cm length, found on rock south east of East Inishtravin, Ireland. **A**. Dorsal view of animal. **B**. Right lateral view with erected gill circlet. **C**. Ventral view of animal. **D**. Detailed lateral view of mantle surface. **E**. Detailed anterior margin of grooved and notched foot. **F**. Detailed view of rhinophore. **G**. Detailed view of single gill, lateral view.

Table 5. Synoptic table of diagnostic characters of the currently known valid species of *Jorunna* in Europe, *Jorunna* sp. nov. included. Characters are compared to *Gargamella lemchei*, formerly attributed to the genus *Jorunna*. Character information on *J. tomentosa* is retrieved from cited literature and supplemented with findings from this study. No differentiation has been made for the two lineages *J. tomentosa* A and *J. tomentosa* B due to the lack of morpho-anatomical differences.

	***Jorunna* sp. nov.** Present study	***Jorunna tomentosa*** (Cuvier, 1804)	***Jorunna efe*** Ortea & Moro, 2014	***Jorunna evansi*** (Eliot, 1906)	***Jorunna onubensis*** Cervera, García-Gómez & García, 1986	***Jorunna spazzola*** (Er. Marcus, 1955)	***Gargamella lemchei*** (Ev. Marcus, 1976)
Dorsum	White to yellow with irregular small brown spots	Grey-white, yellow-cream, orange, reddish brown. Dark blotches in two lateral rows, combined with dark spots scattered across notum. Some specimens lack spots	Pale pink, orange, reddish. Darker spots scattered across notum	Violet to violet-cream. Dark blotches of various size scattered across notum, parted by whitish circles	Light brown to pink. Dark blotches of various size scattered across notum	Purplish-whitish grey. Brown spots on each side of notum forming a row, or spots near margin irregularly arranged	Cream to pale brown. May carry minute brown spots
Caryophyllidia	About 200 µm long, dense and uniform	About 150 µm long, dense and uniform	About 400 µm long, dense and uniform	About 200 µm long, dense and uniform	About 180 µm long, dense and uniform	About 300 µm long, dense and uniform	About 200 µm long, dense, some tilted towards each other forming whitish, slightly raised spots
Mantle glands	Present	Present	Present	Present	Present	Present	Not known
Rhinophores	White to yellow-cream, 9–12 lamellae. Not dotted. Apex protruding in knob	Yellow-cream to grey, 9–12 lamellae, dotted in upper part. Apex protruding in knob	Yellow-cream to pale pink, 12–14 lamellae, dotted. White apex protruding in knob	Violet to violet-cream, 10–12 lamellae, dotted in lower part. White upper part with apex protruding in knob	Light brown to pink, 9–15 lamellae, dotted. Apex protruding in knob	Light grey, 8–10 lamellae, dotted. Opaque white tips with apex protruding in knob	Cream-whitish, up to 20 lamellae, lacking dots. Apex protruding in knob
Gills	9–14 bi- to tripinnate leaves similar to dorsal colour. Not dotted	9–14 bi- to tripinnate leaves forming a cup. Yellow-cream to grey, sometimes dotted	9 bi- to tripinnate leaves arranged in a circle. Similar to dorsal colour with lighter apices	10 uni- to bipinnate leaves arranged in a circle. Similar to dorsal colour with white apices	9–12 bi- to tripinnate leaves arranged in a circle. Light-brown to transparent, dotted	5–10 bi- to tripinnate leaves arranged in a circle. Light grey, speckled with minute brown spots	11–12 bi- to tripinnate leaves arranged in a circle, cup-like. Whitish, slightly dotted

	***Jorunna* sp. nov.** Present study	***Jorunna tomentosa*** (Cuvier, 1804)	***Jorunna efe*** Ortea & Moro, 2014	***Jorunna evansi*** (Eliot, 1906)	***Jorunna onubensis*** Cervera, García-Gómez & García, 1986	***Jorunna spazzola*** (Er. Marcus, 1955)	***Gargamella lemchei*** (Ev. Marcus, 1976)
Foot	Grooved and notched anteriorly	Posteriorly visible when animal in motion. Grooved and notched anteriorly	Posteriorly visible when animal in motion. Grooved and notched anteriorly	Posteriorly visible when animal in motion. Grooved and notched anteriorly	Posteriorly visible when animal in motion. Grooved and notched anteriorly	Grooved and notched anteriorly	Grooved and notched anteriorly
Oral tentacles	Digitiform	Digitiform	Digitiform	Bulbus with pointy tip	Digitiform, slender	Triangular, flattened	Triangular, flattened
Radular formula	15–40 mm: 19–25 x 21–18.0.18 – 21	16–30 mm: 19–25 x 28–19.0.19–28	22–30 mm: 20–22 x 25–22.0.22–25	14 mm: 19 x 20.0.20	14–18 mm: 18–21 x 24–18.0.18–24	7 mm: 22 x 13.0.13 Size ?: 15 x 20.0.20	12 mm: 31 x 35.0.35 Size ?: 26 x 32.0.32
Radular teeth	Hook-shaped with single cusp. Both innermost and outermost laterals lack denticles	Hook-shaped with single cusp. Outermost laterals slender with up to 8 denticles or smooth	Hook-shaped with single cusp. Outermost 3 laterals slender and sickle-shaped, with up to 2 denticles	Hook-shaped with single cusp. Outermost 6 laterals slender with up to 5 denticles	Hook-shaped with single cusp. Outermost 4–5 laterals slender with small denticles	Hook-shaped with single cusp. Innermost laterals with up to 4 denticles. Outermost slender with finger-like projections	Hook-shaped with single cusp. Outermost 4 laterals slender. Teeth smooth
Labial cuticle	Smooth	Smooth	With jaw elements	With jaw elements	With jaw elements	With jaw elements	Smooth
Copulatory spine	Straight, round base, ~ 1.6 mm	Straight, round base, ~ 920 µm	Present	Curved, rounded base, ~ 300 µm	Straight spine, ~ 100 µm	Straight base, ~ 165 µm	Straight, ~ 500 µm
Bursa copulatrix & seminal receptacle	Bursa copulatrix slightly larger than seminal receptacle	Bursa copulatrix up to 3 times larger than seminal receptacle	Bursa copulatrix up to 3 times smaller than seminal receptacle	Bursa copulatrix up to twice as large as seminal receptacle	Bursa copulatrix up to 3 times larger than seminal receptacle	Bursa copulatrix about twice the size of seminal receptacle	Bursa copulatrix slightly larger than seminal receptacle
Penial hooks	Absent	Absent	Absent	Absent	Absent	Absent	Present

	***Jorunna* sp. nov.** Present study	***Jorunna tomentosa*** (Cuvier, 1804)	***Jorunna efe*** Ortea & Moro, 2014	***Jorunna evansi*** (Eliot, 1906)	***Jorunna onubensis*** Cervera, García-Gómez & García, 1986	***Jorunna spazzola*** (Er. Marcus, 1955)	***Gargamella lemchei*** (Ev. Marcus, 1976)
Deferent duct	Shorter than vagina, convoluted. Longer compared to *J. tomentosa*	Shorter than vagina, convoluted	About 3 times longer than vagina, highly convoluted	About twice the length of vagina, convoluted	Over 3 times longer than vagina, highly convoluted; connected to shorter, convoluted non-prostatic def. duct	Shorter than vagina, convoluted	Shorter than vagina, slightly convoluted
Geographic range	Norwegian coast and offshore North Sea grounds	Norwegian coast, Faroe Islands, Britain, France, Spain, Azores, Canary Islands, Italy, Slovenia, Croatia, Algeria, South Africa	Lanzarote, Tenerife, Azores	Cape Verde Islands (São Vicente), Italy (Naples)	Spain, Canary Islands, Algarve, Portugal	Mediterranean, Barbados, Brazil, Mexico, Costa Rica, Bahamas	Western Ireland (Ballyvaughan Bay)
Type locality	Brattøya, Kristiansund, Norway	La Rochelle, France	El Reducto, Lanzarote	São Vicente, Cape Verde Islands	El Portil, Huelva, Spain	Ilha de São Sebastião, São Paulo, Brazil	Ballyvauhan Bay, Western Ireland
Key references	Present study	Marcus, 1976; Camacho-García & Gosliner, 2008	Ortea *et al*., 2014	Eliot, 1906; Rudman & Avern, 1989; Ortea & Moro, 2016	Cervera, García-Gómez & García, 1986; Malaquias & Morenito, 2000; Cervera *et al.* 2004	Marcus, 1955; Alvim & Pimenta, 2013	Marcus, 1976; Just & Edmunds, 1985; Camacho-García & Gosliner, 2008

5. Discussion and conclusion

5.1 Molecular phylogenetic analysis

Prior to this systematic revision, the putative occurrence of cryptic speciation in the European *Jorunna tomentosa* had never been considered, despite comprehensive morpho-anatomical studies on this species (Alder & Hancock, 1845; Ev. Marcus, 1976; Valdés & Gosliner, 2001; Camacho-García & Gosliner, 2008). The phylogenetic (BI and ML) analyses of the three gene markers (COI, 16S, H3) combined with the ABGD distance method for species delimitation (Figures 4–8; Table 4; Appendix II, Figures I–VI; Appendix III, B, Figures IX–X) revealed the presence of the pseudo-cryptic species *Jorunna* sp. nov., and a putative case of incipient speciation in *J. tomentosa*, resulting in the partially unresolved lineages *J. tomentosa* A and *J. tomentosa* B. The COI gene is used as a primary tool for molecular barcoding of marine invertebrates (Geller *et al.*, 2013) and performs generally well to discern between recently diverged species where interspecific variation does not overlap intraspecific variation (Hebert, Ratnasingham & deWaard, 2003). Studies have shown that this condition often, but not always, applies to COI (Meyer & Paulay, 2005). This degree of uncertainty is supported by the findings in this study since the inclusion of more loci revealed that lineage A and B were not always resolved as two separate clades. From the single-gene alignments, COI was the only marker that recovered all three clades (Figure 4). The same tree topology was obtained when concatenating COI with R16S (Figure 7), even though R16S yielded a sub-clade of lineage A sequences within an unresolved cluster of sequences of lineage B when analyzed as a single gene (Figure 5). The 16S gene is regarded as informative to differentiate between species but does not perform as well in possible cases of recently diverged species compared to COI (Medina & Walsh, 2000; Feng *et al.*, 2011). The number of base pairs in the stringent 16S alignment (382 bp) was assumed to be too low to fully recover the phylogenetic relationships yielded by the relaxed and original 16S datasets (Figure 5; Appendix III, B, Figure IX; Table 3). The gene H3 has a lower evolutionary rate compared to the mitochondrial genes COI and 16S (Malaquias *et al.*, 2009; Pola *et al.*, 2014), which likely explains the poorly resolved topology at species level (Figure 6). The partially unresolved lineages A and B are reflected in the ABGD species delimitation outputs excluding outgroup species. Partitions that yielded four (P = 0.02–0.06) and five (P = 0.005–0.01) groups were considered putatively congruent with the results rendered by the phylogenetic analyses. In both partitions, the ABGD analysis yielded *Jorunna* sp. nov. as a distinct species. As for the tree topologies, *J. tomentosa* lineage A and *J. tomentosa* lineage B were regarded as either one species (P = 0.02–0.06) or separated as two

species (P = 0.005–0.01). Puillandre *et al.* (2012) detected that the number of groups is very close, and sometimes equal, to the number of species defined by authors in their original studies when P = 0.01. Considering this value as a good threshold, the partition rendering five groups is regarded as a better estimate. For the phylogenetic hypotheses this would mean that the COI and the COI + R16S topologies represent a better estimate of the evolutionary process of lineage separation compared to the single-gene datasets of 16S and H3 and the concatenated COI + R16S + H3. Because this study was not able to detect discrete morpho-anatomical differences, the conservative approach of regarding *J. tomentosa* lineage A and *J. tomentosa* lineage B as one species was chosen. It remains to be further researched whether hypothesizing these lineages as being one species can be regarded as valid.

5.2 Remarks on *Jorunna* sp. nov.

Jorunna sp. nov. is considered pseudo-cryptic due to subtle but detectable morphological differences (Korshunova *et al.*, 2017). Its morphotype (Figure 10, row 1; Figure 26) is rather distinct from the external coloration described for *J. tomentosa* (Cuvier, 1804; Alder & Hancock, 1845; Ev. Marcus, 1976; Camacho-García & Gosliner, 2008; present study) and seems to have been overlooked in previous studies. This problem is known for many species of the Discodorididae which depict a strong morphological resemblance (Alvim & Pimenta, 2013; Hoover *et al.*, 2015; Lindsay *et al.*, 2016). The examined radulae of *Jorunna* sp. nov. lack denticles on the outermost lateral teeth (Figures 29–30), a character usually present in *J. tomentosa*. However, according to Ev. Marcus (1976) and Camacho-García & Gosliner (2008), the presence of denticles in the outermost teeth may vary within a single radula in specimens of *J. tomentosa*. This variability was confirmed in the material examined here and is further confirmed for other European species of *Jorunna* (Figures 17–20; Table 5). More material on *Jorunna* sp. nov. is needed to clarify whether the absence of denticulation is a discrete characteristic of this species.

Since the geographic localities of *J. tomentosa* (lineage A) and *Jorunna* sp. nov. overlap in the Norwegian coastal regions of Trondheim and Kristiansund, the species are considered sympatric (Figure 9). This overlap in distribution is frequently observed in cryptic species in general (Bickford *et al.*, 2007), and well-known in many cases of nudibranch molluscs (*e.g.*, Kienberger *et al.*, 2016; Lindsay *et al.*, 2016; Sørensen *et al.*, 2020). In accordance with the Biological Species Concept, speciation is assumed to have occurred through lack of interbreeding caused by reproductive barriers. This assumption is supported by the anatomical

differences in the reproductive system of *Jorunna* sp. nov. compared to those in *J. tomentosa* (lineages A and B). Having an approximately 600 µm longer copulatory spine (Figures 23–24, 33; Appendix IV, Table B) suggests reproductive isolation in the form of premating barriers as the spine is assumed to have a function in copulatory arousal. In addition, a longer vagina and deferent duct could further impede successful mating (Figures 21, 31). These differences possibly account for the lack of gene flow between these two geographically overlapping species (COI uncorrected *p*-distance = 10.3–10.8%). Because the Biological Species Concept is concordant with the Phylogenetic Species Concept for sympatric species, the phylogenetic structure detected here is consistent with that reproductive isolation has occurred.

According to Knowlton (2000), sympatric species often show characteristic differences in ecology and life history. Still little is known about the ecology and life history of *Jorunna* sp. nov. and it was beyond the scope of this thesis to further address the species' ecological biology. Fecal analyses of the specimens studied here in addition to further material is proposed as a method to identify prey preferences that possibly differ from those found in *J. tomentosa*. In addition, the depth of 350 m at the sampling site in the North Sea raises the question whether the depth range of *Jorunna* sp. nov. might exceed the maximum depth of 400 m recorded for *J. tomentosa*. More material from the North Sea plateau is desirable to test this hypothesis.

5.3 Remarks on *J. tomentosa* lineage A and *J. tomentosa* lineage B

Whereas the molecular phylogenetic analysis and morpho-anatomical studies clearly resolved the pseudo-cryptic *Jorunna* sp. nov., a putative case of incipient speciation was detected in *J. tomentosa*. Whereas some genetic datasets (COI, COI + R16S; Figures 4, 7) split the species in two clades, here named lineage A and lineage B, other genes (16S, H3, COI + R16S + H3) rendered these lineages as one clade (Figures 5–6, 8; Appendix III, B, Figures IX–X). As pointed out by Shaffer & Thomson (2007), recently diverged species may not have had sufficient time to achieve monophyly, resulting in an incomplete lineage sorting where hybridization might still occur. This pattern is suggested between lineages A and B and is reflected in the low interspecific genetic distance of 3.2–5.0% compared to the estimated genetic distances of 16.9% between the species *J. funebris* and *J. onubensis* and *J. funebris* and *Jorunna* sp. nov. (Table 4).

In an attempt to define an overall threshold for interspecific genetic divergence that delimits species, Hebert *et al.*, (2003) suggested a value of 3% for the COI gene. In practice, however,

the threshold value indicative of a new species varies across taxa and the choice of genetic markers (Meyer & Paulay, 2005). As for COI, 2.7% is considered the threshold value for birds (Hebert *et al.*, 2004), 3.0–3.5% for fish (Ward *et al.*, 2008), and 1.99–2.85% for marine gastropods (Meyer & Paulay, 2005). Among the Nudibranchia, Carmona *et al.* (2013) applied a cut-off range of 5.5–16.0% (COI uncorrected *p*-distance) between sister species of Aeolidiidae Gray, 1827 and among species of *Polycera* Cuvier, 1816, *P. capensis* Quoy & Gaimard, 1824 and *P. aurantiomarginata* Garía-Gómez & Bobo, 1984 show an estimated COI uncorrected genetic distance of 4.3–5.8% (Sørensen *et al.*, 2020). In another case, Tibiriçá, Pola & Cervera (2018) supported the delimitation of two species of *Halgerda* Bergh, 1880 with a divergence of 3.6% (COI). Bearing these thresholds in mind, the degree of genetic divergence between lineage A and B is considered challenging to decide on whether the clades can be considered as one or two species. However, bearing the inferred genetic distances between all other sister species of *Jorunna* (12.6–16.9% for the COI gene), the 3.2–5.0% estimated between the two putative lineages of *J. tomentosa* is considerably lower.

The external coloration of specimens in lineage A (Figure 10, row 2) resembles the typical colour pattern described for *J. tomentosa* (Alder & Hancock, 1845; Ev. Marcus, 1976; Picton & Morrow, 1994), suggesting that this clade may be consistent with the true *J. tomentosa*. This hypothesis is further supported by the fact that a specimens from nearby the type locality of *J. tomentosa* in La Rochelle, France (ZMBN 125512) clustered with lineage A. In lineage B, specimens depict a high chromatic variability in both notal background colour and their spotted pattern (Figure 10, rows 3–6). The grey-white morphotype (Figure 10, row 4) seems to conform with the description by Bergh (1881) of *Jorunna atypha* based on a single specimen collected in Trieste, Italy. Bergh (1881) described this specimen as having a greyish white to yellow-white background colour covered by caryophyllidia, rhinophores with 20 lamellae, pigmented in the upper part, gills with 11 white bi- to tripinnate leaves, and a radula with simple teeth, hook-shaped, with the outermost teeth carrying up to four denticles. In specimens of lineage B examined here, the number of rhinophoral lamellae and gills ranged from 9–12 and 9–14, respectively (Table 5). The denticles on the outermost teeth ranged from none (ZMBN 127603; Figure 20) to four (ZMBN 87955; Figure 19) and eight (ZMBN 125038; Figure 18), depicting an irregularity of denticulation as such that denticles were completely absent in one examined specimen and varied in quantity and shape in others. Despite the discrepancy in the number of rhinophoral lamellae and radular denticles, the possible "conspecificity" of *J. atypha* with *J. tomentosa* lineage B cannot be completely discarded, considering that Bergh (1881) studied

one specimen only. However, without sequencing and comparing specimens from the type locality in Trieste, Italy, this remains nothing else than a speculative hypothesis. Because of the bad preservation of the examined specimen, Bergh (1881) was not certain about its generic assignment, but nevertheless, used later again the name *J. atypha* to refer to Mediterranean specimens (Bergh, 1892). In fact, the flat and broad oral tentacles in *J. atypha* (Bergh, 1881: pl. J, fig. 22; Pruvot-Fol, 1954: 276, fig. 111a) differ greatly from the otherwise digitiform, slender oral tentacles found in *Jorunna*, questioning and raising doubts on the taxonomic status of *J. atypha* (Table 5; Camacho-García & Gosliner, 2008; Ortea *et al.*, 2014; MolluscaBase, 2020i). Besides *J. atypha*, none of the other European species of *Jorunna* match the morpho-anatomical features found in lineage B (Table 5).

5.4 On the taxonomic status of several elusive European species of *Jorunna*

In comparison to other species of *Jorunna* from Europe, the presence of distinctive morpho-anatomical characters grants *J. efe* and *J. onubensis* a robust taxonomic valid status (MolluscaBase, 2020j, 2020k). In *J. efe*, the bursa copulatrix is up to three times smaller than the seminal receptacle, a ratio usually inverted in other species of *Jorunna* (Table 5; Ortea & Moro, 2014). In *J. onubensis*, the deferent duct is over three times longer than the vagina, highly convoluted and connected to a non-prostatic deferent duct. Within *Jorunna*, this character is so far only found in *J. onubensis* (Table 5; Cervera, García-Gómez & García, 1986). On the other hand, the validity of the species *J. evansi* and *J. spazzola* has been highly debated (Ev. Marcus, 1976; Rudman & Avern, 1989; Camacho-García & Gosliner, 2008; Alvim & Pimenta, 2013). *Jorunna evansi* was originally assigned to the genus *Rostanga* Bergh, 1879 (Eliot, 1906), yet Rudman & Avern (1989) proposed the new combination name *Jorunna evansi* due to its light violet grey colour with numerous darker spots, a dorsum covered with caryophyllidia, and the narrow radula with 20 or less teeth in a half row, the latter clearly being a characteristic trait of *Jorunna* rather than *Rostanga*. The combination name *J. evansi* was accepted by Camacho-García & Gosliner (2008), confirming the distributional range of the species to the restricted to the Cape Verde Islands (Eliot, 1906). Rudman & Avern (1989) additionally argued for a strong possibility that *J. evansi* and *J. spazzola* from Brazil are synonyms, substantiated by their similar coloration patterns and radular morphology, but omitted to discuss the geographic distribution of the respective species. Camacho-García & Gosliner (2008) proposed *J. evansi* to be a synonym of *J. spazzola*, reasoning that the species share a common external morphology and anatomy, with the exception of the absence of a denticle on the innermost teeth in *J. evansi* which is sometimes present in *J. spazzola*. Yet, they stated that only the study of new material

from the Cape Verde Islands can confirm the conspecificity of both taxa. Ortea & Moro (2016) considered *J. spazzola* and *J. evansi* as different species due to the absence of denticles on the inner laterals in *J. spazzola*, a character regarded as doubtful for species separation by Camacho-García & Gosliner (2008) and shown here to be potentially variable within species. To date, *J. spazzola* and *J. evansi* are considered valid taxonomic entities (MolluscaBase, 2020l, 2020m).

Several authors have also elaborated on the possible synonymy of *J. spazzola* and *J. luisae* Ev. Marcus, 1976 (Ev. Marcus, 1976; Camacho-García & Gosliner, 2008; Alvim & Pimenta, 2013; Ortea & Moro, 2016). Ev. Marcus (1967) described the species *J. luisae* based on ten preserved specimens from the Mediterranean Sea, Naples, Italy (Holotype USNM 710702), and stressed the insignificant differences between this species and the Brazilian *J. spazzola*. Yet, she decided to regard both as valid due to their disjunct geographic distributions. Camacho-García & Gosliner (2008) first suggested the synonymy of both taxa after comparing material of *J. spazzola* from Costa Rica with literature descriptions of *J. luisae* from Naples (*in* Schmekel & Portmann 1982). They based their proposal of synonymy on the absence of denticles on the innermost radular teeth and presence of up to four denticles on the outermost teeth. However, they considered the presence of denticles on the innermost teeth as a variable character within these species (Camacho-García & Gosliner, 2008). Alvim & Pimenta (2013) considered *J. spazzola* and *J. luisae* to be both valid species because of differences in the reproductive systems. The authors compared illustrations of the holotype of *J. luisae* (*in* Camacho-García & Gosliner, 2008) with the original description of *J. spazzola* (Er. Marcus, 1955) and their own material of the latter species from Brazil. According to Alvim & Pimenta (2013), the accessory gland is convoluted, short, and wide in *J. luisae*, and non-convoluted, tubular, long, and thin in *J. spazzola*. Furthermore, they considered the deferent duct of *J. spazzola* approximately as thick as the vagina, whereas they considered it thinner than the vagina in *J. luisae*. However, a comparison of the allusions by Alvim & Pimenta (2013) with the original work by Ev. Marcus (1976, figs. 24, 39), does not show such clear differences. The original drawings of both *J. spazzola* and *J. luisae* show a thin vagina originating from the bursa copulatrix, thickening towards the common atrium. Anderson (2015) listed *J. luisae* as a synonym of *J. spazzola* without further remarks.

Despite the extensive debate on a possible synonymity of *J. luisae* and *J. spazzola*, the taxonomic status of *J. spazzola* stands robust (MolluscaBase, 2020l). Ortea & Moro (2016) synonymyzed *J. luisae* with *J. evansi* because of concordant radular morphology and presence

of jaw elements on the labial cuticle (MolluscaBase, 2020n). The species *J. evansi* is only known from Naples, Italy and the Cape Verde Islands, having a disjunct geographic distribution.

5.5 On the generic reassignment of *Jorunna lemchei* to the genus *Gargamella*

The presence of penial hooks in the species originally described as *Jorunna lemchei* by Ev. Marcus (1976) supports the reassignment of this species to a different genus since no species of *Jorunna* depict this character (Ev. Marcus, 1976; Camacho-García & Gosliner, 2008; Edmunds, 2011; Alvim & Pimenta, 2013; Ortea & Moro, 2016). However, none of the species of *Gargamella* are equipped with a copulatory spine (Bergh, 1894; Perrone, 1986; Garovoy, Valdés & Gosliner, 1999; Valdés & Gosliner, 2001; Moro & Ortea, 2015), a character clearly shown in the description of *J. lemchei* (Ev. Marcus, 1976, fig. 47). In addition, the geographical distribution of *G. lemchei*, being only found in Western Ireland, deviates far from the already scattered distributional range of the other species. *G. bovina*, *G. immaculata*, and *G. gravastella* occur in the South Atlantic (Patagonia and South Africa), *G. wareni* in the South Pacific (New Caledonia), and *G. blokoverdensis* and *G. perezi* are distributed in the North Atlantic (Cape Verde Islands, Canary Islands, and Italy). This discrepancy raises the question whether the generic assignment of *J. lemchei* to *Gargamella* is correct. In their work, Ortea *et al.* (2014) base the generic reassignment on morphological characters only. Whereas they highlight the presence of penial hooks as the main character for the generic reassignment, they omit to discuss the presence of the copulatory spine described by Ev. Marcus (1976). It is beyond the scope of this study to further discuss the systematics of *G. lemchei*, however, the absence of the spine in all other species of *Gargamella* elicits the need for further elaborations on this generic assignment, certainly using a molecular phylogenetic framework.

5.6 Concluding remarks

The integrative taxonomic approach used in this study has unraveled the first case of cryptic speciation in the genus *Jorunna*. Additional material of *Jorunna* sp. nov. would be desirable to better understand the intraspecific variability, geographical range, and ecology of the species. The unresolved lineage sorting detected in *J. tomentosa* provides a solid knowledge base for future research on other European species of *Jorunna*, especially considering the extensively debated taxonomic status of *J. evansi* and *J. spazzola*. It will be worth pursuing to include more sequences of all European species in addition to several different *loci* to generate a larger phylogenetic framework that builds up on the work presented here. This way we might unravel

whether *J. tomentosa* is a species with high chromatic variability (lineage A and B combined) or in fact is solely represented by lineage A. This would raise the question whether lineage B is an undescribed species or belongs to a species already described. More data on anatomical and ecological characteristics could furthermore provide valuable information to elucidate the relationships between these lineages. In addition to the unraveled cryptic diversity, this study has initiated a review of the generic classification of traditional *Jorunna* species, namely the relation between the genera *Jorunna* and *Gargamella*. This review is highly recommended to be pursued by the aid of a comparative study, including molecular and morpho-anatomical data from species of both genera, to scrutinize the taxonomic classification of *G. lemchei* which is currently adjudged valid.

6. Bibliography

ADAMS, M., RAADIK, T.A., BURRIDGE, C.P. & GEORGES, A. 2014. Global Biodiversity Assessment and Hyper-Cryptic Species Complexes: More Than One Species of Elephant in the Room? *Systematic Biology*, **63**: 518–533.

ALDER, J. & HANCOCK, A. 1845–1855. *A Monograph of the British Nudibranchiate Mollusca I-VII*. Ray Society, London.

ALLEN, J.A. 1962. Fauna of the Clyde Sea Area. In: *Mollusca,* pp. 88. Scottish Marine Biological Association.

ALVIM, J. & PIMENTA, A.D. 2013. Taxonomic review of the family Discodorididae (Mollusca: Gastropoda: Nudibranchia) from Brazil, with descriptions of two new species. *Zootaxa*, **3745**: 152–198.

ANDERSON, V.P. 2015. *Testing traditional concepts: biodiversity and integrative taxonomy of Brazilian opisthobranchs (Mollusca, Heterobranchia)*. Ludwig-Maximilians-Universität München.

AVISE, J.C. & WOLLENBERG, K. 1997. Phylogenetics and the origin of species. *Proceedings of the National Academy of Sciences of the United States of America*, **94**: 7748–7755.

BALLESTEROS, M. 1984. Adición a la fauna de Opistobranquios de Cubelles (Tarragona). *Miscellanea Zoologica*, **8**: 41–49.

BALLESTEROS, M., MADRENAS, E. & PONTES, M. 2016. Update of the catalog of opisthobranch molluscs (Gastropoda: Heterobranchia) from the Catalan waters. *Associació Catalana de Malacologia*, **6**: 1–28.

BEERMANN, J., WESTBURY, M. V., HOFREITER, M., HILGERS, L., DEISTER, F., NEUMANN, H. & RAUPACH, M.J. 2018. Cryptic species in a well-known habitat: applying taxonomics to the amphipod genus *Epimeria* (Crustacea, Peracarida). *Scientific Reports*, **8**: 1–26

BERGH, L.S.R. 1876. Malacologische Untersuchungen. *Reisen im Archipel der Philippinen von Dr. Carl Gottfried Semper. Zweiter Theil. Wissenschaftliche Resultate, Band 2*, **Theil 2**, Heft 10: 377–427, pls. 49–53. C.W. Kreidel, Wiesbaden.

BERGH, L.S.R. 1878. Malacologische Untersuchungen. *Reisen im Archipel der Philippinen von Dr. Carl Gottfried Semper. Zweiter Theil. Wissenschaftliche Resultate, Band 2,* **Theil 2**, Heft 13: 547–601, pls. 62–65. C.W. Kreidel, Wiesbaden.

BERGH, L.S.R. 1880. On the nudibranchiate gastropod Mollusca of the North Pacific Ocean, with special reference to those of Alaska. Part II. *Proceedings of the Academy of Natural Sciences of Philadelphia*, **32**: 40–127.

BERGH, L.S.R. 1881. Malacologische Untersuchungen. *Reisen im Archipel der Philippinen von Dr. Carl Gottfried Semper. Zweiter Theil. Wissenschaftliche Resultate, Band 2*, **Theil 4**, Heft Supplement 2: 79–128, pls. G, H, J–L. C.W. Kreidel, Wiesbaden.

BERGH, L.S.R. 1884. Malacologische Untersuchungen. *Reisen im Archipel der Philippinen von Dr. Carl Gottfried Semper. Zweiter Theil. Wissenschaftliche Resultate, Band 2*, **Theil 3**, Heft 15: 647–754, pls. 69–76. C.W. Kreidel, Wiesbaden.

BERGH, L.S.R. 1892. Die cryptobranchiaten Dorididen. *Zoologische Jahrbücher*, **6**: 103–144.

BERGH, L.S.R. 1893. Ueber einige verkannte und neue Dorididen. *Verhandlungen der Zoologisch-Botanischen Gesellschaft in Wien*, **43**: 408–420.

BERGH, L.S.R. 1894. Die Opisthobranchen 13. Report of the dredging operations off the West coast of Central America of the Galapagos to the West coast of Mexico and in the Gulf of California, in charge of Alexander Agassiz, carried on by the U.S. Fish Commision Steamer Albat. *Bulletin of the Museum of Comparative Zoology*, **25**: 125–235.

BICKFORD, D., LOHMAN, D.J., SODHI, N.S., NG, P.K.L., MEIER, R., WINKER, K., INGRAM, K.K. & DAS, I. 2007. Cryptic species as a window on diversity and conservation. *Trends in Ecology and Evolution*, **22**: 148–155.

BLOOM, S.A. 1976. Morphological correlations between dorid nudibranch predators and sponge prey. *Veliger*, **18**: 289–301.

BOUCHET, P., ROCROI, J.-P., HAUSDORF, B., KAIM, A., KANO, Y., NÜTZEL, A., PARKHAEV, P., SCHRÖDL, M. & STRONG, E.E. 2017. Revised Classification, Nomenclator and Typification of Gastropod and Monoplacophoran Families. *Malacologia*, **61**: 1–526.

CALADO, G., MALAQUIAS, M.A.E., GAVAIA, C., CERVERA, J.L., MEGINA, C., DAYRAT, B., CAMACHO, Y., POLA, M. & GRANDE, C. 2003. New data on opisthobranchs (Mollusca: Gastropoda) from the southwestern coast of Portugal. *Boletim do Instituto Espanol de Oceanografia*, **19**: 199–204.

CAMACHO-GARCÍA, Y.E. & GOSLINER, T.M. 2008. Systematic revision of *Jorunna* Bergh, 1876 (Nudibranchia: Discodorididae) with a morphological phylogenetic analysis. *Journal of Molluscan Studies*, **74**: 143–181.

CAPA, M., HUTCHINGS, P. & PEART, R. 2012. Systematic revision of Sabellariidae (Polychaeta) and their relationships with other polychaetes using morphological and DNA sequence data. *Zoological Journal of the Linnean Society*, **164**: 245–284.

CARMONA, L., BHAVE, V., SALUNKHE, R., POLA, M., GOSLINER, T.M. & CERVERA, J.L. 2014. Systematic review of *Anteaeolidiella* (Mollusca, Nudibranchia, Aeolidiidae) based on morphological and molecular data, with a description of three new species. *Zoological Journal of the Linnean Society*, **171**: 108–132.

CARMONA, L., POLA, M., GOSLINER, T.M. & CERVERA, J.L. 2013. A Tale That Morphology Fails to Tell: A Molecular Phylogeny of Aeolidiidae (Aeolidida, Nudibranchia, Gastropoda). *PLoS ONE*, **8**: 1–13.

CASTRESANA, J. 2000. Selection of conserved blocks from multiple alignments for their use in phylogenetic analysis. *Molecular biology and evolution*, **17**: 540–52.

CATTANEO-VIETTI, R. 1991. Nudibranch Molluscs from the Ross Sea, Antarctica. *Journal of Molluscan Studies*, **57**: 223–228.

CERVERA, J.L., GARCÍA-GÓMEZ, J.C. & GARCÍA, F.J. 1986. Il genere *Jouruna* Bergh, 1876 (Mollusca: Gastropoda: Nudibranchia) nel litorale Iberico. *Lavori Societa Italiana di Malacologia*, **22**: 111–134.

CERVERA, J.L., CALADO, G., GAVAIA, C., MALAQUIAS, M.A.E., TEMPLADO, J., BALLESTEROS, M., GARCÍA-GÓMEZ, J.C. & MEGINA, C. 2004. An annotated and updated checklist of the opisthobranchs (Mollusca: Gastropoda) from Spain and Portugal (including islands and archipelagos). *Boletin Instituto Espanol de Oceanografia*, **20**: 1–122.

CHURCHILL, C.K.C., VALDÉS, Á. & Ó FOIGHIL, D. 2014. Molecular and morphological systematics of neustonic nudibranchs (Mollusca: Gastropoda: Glaucidae: *Glaucus*), with descriptions of three new cryptic species. *Invertebrate Systematics*, **28**: 174–195.

COATES, D.J., BYRNE, M. & MORITZ, C. 2018. Genetic Diversity and Conservation Units: Dealing With the Species-Population Continuum in the Age of Genomics. *Frontiers in Ecology and Evolution*, **6**: 1–13.

COLGAN, D., MCLAUCHLAN, A., WILSON, G., LIVINGSTON, S., MACARANAS, J., EDGECOMBE, G., CASSIS, G. & GRAY, M. 1998. Molecular phylogenetics of the Arthropoda: relationships based on histone H3 and U2 snRNA DNA sequences. *Australian Journal of Zoology*, **46**: 419–437.

CORDEIRO, R., BORGES, J.P., MARTINS, A.M.F. & ÁVILA, S.P. 2015. Checklist of the littoral gastropods (Mollusca: Gastropoda) from the Archipelago of the Azores (NE Atlantic). *Biodiversity journal*, **6**: 855–900.

CUÉNOT, L. 1904. Contributions a la faune du Bassin D'Arcachon. III. Doridiens. *Bulletin de la Station Biologique D'Arcachon*, **7**: 1–22.

CUVIER, G. 1804. Mémoire Sur le Genre Doris. *Annales de Museum National d' Histoire Naturelle*, **4**: 447–473.

DARRIBA, D., TABOADA, G.L., DOALLO, R. & POSADA, D. 2012. jModelTest2: more models, new heuristics and parallel computing. *Nature Methods*, **9**: 772.

DAVIES, J. 1993. *Aspects of the life history and physiological ecology of long-lived nudibranch Molluscs*. University of St Andrews.

DAWSON, M.N. & JACOBS, D.K. 2001. Molecular evidence for cryptic species of *Aurelia aurita* (Cnidaria, Scyphozoa). *Biological Bulletin*, **200**: 92–96.

DE QUEIROZ, K. 2007. Species concepts and species delimitation. *Systematic Biology*, **56**: 879–886.

DEAN, L.J. & PRINSEP, M.R. 2017. The chemistry and chemical ecology of nudibranchs. *Natural Product Reports*, **34**: 1359–1390.

DONG, S., SCHÄFER-VERWIMP, A., MEINECKE, P., FELDBERG, K., BOMBOSCH, A., PÓCS, T., SCHMIDT, A.R., REITNER, J., SCHNEIDER, H. & HEINRICHS, J. 2012. Tramps, narrow endemics and morphologically cryptic species in the epiphyllous liverwort *Diplasiolejeunea*. *Molecular Phylogenetics and Evolution*, **65**: 582–594.

EDGAR, R.C. 2004. MUSCLE: multiple sequence alignment with high accuracy and high throughput. *Nucleic acids research*, **32**: 1792–7.

EDMUNDS, M. 1971. Opisthobranchiate Mollusca from Tanzania (suborder Doridacea). *Zoological Journal of the Linnean Society*, **59**: 339–369.

EDMUNDS, M. 2011. Opisthobranchiate Mollusca from Ghana: Discodorididae. *Journal of Conchology*, **40**: 617–650.

EKIMOVA, I., KORSHUNOVA, T., SCHEPETOV, D., NERETINA, T., SANAMYAN, N. & MARTYNOV, A. 2015. Integrative systematics of northern and Arctic nudibranchs of the genus *Dendronotus* (Mollusca, Gastropoda), with descriptions of three new species. *Zoological Journal of the Linnean Society*, **173**: 841–886.

ELIOT, C.N.E. 1906. Report upon a collection of Nudibranchiata from the Cape Verd Islands, with notes by C. Crossland. *Proceedings of the Malacological Society of London*, **VII**: 131–159.

EVERTSEN, J. & BAKKEN, T. 2002. Heterobranchia (Mollusca, Gastropoda) from northern Norway, with notes on ecology and distribution. *Fauna norvegica*, **22**: 15–22.

EVERTSEN, J. & BAKKEN, T. 2005. Nudibranch diversity (Gastropoda, Heterobranchia) along the coast of Norway. *Fauna norvegica*, **25**: 1–37.

EVERTSEN, J. & BAKKEN, T. 2013. Diversity of Norwegian sea slugs (Nudibranchia): new species to Norwegian coastal waters and new data on distribution of rare species. *Fauna norvegica*, **32**: 45–52.

EYSTER, L.S. 1981. Observations on the growth, reproduction and feeding of the Nudibranch *Armina tigrina*. *Journal of Molluscan Studies*, **47**: 171–181.

FAHEY, S.J. & GARSON, M.J. 2002. Geographic variation of natural products of tropical nudibranch *Asteronotus cespitosus*. *Journal of Chemical Ecology*, **28**: 1773–1785.

FENG, Y., LI, Q., KONG, L. & ZHENG, X. 2011. DNA barcoding and phylogenetic analysis of Pectinidae (Mollusca: Bivalvia) based on mitochondrial COI and 16S rRNA genes. *Molecular Biology Reports*, **38**: 291–299.

FISCHER, P. 1869. Catalogue des nudibranches et cephalopodes des côtes océaniques de la France (1 Supplement). *Journal de Conchyliologie*, **3**: 5–10.

FISCHER, P. 1880–1887. *Manuel de conchyliologie et de paléontologie conchyliologique ou histoire naturelle des mollusques vivants et fossiles*. F. Savy, Paris.

FISHER, N. 1937. Nudibranchs from N.E. Ireland. *The Irish Naturalists' Journal*, **6**: 200–202.

FLAMMENSBECK, C.K., HASZPRUNAR, G., KORSHUNOVA, T., MARTYNOV, A. V., NEUSSER, T.P. & JÖRGER, K.M. 2019. *Pseudovermis paradoxus* 2.0—3D microanatomy and ultrastructure of a vermiform, meiofaunal nudibranch (Gastropoda, Heterobranchia). *Organisms Diversity and Evolution*, **19**: 41–62.

FOALE, S.J. & WILLAN, R.C. 1987. Scanning and transmission electron microscope study of specialized mantle structures in dorid nudibranchs (Gastropoda: Opisthobranchia: Anthobranchia). *Marine Biology*, **95**: 547–557.

FOLMER, O., BLACK, M., HOEH, W., LUTZ, R. & VRIJENHOEK, R. 1994. DNA primers for amplification of mitochondrial cytochrome *c* oxidase subunit I from diverse metazoan invertebrates. *Molecular marine biology and biotechnology*, **3**: 294–299.

FRANKS, D.W. & NOBLE, J. 2004. Batesian mimics influence mimicry ring evolution. *Proceedings of the Royal Society B: Biological Sciences*, **271**: 191–196.

FUHRMAN, F. A., FUHRMAN, G.J. & DERIEMER, K. 1979. Toxicity and Pharmacology of Extracts from Dorid Nudibranchs. *Biological Bulletin*, **156**: 289–299.

FURFARO, G., VITALE, F., LICCHELLI, C. & MARIOTTINI, P. 2020. Two Seas for One Great Diversity: Checklist of the Marine Heterobranchia (Mollusca; Gastropoda) from the Salento Peninsula (South-East Italy). *Diversity*, **12**: 1–24.

GARCÍA GÓMEZ, J.C. 1983. Opisthobranch Molluscs of the Gibraltar Strait and Algeciras Bay. *Iberus*, **3**: 41–46.

GARCÍA, F.J. & BERTSCH, H. 2009. Diversity and distribution of the Gastropoda Opisthobranchia from the Atlantic Ocean: A global biogeographic approach. *Scientia Marina*, **73**: 153–160.

GAROVOY, J.B., VALDÉS, A. & GOSLINER, T.M. 1999. Two New Species of *Gargamella* (Mollusca, Nudibranchia) from South Africa. *Proceedings of the California Academy of Sciences*, **51**: 245–257.

GARSTANG, W. 1893. Notes on the structure and habits of *Jorunna johnstoni*. *The Conchologist*, **2**: 49–52.

GELLER, J., MEYER, C., PARKER, M. & HAWK, H. 2013. Redesign of PCR primers for mitochondrial cytochrome *c* oxidase subunit I for marine invertebrates and application in all-taxa biotic surveys. *Molecular Ecology Resources*, **13**: 851–861.

GOSLINER, T.M. 1994. Gastropoda: Opisthobranchia. In: *Microscopic Anatomy of Invertebrates*Volume 5 (F. W. Harrison & A. J. Kohn, eds), pp. 235–355. Wiley-Liss Inc., New York.

GOSLINER, T.M. & FAHEY, S.J. 2011. Previously undocumented diversity and abundance of cryptic species: A phylogenetic analysis of Indo-Pacific Arminidae Rafinesque, 1814 (Mollusca: Nudibranchia) with descriptions of 20 new species of *Dermatobranchus*. *Zoological Journal of the Linnean Society*, **161**: 245–356.

GRIEG, J.A. 1912. Nudibranchiate Mollusker indsamlede av Den Norske Fiskeridamper "Michael Sars." *Det Kgl. Norske Videnskabers Selskabs Skrifter*, **13**: 1–13.

GUINDON, S. & GASCUEL, O. 2003. A simple, fast and accurate method to estimate large phylogenies by maximum-likelihood. *Systematic Biology*, **52**: 696–704.

HANCOCK, A. & EMBLETON, D. 1852. On the Anatomy of *Doris*. *Philosophical Transactions of the Royal Society of London*, **2**: 207–252.

HANSSON, H.G. 1998. Scandinavian marine Mollusca Check-List, available at https://www.tmbl.gu.se/libdb/taxon/neat_pdf/NEAT*Mollusca.pdf

HAYWARD, P.J. & RYLAND, J.S. 2017. *Handbook of the Marine Fauna of North-West Europe*. Oxford University Press, Oxford.

HEBERT, P.D.N., CYWINSKA, A., BALL, S.L. & DEWAARD, J.R. 2003. Biological identifications through DNA barcodes. *Proceedings of the Royal Society B: Biological Sciences*, **270**: 313–321

HEBERT, P.D.N., RATNASINGHAM, S. & deWAARD, J.R. 2003. Barcoding animal life: cytochrome *c* oxidase subunit 1 divergences among closely related species. *Proceedings of the Royal Society B: Biological Sciences*, **270**: S96–S99.

HEBERT, P.D.N., PENTON, E.H., BURNS, J.M., JANZEN, D.H. & HALLWACHS, W. 2004. Ten species in one: DNA barcoding reveals cryptic species in the neotropical skipper butterfly *Astraptes fulgerator*. *Proceedings of the National Academy of Sciences of the United States of America*, **101**: 14812–14817.

HEBERT, P.D.N, STOECKLE, M.Y., ZEMLAK, T.S. & FRANCIS, C.M. 2004. Identification of Birds through DNA Barcodes. *PLoS Biology*, **2**: 1657–1663.

HOFFMANN, H. 1926. Opisthobranchia. In: *Die Tierwelt der Nord- und Ostsee*, Vol. IX (G. Grimpe & E. Wagler, ed.), pp. 1-52. Akademische Verlagsgesellschaft, Leipzig.

HOOVER, C., LINDSAY, T., GODDARD, J.H.R. & VALDÉS, Á. 2015. Seeing double: pseudocryptic diversity in the *Doriopsilla albopunctata-Doriopsilla gemela* species complex of the north-eastern Pacific. *Zoologica Scripta*, **44**: 612–631.

HUELSENBECK, J.P. & RONQUIST, F. 2001. MRBAYES: Bayesian inference of phylogenetic trees. *Bioinformatics*, **17**: 754–755.

HUNNAM, P. & BROWN, G. 1975. Sublittoral Nudibranch Mollusca (sea slugs) in Pembrokeshire Waters. *Field Studies*, **4**: 131–159.

INTERNATIONAL COMMISSION ON ZOOLOGICAL NOMENCLATURE (ICZN). 1999. *International Code of Zoological Nomenclature*. International Trust for Zoological Nomenclature, London.

IREDALE, T. & O'DONOGHUE, C.H. 1923. List of British Nudibranchiate Mollusca. *Proceedings of the Malacological Society of London*, **15**: 195–233.

JOHNSTON, G. 1838. VI.- Miscellanea Zoologica. The Scottish Mollusca Nudibranchia. *Annals of Natural History*, **1**: 44–56; 115-125, pls. 2, 3.

JÖRGER, K.M., STÖGER, I., KANO, Y., FUKUDA, H., KNEBELSBERGER, T. & SCHRÖDL, M. 2010. On the origin of Acochlidia and other enigmatic euthyneuran gastropods, with implications for the systematics of Heterobranchia. *BMC Evolutionary Biology*, **10**.

JÖRGER, K.M., STOSCHEK, T., MIGOTTO, A.E., HASZPRUNAR, G. & NEUSSER, T.P. 2014. 3D-microanatomy of the mesopsammic *Pseudovermis salamandrops* Marcus, 1953 from Brazil (Nudibranchia, Gastropoda). *Marine Biodiversity*, **44**: 327–341.

JUST, H. & EDMUNDS, M. 1985. *North Atlantic Nudibranchs (Mollusca) Seen By Henning Lemche*. Ophelia Publications, Helsingør.

KARLSSON, A. & HAASE, M. 2002. The enigmatic mating behaviour and reproduction of a simultaneous hermaphrodite, the nudibranch *Aeolidiella glauca* (Gastropoda, Opisthobranchia). *Canadian Journal of Zoology*, **80**: 260–270.

KAY, E. & YOUNG, D. 1969. The Doridacea (Opisthobranchia: Mollusca) of the Hawaiian Islands. *Pacific Science*, **23**: 172–231.

KEARSE, M., MOIR, R., WILSON, A., STONES-HAVAS, S., CHEUNG, M., STURROCK, S., BUXTON, S., COOPER, A., MARKOWITZ, S., DURAN, C., THIERER, T., ASHTON, B., MEINTJES, P. & DRUMMOND, A. 2012. Geneious Basic: An integrated and extendable desktop software platform for the organization and analysis of sequence data. *Bioinformatics*, **28**: 1647–1649.

KIENBERGER, K., CARMONA, L., POLA, M., PADULA, V., GOSLINER, T.M. & CERVERA, J.L. 2016. *Aeolidia papillosa* (Linnaeus, 1761) (Mollusca: Heterobranchia: Nudibranchia), single species or a cryptic species complex? A morphological and molecular study. *Zoological Journal of the Linnean Society*, **177**: 481–506.

KNOWLTON, N. 2000. Molecular genetic analyses of species boundaries in the sea. *Hydrobiologia*, **420**: 73–90.

KORSHUNOVA, T., LUNDIN, K., MALMBERG, K., PICTON, B. & MARTYNOV, A. 2018. First true brackish-water nudibranch mollusc provides new insights for phylogeny and biogeography and reveals paedomorphosis-driven evolution. *PLoS ONE*, **13**: 1–20.

KORSHUNOVA, T., MALMBERG, K., PRKIĆ, J., PETANI, A., FLETCHER, K., LUNDIN, K. & MARTYNOV, A. 2020. Fine-scale species delimitation: Speciation in process and periodic patterns in nudibranch diversity. *ZooKeys*, **917**: 15–50.

KORSHUNOVA, T., MARTYNOV, A., BAKKEN, T. & PICTON, B. 2017. External diversity is restrained by internal conservatism: New nudibranch mollusc contributes to the cryptic species problem. *Zoologica Scripta*, **46**: 683–692.

KORSHUNOVA, T., PICTON, B., FURFARO, G., MARIOTTINI, P., PONTES, M., PRKIĆ, J., FLETCHER, K., MALMBERG, K., LUNDIN, K. & MARTYNOV, A. 2019. Multilevel fine-scale diversity challenges the 'cryptic species' concept. *Scientific Reports*, **9**: 6732.

KRESS, A. 1981. A scanning electron microscope study of notum structures in some dorid nudibranchs (Gastropoda: Opisthobranchia). *Journal of the Marine Biological Association of the United Kingdom*, **61**: 177–191.

KUMAR, S., STECHER, G., LI, M., KNYAZ, C. & TAMURA, K. 2018. MEGA X: Molecular evolutionary genetics analysis across computing platforms. *Molecular Biology and Evolution*, **35**: 1547–1549.

LABBÉ, A. 1929. Les organes palléaux (caryophillidies) et le tissu conjonctif du manteau de *Rostanga coccinea* Forbes. *Archives d'anatomie microscopique*, **25**: 87–103.

LABBÉ, A. 1933. Les organes palléaux (caryophyllidies) des Doridiens. *Archives de Zoologie Expérimentale et Générale*, **75**: 211–220.

LINDSAY, T., KELLY, J., CHICHVARKHIN, A., CRAIG, S., KAJIHARA, H., MACKIE, J. & VALDÉS, Á. 2016. Changing spots: pseudocryptic speciation in the North Pacific dorid nudibranch *Diaulula sandiegensis* (Cooper, 1863) (Gastropoda: Heterobranchia). *Journal of Molluscan Studies*, **82**: 564–574.

LONGLEY, A.J. & LONGLEY, R.D. 1984. Mating in the gastropod *Aeolidiella papillosa*: behaviour and anatomy. *Canadian Journal of Zoology*, **62**: 8–14.

MALAQUIAS, M.A.E. & MORENITO, P.M. 2000. The Opisthobranchs (Mollusca: Gastropoda) of the Coastal Lagoon "Ria Formosa" in Southern Portugal. *Bollettino Malacologico*, **36**: 117–124.

MALAQUIAS, M.A.E. 2001. Updated and annotated checklist of the opisthobranch molluscs (excluding Thecosomata and Gymnosomata) from the Azores archipelago (North Atlantic Ocean, Portugal). *Iberus*, **19**: 37–48.

MALAQUIAS, M.A.E., CALADO, G.P., PADULA, V., VILLANI, G. & CERVERA, J.L. 2009. Molluscan diversity in the North Atlantic Ocean: new records of opisthobranch gastropods from the Archipelago of the Azores. *Marine Biodiversity Records*, **2**: 1–9.

MALAQUIAS, M.A.E., CALADO, C., CRUZ, J.F. & JENSEN, K. 2014. Opisthobranch molluscs of the Azores: results of the IV International Workshop of Malacology and Marine Biology. *IV International Workshop on Malacology and Marine Biology*, 139–147.

MALMBERG, K. & LUNDIN, K. 2015. *Svenska Nakensnäckor*. Waterglobe Productions.

MARCUS, Er. 1955. Opisthobranchia from Brazil. *Boletim da Facultadede Filosofia, Ciências e Letras da Universidade de São Paulo, Zoologica*, **20**: 89–261.

MARCUS, Ev. 1976. On *Kentrodoris* and *Jorunna* (Gastropoda Opisthobranchia). *Boletim de Zoologica, Universidad de São Paulo*, **1**: 11–68.

MARRONE, F., LO BRUTTO, S., HUNDSDOERFER, A.K. & ARCULEO, M. 2013. Overlooked cryptic endemism in copepods: Systematics and natural history of the calanoid subgenus *Occidodiaptomus* Borutzky 1991 (Copepoda, Calanoida, Diaptomidae). *Molecular Phylogenetics and Evolution*, **66**: 190–202.

MAYR, E. 1942. *Systematics and the Origin of Species*. Columbia University Press, New York.

MCDONALD, G.R. & NYBAKKEN, J.W. 1997. List of the Worldwide Food Habits of Nudibranchs. *Veliger*, **40**.

MEBS, D. 1985. Chemical defense of a dorid nudibranch, *Glossodoris quadricolor*, from the Red Sea. *Journal of Chemical Ecology*, **11**: 713–716.

MEDINA, M. & WALSH, P.J. 2000. Molecular systematics of the order Anaspidea based on mitochondrial DNA sequence (12S, 16S, and COI). *Molecular Phylogenetics and Evolution*, **15**: 41–58.

MEGINA, C. & CERVERA, J.L. 2003. Diet, prey selection and cannibalism in the hunter opisthobranch *Roboastra europaea*. *Jorunal of the Marine Biological Association of the United Kingdom*, **83**: 489–495.

MEYER, C.P. & PAULAY, G. 2005. DNA Barcoding: Error Rates Based on Comprehensive Sampling. *PLoS Biology*, **3**: 2229–2238.

MEYER-WACHSMUTH, I., CURINI GALLETTI, M. & JONDELIUS, U. 2014. Hyper-cryptic marine meiofauna: Species complexes in Nemertodermatida. *PLoS ONE*, **9**: 1–25.

MILLER, M.A., PFEIFFER, W. & SCHWARTZ, T. 2010. Creating the CIPRES Science Gateway for inference of large phylogenetic trees. *Proceedings of the Gateway Computing Environments Workshop*. New Orleans.

MILLER, M.C. 1958. *Studies on the nudibranchiate Mollusca of the Isle of Man*. University of Liverpool.

MILLER, M.C. 1962. Annual Cycles of Some Manx Nudibranchs, with a Discussion of the Problem of Migration. *Journal of Animal Ecology*, **31**: 545–569.

MILLOTT, N. 1937. On the morphology of the alimentary canal, process of feeding, and physiology of digestion of the nudibranch mollusc *Jorunna tomentosa* (Cuvier). *Philosophical Transactions of the Royal Society of London*, **228**: 173–218.

MOEN, F.E. & SVENSEN, E. 2014. *Dyreliv i havet*. Kom Forlag, Son, Norway.

MOLLUSCABASE 2020a. MolluscaBase. Doridoidei. Accessed through World Register of Marine Species, accessed April 4, 2020, available at http://www.marinespecies.org/aphia.php?p=taxdetails&id=246038.

MOLLUSCABASE 2020b. MolluscaBase. Okadaiidae Baba, 1930. Accessed through World Register of Marine Species, accessed April 4, 2020, available at http://www.marinespecies.org/aphia.php?p=taxdetails&id=412584.

MOLLUSCABASE 2020c. MolluscaBase. Discodorididae Bergh, 1891. Accessed through World Register of Marine Species, accessed April 5, 2020, available at http://www.marinespecies.org/aphia.php?p=taxdetails&id=1761.

MOLLUSCABASE 2020d. MolluscaBase eds. *Jorunna* Bergh, 1876. Accessed through World Register of Marine Species, accessed February 9, 2020, available at http://www.marinespecies.org/aphia.php?p=taxdetails&id=138098.

MOLLUSCABASE 2020e. MolluscaBase. *Jorunna maima* (Bergh, 1878). Accessed through World Register of Marine Species, accessed April 7, 2020, available at https://www.marinespecies.org/aphia.php?p=taxdetails&id=534408.

MOLLUSCABASE 2020f. MolluscaBase. *Doris obvelata* O. F. Müller, 1776. Accessed through World Register of Marine Species, accessed April 24, 2020, available at http://www.marinespecies.org/aphia.php?p=taxdetails&id=153311.

MOLLUSCABASE 2020g. MolluscaBase. *Gargamella lemchei* (Ev. Marcus, 1976). Accessed through World Register of Marine Species, accessed June 8, 2020, available at http://www.marinespecies.org/aphia.php?p=taxdetails&id=828314.

MOLLUSCABASE 2020h. MolluscaBase. *Gargamella novozealandica* Eliot, 1907. Accessed through World Register of Marine Species, accessed July 4, 2020, available at http://www.marinespecies.org/aphia.php?p=taxdetails&id=534388.

MOLLUSCABASE 2020i. MolluscaBase. *Jorunna atypha* Bergh, 1881, Accessed through World Register of Marine Species, accessed April 15, 2020, available at http://www.marinespecies.org/aphia.php?p=taxdetails&id=140164.

MOLLUSCABASE 2020j. MolluscaBase. *Jorunna efe* Ortea & Moro, 2014. Accessed through World Register of Marine Species, accessed July 28, 2020, available at http://www.marinespecies.org/aphia.php?p=taxdetails&id=828313.

MOLLUSCABASE 2020k. MolluscaBase. *Jorunna onubensis* Cervera, García-Gómez & García, 1986. Accessed through World Register of Marine Species, accessed July 28, 2020, available at http://www.marinespecies.org/aphia.php?p=taxdetails&id=140165.

MOLLUSCABASE 2020l. MolluscaBase. *Jorunna evansi* (Eliot, 1906). Accessed through World Register of Marine Species, accessed April 10, 2020, available at http://www.marinespecies.org/aphia.php?p=taxdetails&id=224400.

MOLLUSCABASE 2020m. MolluscaBase. *Jorunna spazzola* (Er. Marcus, 1955). Accessed through World Register of Marine Species, accessed April 15, 2020, available at http://www.marinespecies.org/aphia.php?p=taxdetails&id=420601.

MOLLUSCABASE 2020n. MolluscaBase. *Jorunna luisae* Ev. Marcus, 1976. Accessed through World Register of Marine Species, accessed July 28, 2020, available at http://www.marinespecies.org/aphia.php?p=taxdetails&id=534399.

MOORE, H.B. & SPROSTON, N.G. 1940. Further Observations on the Colonization of a New Rocky Shore at Plymouth. *Journal of Animal Ecology*, **9**: 319–327.

MORO, L. & ORTEA, J. 2015. New taxa ofsea slugs ofthe Canary Islands and Cape Verde Islands (Mollusca: Heterobranchia). *VIERAEA*, **43**: 21–86.

NAKANO, R. & HIROSE, E. 2011. Field Experiments on the Feeding of the Nudibranch *Gymnodoris* spp . (Nudibranchia: Doridina: Gymnodorididae) in Japan. *The Veliger*, **51**: 66–75.

NAKANO, R., UOCHI, J., FUJITA, T. & HIROSE, E. 2011. *Kalinga ornata* Alder & Hancock, 1864 (Nudibranchia: Polyceridae): A unique case of a sea slug feeding on echinoderms. *Journal of Molluscan Studies*, **77**: 413–416.

NIXON, K.C. & WHEELER, Q.D. 1990. An Amplification of the Phylogenetic Species Concept. *Cladistics*, **6**: 211–223.

NOBRE, A. 1938. Moluscos marinhos e das águas salobras. *Fauna Malacológica do Portugal*, **32**: 808.

NYGREN, A., EKLÖF, J. & PLEIJEL, F. 2010. Cryptic species of *Notophyllum* (Polychaeta: Phyllodocidae) in Scandinavian waters. *Organisms Diversity and Evolution*, **10**: 193–204.

NYLANDER, J.A.A., RONQUIST, F., HUELSENBECK, J.P. & NIEVES-ALDREY, J.L. 2004. Bayesian Phylogenetic Analysis of Combined Data. *Systematic Biology*, **53**: 47–67.

ODHNER, N.H. 1907. Northern and Arctic invertebrates in the collection of the Swedish State Museum (Riksmuseum). III. Opisthobranchia and Pteropoda. *Kongliga Svenska vetenskaps-akademiens handlingar*, **41**: 1–118.

ODHNER, N.H. 1926. Nudibranchs and lamellarids from the Trondhjem fjord. *Det Kongelige Norske Videnskabers Selskabs Skrifter*, 1–36.

ODHNER, N.H. 1939. Opisthobranchiate mollusca from the western and northern coasts of Norway. *Det Kongelige Norske Videnskabers Selskabs Skrifter*, 1–92.

ORTEA, J., PÉREZ, J. & LLERA, E.M. 1982. Moluscos opistobranquios recolectados durante el plan de bentos circuncanario. *Cuadernos del CRINAS*, **3**: 1–48.

ORTEA, J. & MORO, L. 2016. New data on the genus *Jorunna* Bergh, 1876 (Mollusca: Nudibranchia: Discodorididae) in Macaronesia and the Caribbean Sea. *Vieraea*, **44**: 25–52.

ORTEA, J., MORO, L., BACALLADO, J.J. & CABALLER, M. 2014. New species and first records of sea slugs (Mollusca: Opisthobranchia) in the Canary Islands and other archipelagos in the Macaronesia. *Vieraea*, **42**: 47–77.

PALUMBI, S.R., MARTIN, A., ROMAN, S., MCMILLAN, W., STICE, L. & GRABOWSKI, G. 1991. The Simple Fool's guide to PCR. *Department of Zoology and Kewalo Laboratory (Online)*.

PENNEY, B.K. 2008. Phylogenetic comparison of spicule networks in cryptobranchiate dorid nudibranchs (Gastropoda, Euthyneura, Nudibranchia, Doridina). *Acta Zoologica*, **89**: 311–329.

PERRONE, A.S. 1983. Opistobranchi (Aplysiomorpha, Pleurobrancomorpha, Sacoglossa, Nudibranchia) del litorale salentino (Mar Jonio) (Elenco — contributo secondo). *Thalassia Salentina*, **13**: 118–144.

PERRONE, A.S. 1986. Il genere *Baptodoris* in Mediterraneo: Nuovi dati sulla morfologia di *Baptodoris perezi* Llera & Ortea, 1982 dal Golfo di Taranto (Opisthobranchia Nudibranchia). *Bollettino Malacologico*, **22**: 277–284.

PFENNINGER, M. & SCHWENK, K. 2007. Cryptic animal species are homogeneously distributed among taxa and biogeographical regions. *BMC Evolutionary Biology*, **7**: 1–6.

PICTON, B.E. & MORROW, C.C. 1994. *A Field Guide to the Nudibranchs of the British Isles*. Immel Publishing Limited, London.

POLA, M. & GONZÁLEZ DUARTE, M.M. 2008. Is self-fertilization possible in nudibranchs? *Journal of Molluscan Studies*, **74**: 305–308.

POLA, M., PADULA, V., GOSLINER, T.M. & CERVERA, J.L. 2014. Going further on an intricate and challenging group of nudibranchs: Description of five novel species and a more complete molecular phylogeny of the subfamily Nembrothinae (Polyceridae). *Cladistics*, **30**: 607–634.

POLA, M., ROLDÁN, P. & PADILLA, S. 2014. Molecular data on the genus *Okenia* (Nudibranchia: Goniodorididae) reveal a new cryptic species from New South Wales (Australia). *Journal of the Marine Biological Association of the United Kingdom*, **94**: 587–598.

PRKIĆ, J., PETANI, A., IGLIĆ, Đ. & LANČA, L. 2018. *Opisthobranchs of the Adriatic Sea: Photographic Atlas and List of Croatian species*. Ronilački klub Sveti Roko, Bibinje.

PRUVOT-FOL, A. 1954. Mollusques Opisthobranches. *Faune de France*, **58**: 1–460.

PUILLANDRE, N., LAMBERT, A., BROUILLET, S. & ACHAZ, G. 2012. ABGD, Automatic Barcode Gap Discovery for primary species delimitation. *Molecular Ecology*, **21**: 1864–1877.

RAMBAUT, A. 2009. *FigTree: tree figure drawing tool version*.

RAMBAUT, A., DRUMMOND, A.J., XIE, D., BAELE, G. & SUCHARD, M.A. 2018. Posterior summarization in Bayesian phylogenetics using Tracer 1.7. *Systematic Biology*, **67**: 901–904.

RAUCH, C. & MALAQUIAS, M.A.E. 2019. Sea slugs of southern Norway - an example of citizens contributing to science. *The Malacologist*, **73**: 23–27.

RICHARDS, R.A. 2010. *The Species Problem: A Philosophical Analysis*. Cambridge University Press, New York.

RIVEST, B.R. 1984. Copulation by Hypodermic Injection in the Nudibranchs *Palio zosterae* and *P. dubia* (Gastropoda, Opisthobranchia). *The Biological Bulletin*, **167**: 543–554.

ROS, J. 1978. Distribució en l'espai i en el temps dels opistobranquis Ibèrics, amb especial referència als del litoral Català. *Butlletí de la Institució Catalana d'Història Natural*, **42**: 23–32.

RUDMAN, W.B. & AVERN, G.J. 1989. The genus *Rostanga* Bergh, 1879 (Nudibranchia: Doridiidae) in the Indo-West Pacific. *Zoological Journal of the Linnean Society*, **96**: 281–338.

RUDMAN, W.B. & WILLAN, R. 1998. Opisthobranchia. In: *Mollusca: The Southern Synthesis.* Vol. 5 (P.L. Beesley, G.J.B. Ross & A.Wells, eds), pp. 915–942. CSIRO Publishing, Melbourne.

SAKAMOTO, Y., ISHIGURO, M. & KITAGAWA, G. 1986. *Akaike information criterion statistics*. D. Reidel, Dordrecht: The Netherlands.

SALES, L., QUEIROZ, V., PADULA, V., NEVES, E.G. & JOHNSSON, R. 2013. New records of nudibranchs (Mollusca: Gastropoda) from Bahia State, northeastern Brazil. *Check List*, **9**: 689–691.

SALTIK, A.T. 2005. Sea Slug Forum, accessed July 15, 2020, available at http://www.seaslugforum.net/find/14848.

SALVINI-PLAWEN, L. 1972. Cnidaria as Food-Sources for Marine Invertebrates. *Cahiers de Biologie Marine*, **13**: 385–400.

SÁNCHEZ TOCINO, L. 2003. *Aspectos taxonómicos y biológicos de los Doridoidea (Mollusca: Nudibranchia) del litoral Granadino*. Universidad de Granada.

SCARPA, F., COSSU, P., LAI, T., SANNA, D., CURINI-GALLETTI, M. & CASU, M. 2016. Meiofaunal cryptic species challenge species delimitation: The case of the *Monocelis lineata* (Platyhelminthes: Proseriata) species complex. *Contributions to Zoology*, **85**: 123–145.

SCHMEKEL, L. & PORTMANN, A. 1982. *Opisthobranchia des Mittelmeeres. Nudibranchia und Sacoglossa*. Springer Verlag, Heidelberg.

SHAFFER, H.B. & THOMSON, R.C. 2007. Delimiting Species in Recent Radiations. *Systematic Biology*, **56**: 896–906.

SØRENSEN, C.G., RAUCH, C., POLA, M. & MALAQUIAS, M.A.E. 2020. Integrative taxonomy reveals a cryptic species of the nudibranch genus *Polycera* (Polyceridae) in European waters. *Journal of the Marine Biological Association of the United Kingdom*, 1–20.

STAMATAKIS, A. 2014. RAxML version 8: A tool for phylogenetic analysis and post-analysis of large phylogenies. *Bioinformatics*, **30**: 1312–1313.

STRUCK, T.H., FEDER, J.L., BENDIKSBY, M., BIRKELAND, S., CERCA, J., GUSAROV, V.I., KISTENICH, S., LARSSON, K.-H., LIOW, L.H., NOWAK, M.D., STEDJE, B., BACHMANN, L. & DIMITROV, D. 2018. Finding Evolutionary Processes Hidden in Cryptic Species. *Trends in Ecology and Evolution*, **33**: 153–163.

STUART, B.L., INGER, R.F. & VORIS, H.K. 2006. High level of cryptic species diversity revealed by sympatric lineages of Southeast Asian forest frogs. *Biology Letters*, **2**: 470–474.

SWEDMARK, B. 1964. The interstitial fauna of marine sand. *Biological Reviews*, **39**: 1–42.

SWENNEN, C. 1961. Data on Distribution, Reproduction and Ecology of the Nudibranchiate Molluscs Occurring in the Netherlands. *Netherlands Journal of Sea Research*, **1**: 191–240.

THERMO FISCHER SCIENTIFIC. 2019. Loading Dyes and Buffers-Thermo Scientific: Buffer for electrophoresis, accessed February 26, 2020, available at https://www.thermofisher.com/no/en/home/brands/thermo-scientific/molecular-biology/thermo-scientific-nucleic-acid-electrophoresis-purification/dna-electrophoresis-thermo-scientific/loading-dyes-buffers.html#buffers.

THOMPSON, T.E. 1960. Defensive Adaptations in Opisthobranchs. *Journal of the Marine Biological Association of the UK*, **39**: 123–134.

THOMPSON, T.E. 1961. The importance of the larval shell in the classification of the Sacoglossa and the Acoela (Gastropoda Opisthobranchia). *Proceedings of the Zoological Society of London*, **34**: 233–238.

THOMPSON, T.E. 1966. Studies on the Reproduction of *Archidoris pseudoargus* (Rapp) (Gastropoda Opisthobranchia). *Philosophical Transactions of the Royal Society of London*, **250**: 343–374.

THOMPSON, T.E. 1967. Direct development in a nudibranch, *Cadlina laevis*, with a discussion of developmental processes in Opisthobranchia. *Journal of the Marine Biological Association of the United Kingdom*, **47**: 1–22.

THOMPSON, T.E. 1976. *Biology of Opisthobranch Molluscs Volume I*. Ray Society, London.

THOMPSON, T.E. 1988. *Molluscs: Benthic Opisthobranchs*. (D.M. Kermack & R.S.K. Barnes, eds). Brill, E.J. and Dr. W. Backhuys, Bristol.

THOMPSON, T.E. & BROWN, G.H. 1984. *Biology of Opisthobranch Molluscs Volume II*. Ray Society, London.

TIBIRIÇÁ, Y., MALAQUIAS, M.A.E., POLA, M., GOSLINER, T.M. & CERVERA, J.L. 2019. How the Famous Nudibranch *Hexabranchus sanguineus* (Rüppell & Leuckart, 1830) has Fooled Everyone - Preliminary Results. *Abstract Volume*pp. 296. World Congress of Malacology, Pacific Grove, California.

TIBIRIÇÁ, Y., POLA, M. & CERVERA, J.L. 2017. Astonishing diversity revealed: an annotated and illustrated inventory of Nudipleura (Gastropoda: Heterobranchia) from Mozambique. *Zootaxa*, **4359**: 1–133.

TIBIRIÇÁ, Y., POLA, M. & CERVERA, J.L. 2018. Systematics of the genus *Halgerda* Bergh, 1880 (Heterobranchia: Nudibranchia) of Mozambique with descriptions of six new species. *Invertebrate Systematics*, **32**: 1388–1421.

TODD, C.D. 1979. The population ecology of *Onchidoris bilamellata* (L.) (Gastropoda: Nudibranchia). *Journal of Experimental Marine Biology and Ecology*, **41**: 213–255.

TODD, C.D. 1981. The Ecology of Nudibranch Molluscs. *Oceanography and Marine Biology, An Annual Review*, **19**: 141–234.

TODD, C.D. 1983. *Reproductive and Trophic Ecology of Nudibranch Molluscs*. *Ecology*. Academic Press, Inc.

TODD, C.D. & HAVENHAND, J.N. 1985. Preliminary observations on the embryonic and larval development of three dorid nudibranchs. *Journal of Molluscan Studies*, **51**: 97–99.

TODD, C.D., LAMBERT, W.J. & DAVIES, J. 2001. Some perspectives on the biology and ecology of nudibranch molluscs: generalisations and variations on the theme that prove the rule. *Malacologico*, **37**: 105–120.

VALDÉS, Á. 2002. A phylogenetic analysis and systematic revision of the cryptobranch dorids (Mollusca, Nudibranchia, Anthobranchia). *Zoological Journal of the Linnean Society*, **136**: 535–636.

VALDÉS, Á. 2003. Preliminary molecular phylogeny of the radula-less dorids (Gastropoda: Opisthobranchia), based on 16S mtDNA sequence data. *Journal of Molluscan Studies*, **69**: 75–80.

VALDÉS, Á. & GOSLINER, T.M. 2001. Systematics and phylogeny of the caryophyllidia-bearing dorids (Mollusca, Nudibranchia), with descriptions of a new genus and four new species from Indo-Pacific deep waters. *Zoological Journal of the Linnean Society*, **133**: 103–198.

VALDÉS, Á., MURILLO, F.J., MCCARTHY, J.B. & YEDINAK, N. 2017. New deep-water records and species of North Atlantic nudibranchs (Mollusca, Gastropoda: Heterobranchia) with the description of a new species. *Journal of the Marine Biological Association of the United Kingdom*, **97**: 303–319.

VON IHERING, H. 1886. Beiträge zur Kenntnis der Nudibranchien des Mittelmeeres II. 4. Die Polyceraden. *Malakozoologische Blätter*, **8**: 12–48.

WARD, R.D., COSTA, F.O., HOLMES, B.H. & STEINKE, D. 2008. DNA barcoding of shared fish species from the North Atlantic and Australasia: minimal divergence for most taxa, but *Zeus faber* and *Lepidopus caudatus* each probably constitute two species. *Aquatic Biology*, **3**: 71–78.

WÄGELE, H. 1989. Diet of some Antarctic nudibranchs (Gastropoda, Opisthobranchia, Nudibranchia). *Marine Biology*, 439–441.

WÄGELE, H.. 1991. The Distribution of Some Endemic Antarctic Nudibranchia. *Journal of Molluscan Studies*, **57**: 337–345.

WÄGELE, H. 1998. Histological Investigation of Some Organs and Specialised Cellular Structures in Opisthobranchia (Gastropoda) with the Potential to Yield Phylogenetically Significant Characters. *Zoologischer Anzeiger*, **236**: 119–131.

WÄGELE, H. & KLUSSMANN-KOLB, A. 2005. Opisthobranchia (Mollusca, Gastropoda) - More than just slimy slugs. Shell reduction and its implications on defence and foraging. *Frontiers in Zoology*, **2**: 1–18.

WÄGELE, H., KLUSSMANN-KOLB, A., VERBEEK, E. & SCHRÖDL, M. 2014. Flashback and foreshadowing - A review of the taxon Opisthobranchia. *Organisms Diversity and Evolution*, **14**: 133–149.

WÄGELE, H. & WILLAN, R.C. 2000. Phylogeny of the Nudibranchia. *Zoological Journal of the Linnean Society*, **130**: 83–181.

WEISS, M., MACHER, J.N., SEEFELDT, M.A. & LEESE, F. 2014. Molecular evidence for further overlooked species within the *Gammarus fossarum* complex (Crustacea: Amphipoda). *Hydrobiologia*, **721**: 165–184.

WHEELER, Q.D. & MEIER, R. 2000. *Species concepts and phylogenetic theory*. Columbia University Press, New York.

WIECZOREK, J., DÖRING, M., DE GIOVANNI, R. ROBERTSON, T. & VIEGLAIS, D. 2009. Darwin Core, accessed February 18, 2020, available at http://www.tdwg.org/standards/450/.

WILSON, N.G. & BURGHARDT, I. 2015. Here be dragons - phylogeography of *Pteraeolidia ianthina* (Angas, 1864) reveals multiple species of photosynthetic nudibranchs (Aeolidina: Nudibranchia). *Zoological Journal of the Linnean Society*, **175**: 119–133.

WOLTER, H. 1967. Beiträge zur Biologie, Histologie und Sinnesphysiologie (insbesondere der Chemorezeption) einiger Nudibranchia (Mollusca, Opisthobranchia) der Nordsee. *Zeitschrift für Morphologie und Ökologie der Tiere*, **60**: 275–337.

YONOW, N. 2015. Sea Slugs: Unexpected Biodiversity and Distribution. In: *Sea Slugs of the Red Sea*, pp. 531–550. Pensoft Publishers.

ZACHOS, F.E. 2016. *Species Concepts in Biology. Historical Development, Theoretical Foundations and Practical Relevance*. Springer International Publishing Switzerland.

ZENETOS, A., MACIC, V., JAKLIN, A., LIPEJ, L., POURSANIDIS, D., CATTANEO-VIETTI, R., BEQIRAJ, S., BETTI, F., POLONIATO, D., KASHTA, L., KATSANEVAKIS, S. & CROCETTA, F. 2016. Adriatic "opisthobranchs" (Gastropoda, Heterobranchia): shedding light on biodiversity issues. *Marine Ecology*, **37**: 1–17.

Appendix I: Molecular work

A. DNA extraction using the Qiagen DNeasy Blood and Tissue Kit (Ref. No. 69506)

Prior to DNA extraction, tissue samples were exposed to air for the ethanol to evaporate to prevent the alcohol from inhibiting the DNA extraction. When dry, 180 µl of lysis ATL buffer and 20 µl proteinase K were added to each sample, relaxing the DNA helix and denaturing proteins, respectively. Each tube was vortexed for 3 seconds, centrifuged and set to over-night incubation on a heat block (56°C) for the lysis and denaturation to take place. Next, samples were vortexed for 15 seconds and centrifuged. 200 µl AL buffer was added, followed by an immediate quick vortex to assure a homogenous solution. Thereafter, 200µl absolute ethanol was added prior to another quick vortex. Both the AL buffer and the ethanol help attaching the DNA to the filter. The solutions were so transferred to mini spin columns (filtering tubes inside a collection tube). The columns were centrifuged for 1 minute at 8000 rounds per minute (rpm) and fluids that had run through the filter into the collection tube were discarded as waste. DNA was so washed adding 500 µl AW1 precisely onto each filter followed by centrifugation (1 min., 8000 rpm). Waste was discarded and the protocol repeated adding 500 µl AW2 washing buffer. After centrifugation, waste fluid was discarded from the columns. Filtering tubes were so placed back in the respective collection tubes and centrifugation (3 min., 13000 rpm) was repeated to ensure removal of all liquid contamination and ethanol leftovers. Next, the filtering tubes were transferred to Eppendorf tubes (1.5 ml) and 200 µl AE buffer added onto the filter. To assure the DNA to be released from the filter, samples were incubated on the bench for 2-5 minutes (~25°C) prior to centrifugation (1 min., 8000 rpm). The protocol was repeated, adding 100 µl AE buffer. The filtering tubes were so discarded and each Eppendorf tube, containing the DNA extract, annotated with the respective sample ID (code J, number 1–71; Table A).

B. Preparing for polymerase chain reaction (PCR)

Polymerase chain reaction (PCR) amplifications were run on the three gene markers COI, 16S, and H3 with a total amplification volume of 50 µl. Universal primers were diluted from 100 µM to 10 µM (total volume 100 µl) adding 10 µl primer and 90 µl Sigma-Aldrich water. Master cocktails were generated multiplying the volumes of each reagent needed for one sample by the number of samples to be amplified plus one positive control, one negative control and one extra sample to ensure for pipetting errors. Due to the use of the heat sensitive Taq DNA polymerase I, master cocktails were generated on ice, keeping the cocktails' temperature low. Taq DNA polymerase I was added at last to prevent the enzyme from activating too early and immediately

placed back in the freezer when done. After a quick vortex and spin, each 49 µl of the master cocktail was added to the microfuge tubes (0.2 ml) designated with each their sample ID. To prevent pre-PCR preparations to be contaminated with DNA, DNA from each sample (1 µl) was added in a separate room, being the last step before the microfuge tubes were placed in the thermal cycler for PCR.

Remarks

Reducing the total PCR amplification volume from 50 µl to 25 µl showed to result in equal outcomes. To save reagents and expenses, the volume for most samples amplified was halved to 25 µl. Reagent volumes for generating the master cocktails were halved, respectively (see 3.2).

C. Preparation of agarose gel

The agarose gel was generated adding 2 grams agarose (dry weight) to 200 ml 1% TAE (Tris-acetate-EDTA) buffer, commonly used to run agarose gel electrophoresis on longer nucleic acid fragments. The buffer is compatible with the enzyme reactions and works by separating the DNA and/or RNA (Thermo Fischer Scientific, 2019). Processing of the agarose gel was initiated using microwave heating followed by magnetic mixing using the IKARRCT basic safety control mixer. The gel was properly mixed when turned from milky to transparent. When not in use, the agarose gel was stored at 65°C to prevent stiffening.

D. Gel electrophoresis

Gel electrophoresis was performed using an electrophoresis chamber and a UVT gel-tray. The tray was placed into the chamber in a casting position functioning as an agarose gel platform preventing the gel from leaking out into the chamber pools. Combs were placed in the tray to create wells for the PCR products to be pipetted in. Warm and fluent agarose gel (30 ml/50 ml; total volume depending on size of chamber) was blended with GelRed (1 µl/3µl) prior to adding the solution to the tray. The agarose gel was left on the bench for approximately 20 minutes to stiffen. When stiffened, the combs were removed. 1x TAE buffer was added to the chamber pools, covering the agarose gel, and filling the wells. Four µl PCR product was blended with 1 µl Ficoll 5x loading dye (bromophenol blue dye) for the liquid to sink down into the wells. In addition, one well of each row was added 5 µl of FastRuler ladder marker as a reference for the DNA band lengths and concentrations. At last, the chamber was closed and run on 80V for about 20 minutes. The results were studied placing the gel in a UV-radiation machine (Syngene,

Cambridge, UK), equipped with a chemiluminescent sensitive video camera. Gel bands were visualized, and DNA quantity estimated using GeneSnap (v. 701) and GeneTools (v. 4.0) (Syngene, Cambridge, UK). Radiation exposure was set to 560 milliseconds.

An excessive quantity of DNA in the PCR sequencing reactions can result in deficits of the BigDye products, using up the BigDye before all samples have been sequenced. To prevent this, band lengths (number of base pairs) and DNA content (measured in nano grams) were estimated with the aid of the ladder. This way, PCR products containing too high quantities of DNA were diluted prior to sequencing.

E. Purification of PCR products

PCR products were purified using EXOSAP, a combination of Exonuclease I (EXO I) and Shrimp Alkaline Phosphatase (SAP). The master cocktail for one sample contained 0.1 µl EXO, 1.0 µl SAP, and 0.9 µl Sigma-Aldrich water and was prepared in a tube kept on ice. Standard quantities were multiplied according to the number of samples to be purified plus one extra unit to account for pipetting error. The master cocktail was gently mixed and centrifuged. Two µl cocktail were so added to 8 µl PCR product in each its 0.2 ml microfuge tube kept on ice, and gently mixed and centrifuged. The samples were so transferred to a thermal cycler and purified setting the conditions to 37°C for 30 minutes, 85°C for 15 minutes, and a final 4°C for cooling.

Remarks

PCR products containing too high quantities of DNA were diluted prior to the purification. Instead of adding the standard volume of 8 µl PCR product, the volume was decreased to 1 or 2 µl DNA product (depending on the DNA quantity estimation), replacing the excess volume with Sigma-Aldrich water (7 or 6 µl, respectively). Next, each 2 µl EXOSAP master cocktail were added to the diluted samples, resulting in a total reaction volume of 10 µl. The thermal cycling protocol was kept the same for both diluted and non-diluted samples.

F. Preparing the sequencing reactions

Each universal primer was diluted to 3.2 µM adding 34 µl of Sigma-Aldrich water to 16 µl of 10 µM primer. For the primers to be sequenced separately, each one master cocktail was prepared for each of the primers (forward 5’→ 3’ and reverse 3’ → 5’). Master cocktails for each primer were blended in reaction tubes kept on ice, adding 6 µl Sigma-Aldrich water, 1 µl of primer (3.2 µM), 1 µl BigDye and 1 µl sequencing buffer. One µl of each purified PCR

product was pipetted to a 0.2 ml microfuge tube, added by 9 µl master cocktail. The protocol was followed twice, given one set containing the forward, and one set containing the reverse primer. After a gentle mix and spin the samples were transferred to a thermal cycler setting the conditions to 96°C for 5 minutes, 96°C for 10 seconds, 50°C for 5 seconds, 60°C for 4 minutes, 72°C for 5 minutes, and a final 8°C for cooling. Prior to sending the samples to the sequencing laboratory facility at the Department of Biological Sciences, University of Bergen, 10 µl of Sigma-Aldrich water were added to each to obtain a final volume of 20 µl. Sequencing reactions were run on the capillary-based Applied Biosystems 3730XL DNA Analyzer. Chromatograms were obtained from the facilities web portal (accessible at: https://www.uib.no/en/seqlab).

Appendix II: Automatic Barcode Gap Discovery (ABGD)

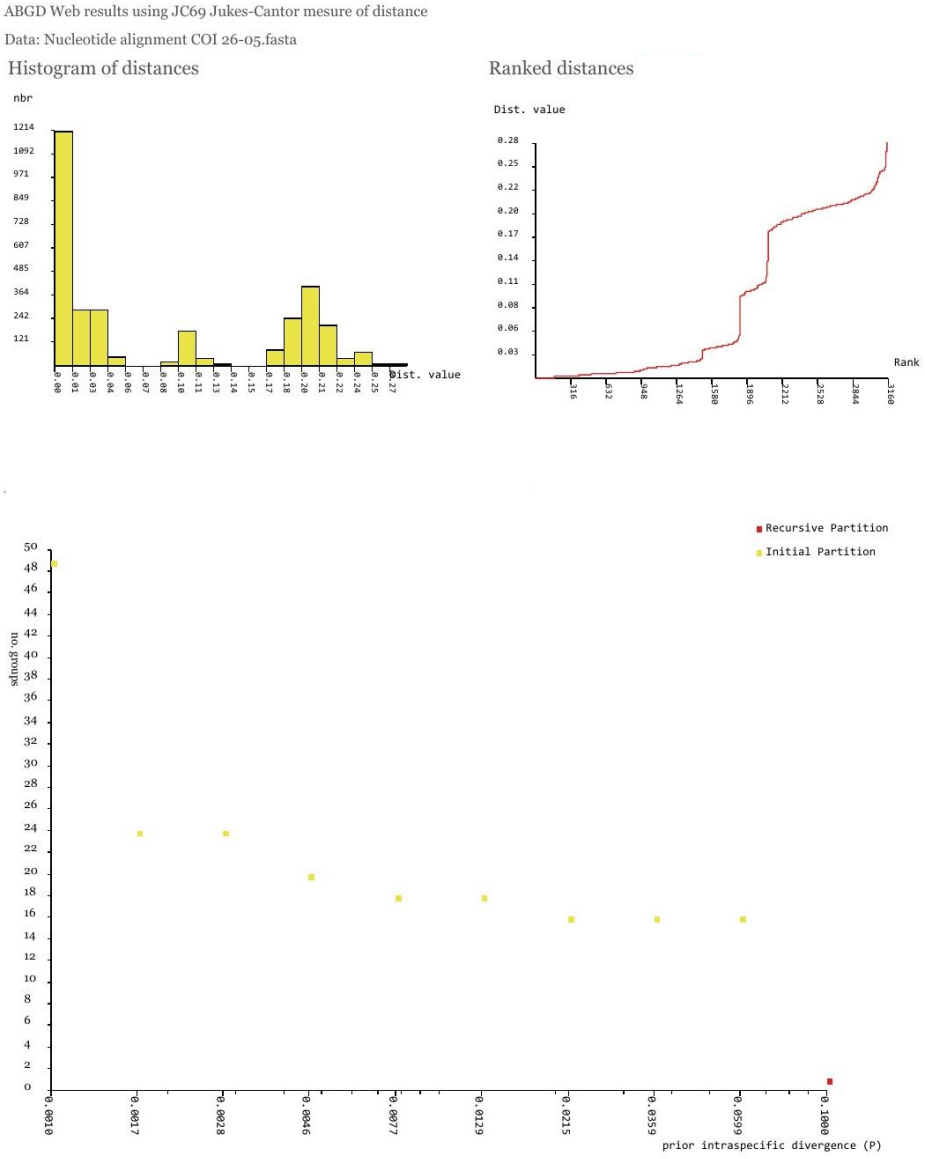

Figure I. ABGD analysis output of the COI alignment including all outgroup species, applying the evolutionary model Jukes Cantor 69.

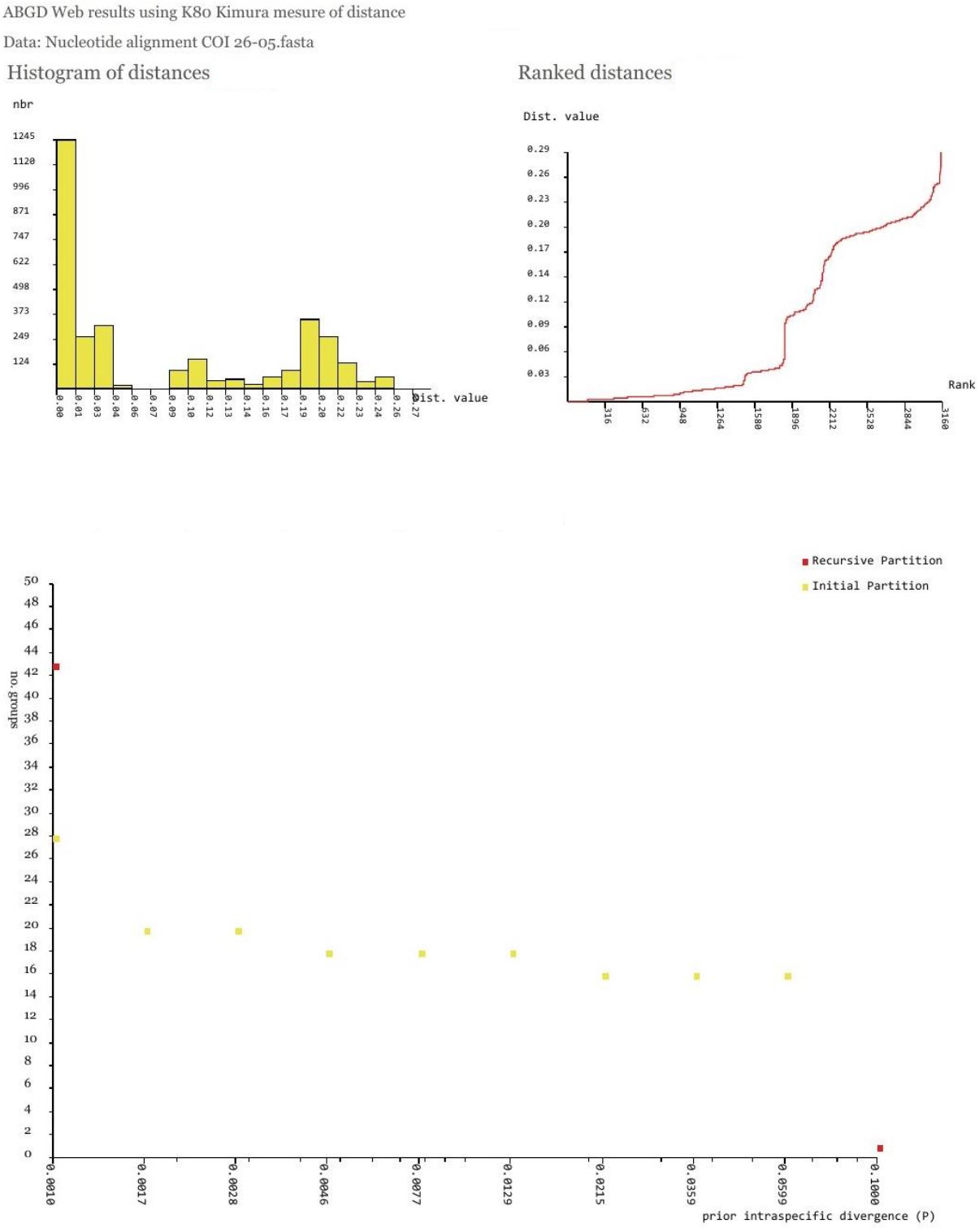

Figure II. ABGD analysis output of the COI alignment including all outgroup species, applying the evolutionary model Kimura 80.

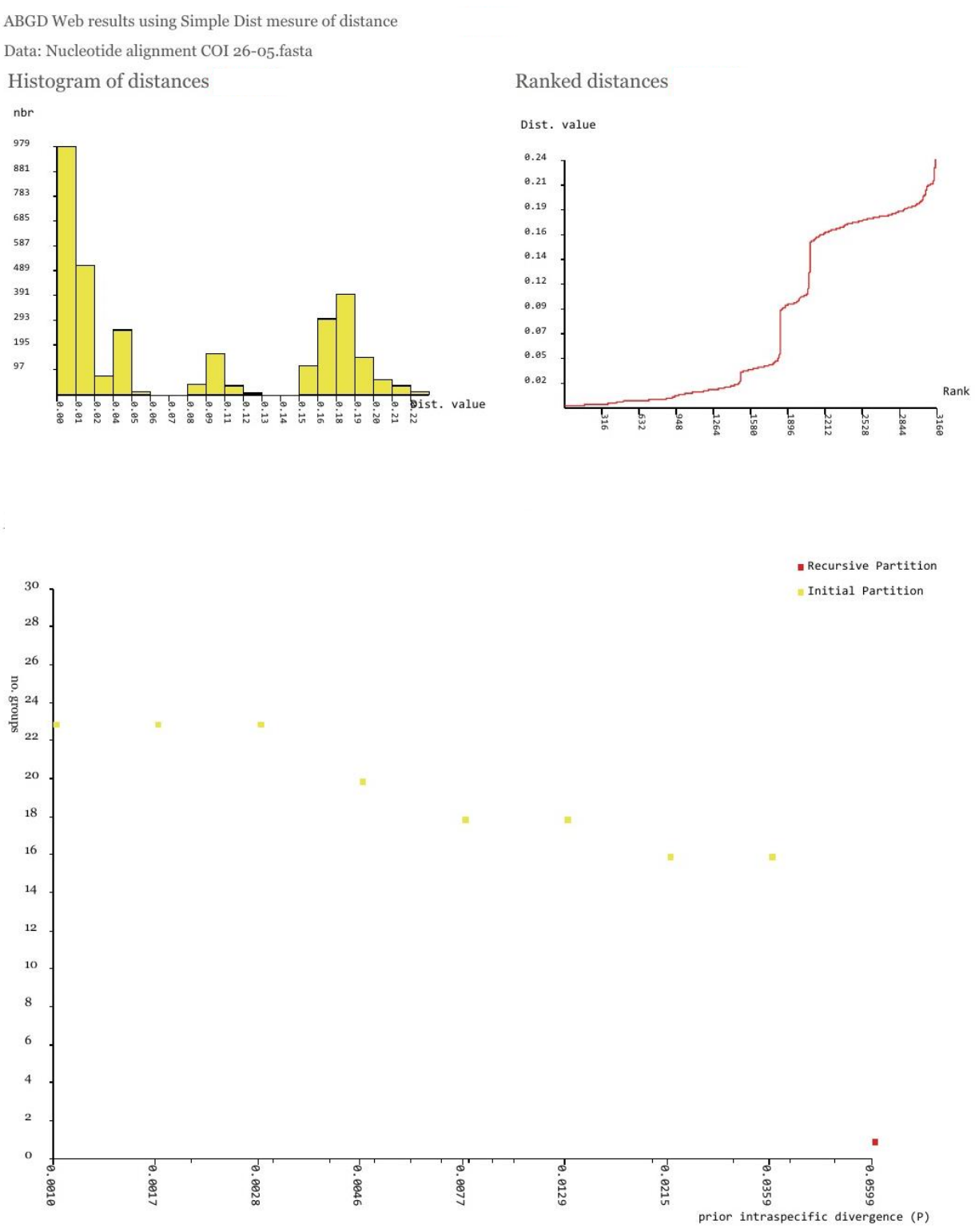

Figure III. ABGD analysis output of the COI alignment including all outgroup species, applying the evolutionary model Simple distance.

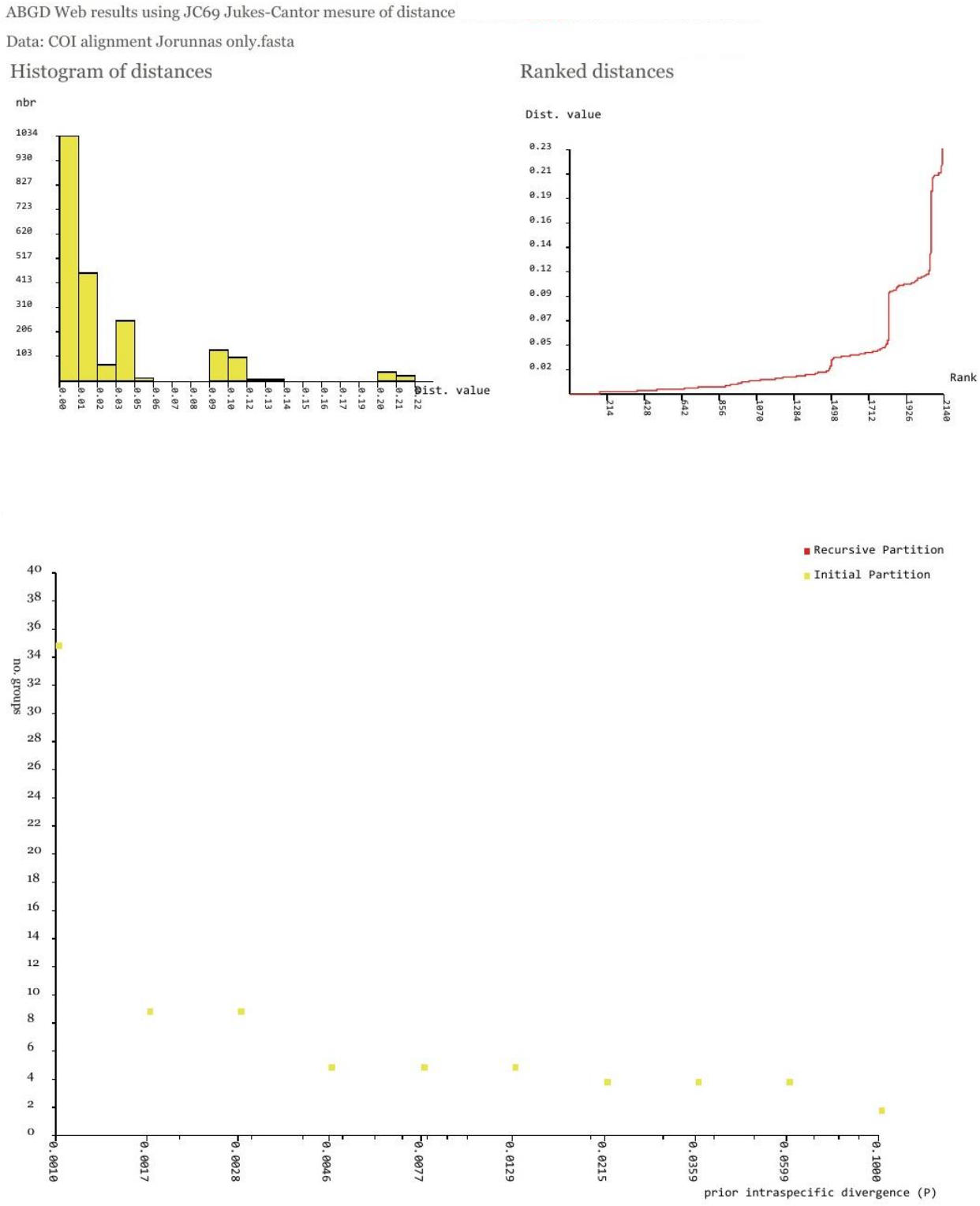

Figure IV. ABGD analysis output of the COI alignment including only species of the genus *Jorunna*, applying the evolutionary model Jukes Cantor 69.

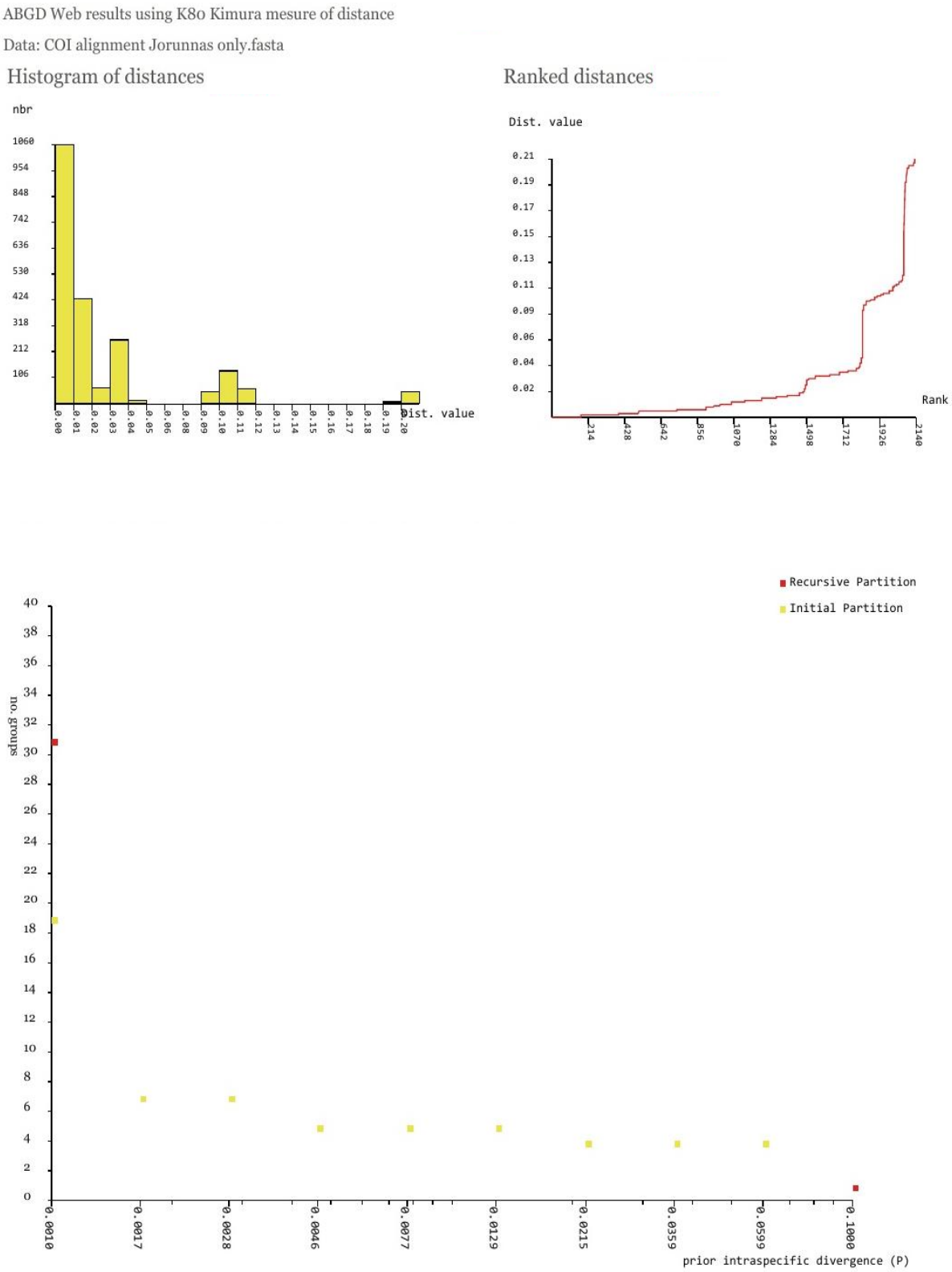

Figure V. ABGD analysis output of the COI alignment including only species of the genus *Jorunna*, applying the evolutionary model Kimura 80.

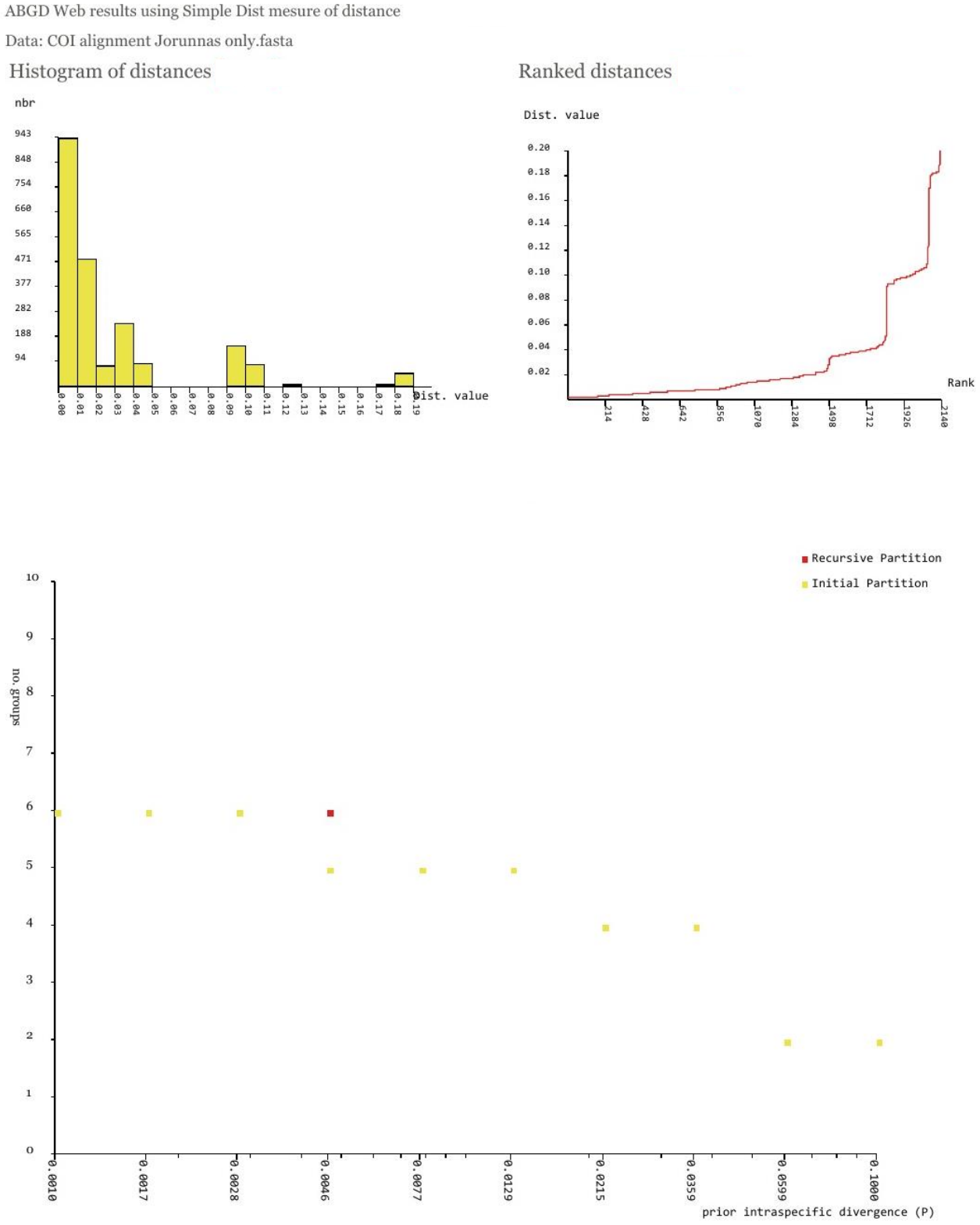

Figure VI. ABGD analysis output of the COI alignment including only species of the genus *Jorunna*, applying the evolutionary model Simple Distance.

Appendix III: Phylogenetic analyses

A. Saturation plots

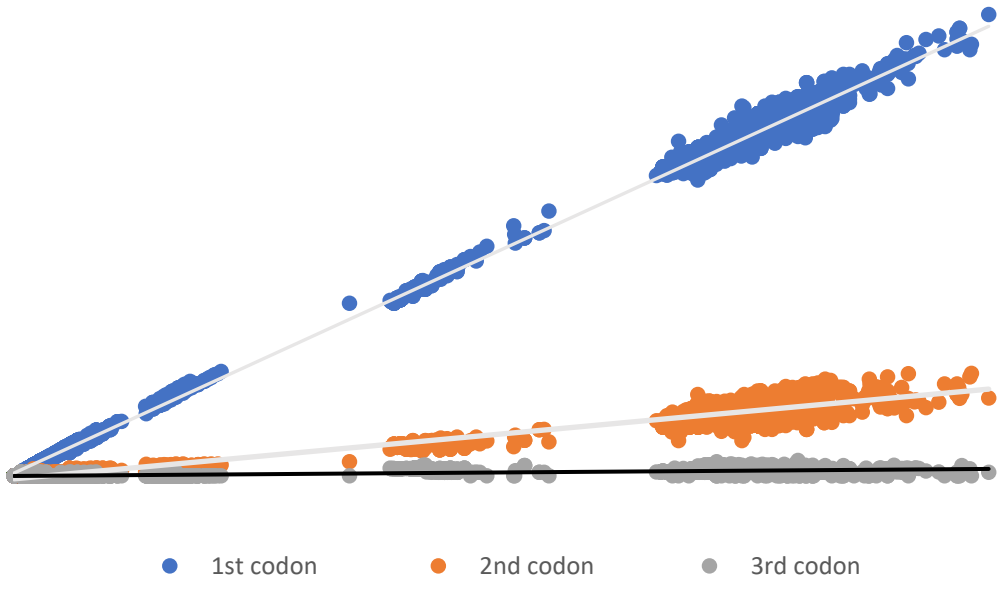

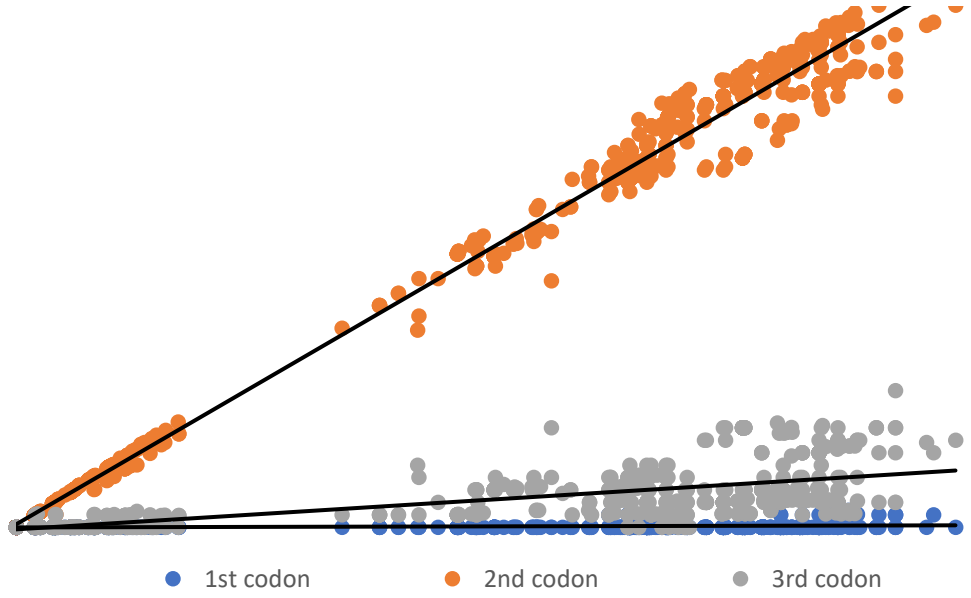

Figure VII. Saturation was tested for first, second, and third codon positions for the protein-coding genes COI (top) and H3 (bottom). No saturation was found.

B. Bayesian inference

```
begin mrbayes;

        set autoclose=yes nowarn=yes;

        charset Subset1 = 1-656;
        charset Subset2 = 657-1140;
        charset Subset3 = 1141-1480;


        partition gene = 3:Subset1, Subset2, Subset3;
        set partition=gene;

        lset applyto=(1) nst=6 rates=invgamma;
        lset applyto=(2) nst=6 rates=invgamma;
        lset applyto=(3) nst=6 rates=propinv;

        prset applyto=(all) ratepr=variable;
        unlink statefreq=(all) revmat=(all) shape=(all) pinvar=(all) tratio=    (all);

        mcmcp ngen=15000000 nruns=3 nchains=4 samplefreq=100 printfreq=10000    savebrlens=yes;
        mcmc;

        sump burnin=37500;
        sumt burnin=37500 contype=halfcompat;


end;
```

Figure VIII. Data script used for the phylogenetic analysis with MrBayes. Here, the alignment used contained three partitions (COI, 16S, H3). For datasets with less partitions, the script was respectively modified

Explanation of the commands

The program was commanded (Figure VIII) not to prompt the user during execution and not prompt the user before overwriting output files (*set autoclose = yes; nowarn = yes).* Starting and ending positions of the concatenated sequences were defined by three subsets (*charset Subset1; Subset2;* Subset3) with respective base pair settings. Partitions were generated for each gene marker (*n* = 3), arranged by subsets. Settings for likelihood models were applied to the three data partitions with each 6 substitution types (*lset applyto=(1);(2);(3) nst=6*). Prior to the Bayesian analysis, evolutionary models were obtained using jModeltest (Darriba *et al.*, 2012; see section 3.3). Each evolutionary model was set for among-site rate variation (*rates*). For COI and 16S (Subset 1 and Subset 2), the evolutionary model was set to General Time Reversible model (GTR) accounting for gamma-distribution (G) across sites and a proportion of invariable sites (I) (*invgamma*). For H3, a model that allows a proportion of sites to be invariable was applied (*propinv*). The parameter settings (*prset*) were applied to all data, using different state frequencies (*statefreq*) between partitions. Parameters for the Markov Chain Monte Carlo (*mcmc*) were set to 15 million generations (*ngen*) run on four parallel chains (*nchains*) for each

of the three independent analyses (*nruns*). Trees were sampled at a frequency of 100 (*samplefreq*) and printed at a frequency of 10000 (*printfreq*). Branch lengths of all trees were saved (*savebrlens=yes*). Posterior probabilities on trees and their respective parameters were obtained in postrun analyses (*sumt, sump*). Here, 25% of the trees were discarded while computing the posterior probabilities (*burnin=37500*). The type of consensus tree was set to a 50% majority rule tree (*contype=halfcompat*) (Huelsenbeck & Ronquist, 2001).

Bayesian inference phylograms: 16S and S16S

(see next page)

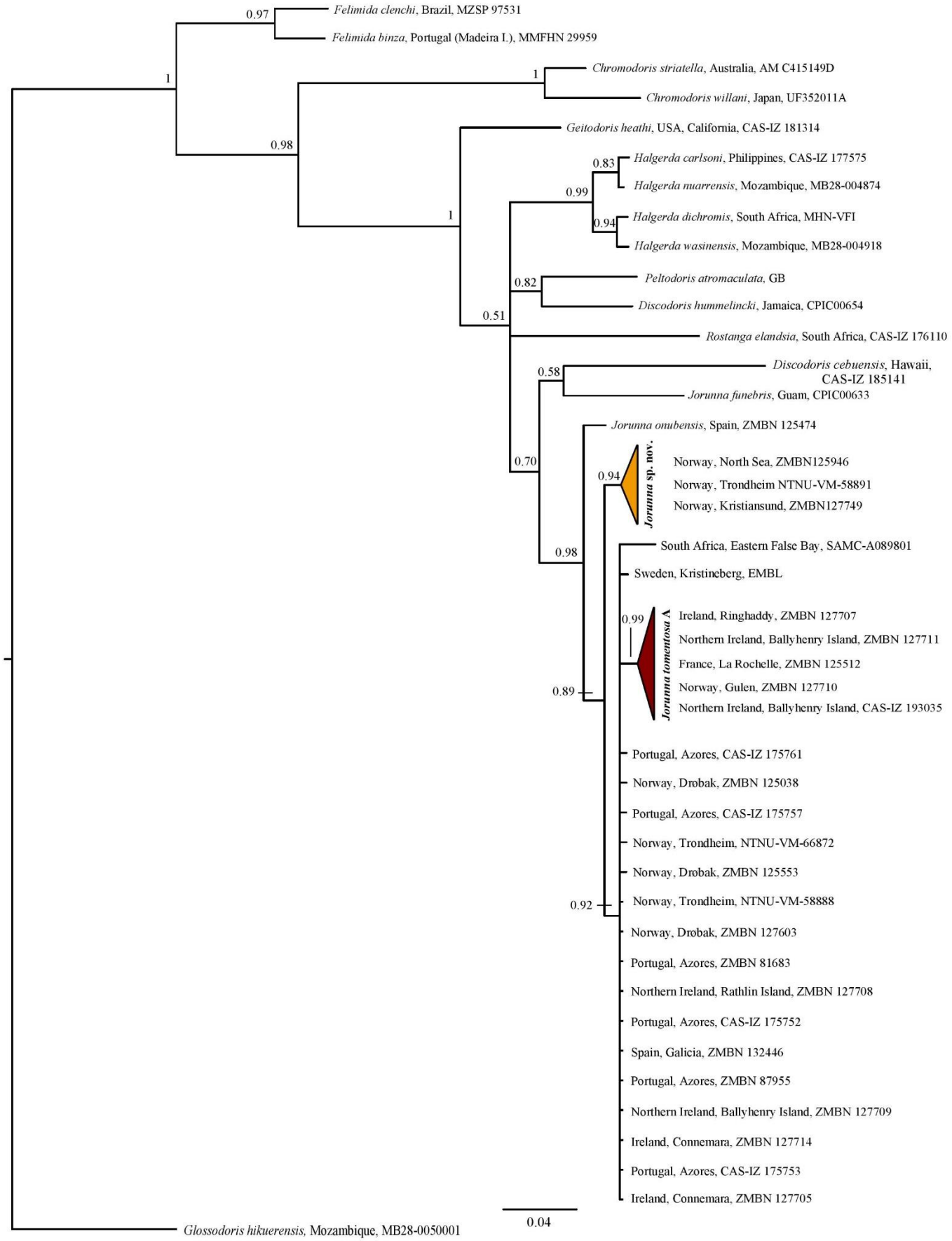

Figure IX. Phylogenetic hypothesis resulting from the 16S dataset based on Bayesian analysis. Numbers on branches refer to posterior probabilities. Tree rooted with *Glossodoris hikuerensis*.

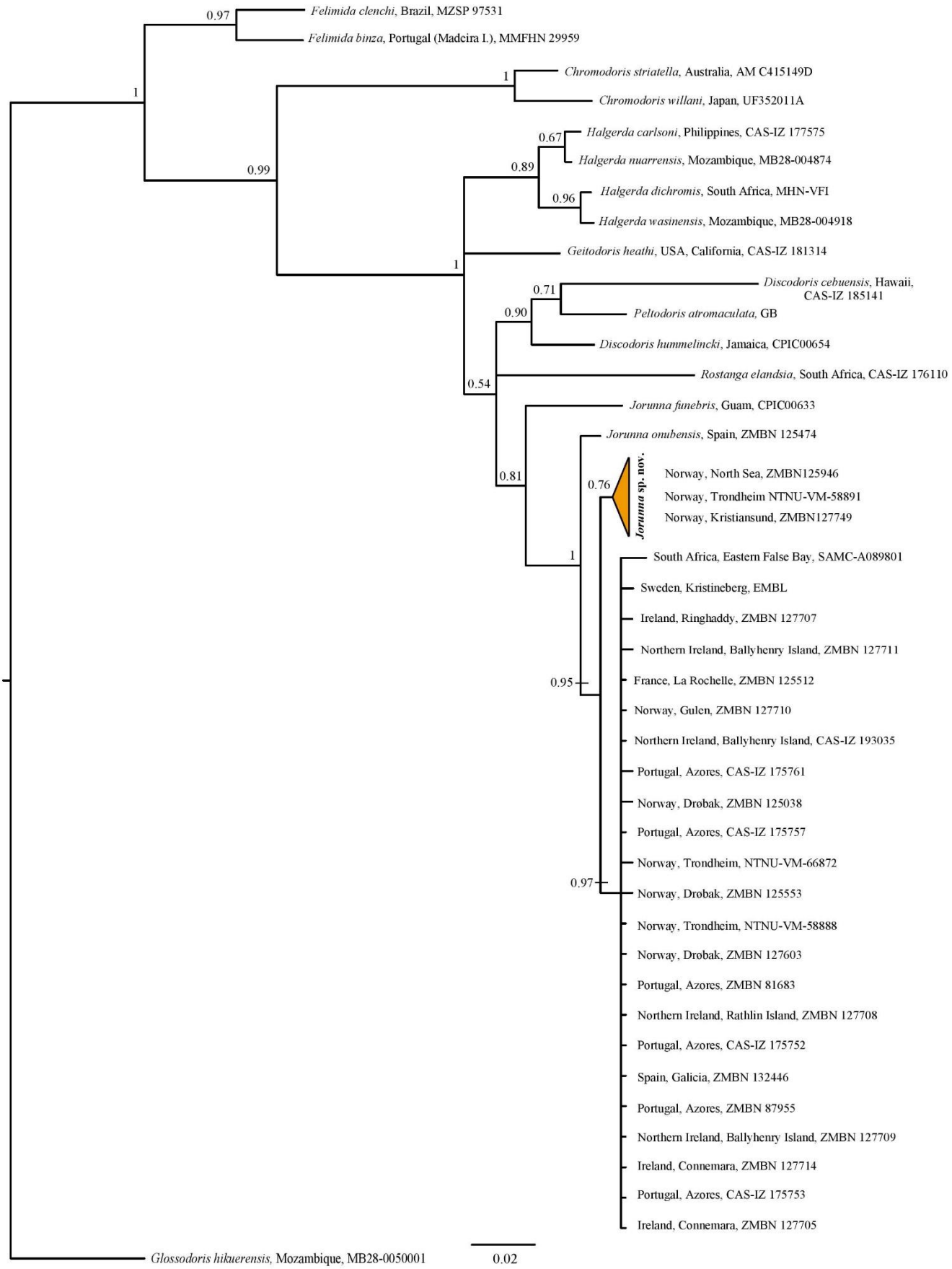

Figure X. Phylogenetic hypothesis resulting from the stringent 16S (S16S) dataset based on Bayesian analysis. Numbers on branches refer to posterior probabilities. Tree rooted with *Glossodoris hikuerensis*.

Appendix IV: Examined material

(see next page for Table A and Table B)

Table A. List of specimens used for DNA amplification with information on respective sampling coordinates and fixed specimen length. Species names are given according to the phylogenetic hypotheses, yielding *Jorunna* sp. nov. and two lineages of J. *tomentosa* (A and B). DNA amplification failed for samples marked with an asterisk (*).

Sample ID	Voucher no.	Species name	Locality	Latitude	Longitude	Fixed length (mm)
J01	NTNU-VM-66876	*Jorunna tomentosa* B	Norway: Gulen	60.960225	5.128899	12
J02	NTNU-VM-213	*Jorunna tomentosa* B	Norway: Lofoten	68.334701	13.813291	20
J03	NTNU-VM-66873	*Jorunna tomentosa* B	Norway: Trondheim	63.441109	10.348831	13
J04	NTNU-VM-58888	*Jorunna tomentosa* B	Norway: Trondheim	63.792438	8.89163	10
J05	NTNU-VM-66874	*Jorunna tomentosa* B	Norway: Gulen	60.960225	5.128899	12
J06	NTNU-VM-68601	*Jorunna tomentosa* B	Norway: Gulen	60.960225	5.128899	13
J07*	NTNU-VM-5521	*Jorunna* cf. *tomentosa*	Norway: Trondheim	63.845076	8.631778	10
J08	NTNU-VM-58891	*Jorunna* sp. nov.	Norway: Trondheim	63.845076	8.631778	15
J09	ZMBN 125057	*Jorunna tomentosa* B	Norway: Drøbak	59.64901	10.636139	26
J10	ZMBN 125512	*Jorunna tomentosa* A	France: La Rochelle	46.202646	-1.186523	n/a
J11	NTNU-VM-68525	*Jorunna tomentosa* B	Norway: Gulen	60.960225	5.128899	17
J12	NTNU-VM-66875	*Jorunna tomentosa* B	Norway: Gulen	60.960225	5.128899	12
J13	NTNU-VM-66872	*Jorunna tomentosa* B	Norway: Trondheim	63.441109	10.348831	14
J14	ZMBN 125038	*Jorunna tomentosa* B	Norway: Drøbak	59.64901	10.636139	30
J15	ZMBN 125651	*Jorunna tomentosa* B	Norway: Kristiansund	63.062076	7.695494	26
J16	ZMBN 125644	*Jorunna tomentosa* B	Norway: Kristiansund	63.062076	7.695494	15
J17	ZMBN 125591-1	*Jorunna tomentosa* B	Norway: Averøy	63.114832	7.662235	28
J18	ZMBN 125591-2	*Jorunna tomentosa* B	Norway: Averøy	63.114832	7.662235	n/a
J19	ZMBN 125553	*Jorunna tomentosa* B	Norway: Drøbak	59.64901	10.636139	25
J20	ZMBN 125090	*Jorunna tomentosa* B	Norway: Drøbak	59.64901	10.636139	10
J21	ZMBN 125632	*Jorunna tomentosa* B	Norway: Kristiansund	63.062076	7.695494	25
J22	ZMBN 125878	*Jorunna tomentosa* B	Norway: Haugesund	59.408210	5.377251	13
J23	ZMBN 125946	*Jorunna* sp. nov.	Norway: North Sea	60.726944	0.505371	30
J24	ZMBN 125563	*Jorunna tomentosa* B	Norway: Drøbak	59.64901	10.636139	23
J25	ZMBN 125560	*Aldisa zetlandica*	Norway: Drøbak	59.64901	10.636139	n/a
J26	ZMBN 127553	*Jorunna tomentosa* B	Norway: Egersund	58.417110	5.998327	15
J27	ZMBN 127567	*Jorunna tomentosa* B	Norway: Egersund	58.417110	5.998327	18

Table A. *Continued*.

Sample ID	Voucher no.	Species name	Locality	Latitude	Longitude	Fixed length (mm)
J28	ZMBN 127533	*Doris pseudoargus*	Norway: Egersund	58.417110	5.998327	n/a
J29	ZMBN 125581	*Jorunna tomentosa* B	Norway: Drøbak	59.64901	10.636139	18
J30	ZMBN 127568	*Jorunna tomentosa* B	Norway: Egersund	58.417110	5.998327	12
J31	ZMBN 127577	*Jorunna tomentosa* B	Norway: Drøbak	59.64901	10.636139	17
J32	ZMBN 127603	*Jorunna tomentosa* B	Norway: Drøbak	59.64901	10.636139	25
J33	ZMBN 127593	*Jorunna tomentosa* B	Norway: Drøbak	59.64901	10.636139	12
J34	ZMBN 81683	*Jorunna tomentosa* B	Azores: Faial Island	38.590668	-28.697813	9
J35	ZMBN 87955	*Jorunna tomentosa* B	Azores: São Miguel Island	37.898156	-25.821991	30
J36*	ZMBN 81684	*Jorunna* cf. *tomentosa*	Azores: Faial Island	38.590668	-28.697813	5
J37	ZMBN 127709	*Jorunna tomentosa* B	Northern Ireland: Ballyhenry Island	54.394951	-5.583801	29
J38	ZMBN 127715	*Jorunna tomentosa* B	Ireland, Connemara	53.636815	-9.919531	13
J39	ZMBN 127710	*Jorunna tomentosa* A	Norway: Gulen	60.960225	5.128899	23
J40	ZMBN 127708	*Jorunna tomentosa* B	Northern Ireland: Rathlin Island	55.31138	-6.25667	17
J41	ZMBN 127714	*Jorunna tomentosa* B	Ireland: Connemara	53.62906	-9.872399	14
J42	ZMBN 127704	*Jorunna tomentosa* B	Northern Ireland: Ballyhenry Island	54.393969	-5.578313	32
J43	ZMBN 127713	*Jorunna tomentosa* B	Ireland: Connemara	53.62906	-9.872399	12
J44	ZMBN 127712	*Jorunna tomentosa* B	Norway: Gulen	60.960225	5.128899	14
J45	ZMBN 127706	*Jorunna tomentosa* B	Northern Ireland: Stangford	54.537024	-5.615899	21
J46	ZMBN 127705	*Jorunna tomentosa* B	Ireland: Connemara	53.62906	-9.872399	25
J47	ZMBN 127707	*Jorunna tomentosa* A	Ireland: Ringhaddy	54.451046	-5.631184	30
J48	ZMBN 127711	*Jorunna tomentosa* A	Northern Ireland: Ballyhenry Island	54.394951	-5.583801	30
J49	ZMBN 127749	*Jorunna* sp. nov.	Norway: Kristiansund	63.062076	7.695494	40
J50	ZMBN 127775	*Jorunna tomentosa* B	Norway: Kristiansund	63.062076	7.695494	35
J51*	ZMBN 127740	n/a	Norway: Surnadal	63.008601	8.360252	20
J52	ZMBN 127730	*Jorunna tomentosa* B	Norway: Gjemnes	62.973522	7.784554	12
J53	ZMBN 125474	*Jorunna onubensis*	Spain: Huelva	37.206167	-7.055722	5
J54	CAS-IZ 175753	*Jorunna tomentosa* B	Azores: Faial Island	38.590668	-28.697813	n/a

Table A. *Continued*.

Sample ID	Voucher no.	Species name	Locality	Latitude	Longitude	Fixed length (mm)
J55	CAS-IZ 175752	*Jorunna tomentosa* B	Azores: Faial Island	38.590668	-28.697813	n/a
J56*	CAS-IZ 115215	*Jorunna tomentosa* B	Spain: Asturias, Ovinana	43.582988	-5.976972	30
J57	CAS-IZ 175757	*Jorunna tomentosa* B	Azores: Faial Island	38.590668	-28.697813	12
J58	CAS-IZ 175761	*Jorunna tomentosa* B	Azores: Faial Island	38.590668	-28.697813	9
J59	CAS-IZ 193035	*Jorunna tomentosa* A	Northern Ireland: Ballyhenry Island	54.394951	-5.583801	n/a
J60	CAS-IZ 176820	*Jorunna tomentosa* A	Portugal: Parque Natural da Arrábida	38.439806	-9.053361	n/a
J61*	CAS-IZ 176801	*Jorunna* cf. *tomentosa*	Portugal: Parque Natural da Arrábida	38.439806	-9.053361	n/a
J62	CAS-IZ 176819	*Jorunna tomentosa* B	Portugal: Parque Natural da Arrábida	38.439806	-9.053361	n/a
J63*	ZMBN 132443	n/a	Greece: Elounda, Crete	35.264306	25.738583	18
J64*	ZMBN 132444	n/a	Greece: Elounda, Crete	35.264307	25.738584	15
J65*	ZMBN 132445	n/a	Spain: San Vicente do Grove, Pontevedra	42.455300	-8.922587	10
J66	ZMBN 132446	*Jorunna tomentosa* B	Spain: San Vicente do Grove, Pontevedra	42.455301	-8.922588	10
J67*	ZMBN 132447	n/a	Spain: San Vicente do Grove, Pontevedra	42.455302	-8.922589	5
J68*	MNHN-IM-2019-1512	*Jorunna* cf. *tomentosa*	Spain: El Riconin, Gijou, Asturias	43.545621	-5.682680	n/a
J69*	MNHN-IM-2019-1513	*Jorunna* cf. *tomentosa*	Spain: El Riconin, Gijou, Asturias	43.545622	-5.682681	n/a
J70*	ZMH 71707	*Jorunna* cf. *tomentosa*	Germany: Helgoland, West coast	54.182372	7.879751	10
J71*	ZMH 71773	*Jorunna* cf. *tomentosa*	Germany: North Sea	n/a	n/a	18

Table B. Remarks on radulae, copulatory spines, caryophyllidia, and penial structures of the examined material of *Jorunna* sp. nov., *J. tomentosa* lineage A, and *J. tomentosa* lineage B.

Sample ID	Voucher no.	Species name	Radular formula	Remarks on innermost radular teeth	Remarks on sickle-shaped (ss) outermost radular teeth	Total length (TL) and remarks on copul. spine
J08	NTNU-VM-58891	*Jorunna* sp. nov.	19x 18.0.18	Denticles absent	5 to 6 ss, denticles absent	n/a
J23	ZMBN 125946	*Jorunna* sp. nov.	25x 20.0.20	Denticles absent	3 to 4 ss, denticles absent	TL = 1600 µm
J49	ZMBN 127749	*Jorunna* sp. nov.	23x 21.0.21	One tooth with round swelling	3 to 4 ss, denticles absent	TL = 1700 µm; broken tip
J39	ZMBN 127710	J. *tomentosa* lineage A	21x 23.0.23	One tooth with 1 denticle	4 to 5 ss, up to 2 denticles	TL = 1100 µm
J47	ZMBN 127707	*J. tomentosa* lineage A	25x 25.0.25	Denticles absent	2 to 3 ss, denticles absent	TL = 500 µm; broken base
J48	ZMBN 127711	J. *tomentosa* lineage A	19x 26.0.26	Denticles absent	3 to 4 ss, denticles absent	TL = 750 µm; broken tip
J02	NTNU-VM-213	J. *tomentosa* lineage B	18x 26.0.26	Denticles absent	3 to 4 ss, up to 6 denticles	n/a
J14	ZMBN 125038	J. *tomentosa* lineage B	22x 23.0.23	Several teeth with each 1 denticle	4 to 8 ss, up to 6 denticles	TL = 1100 µm
J19	ZMBN 125553	J. *tomentosa* lineage B	25x 20.0.20	One tooth with 1 denticle	3 to 4 ss, up to 7 denticles	TL = 990 µm
J32	ZMBN 127603	J. *tomentosa* lineage B	20x 19.0.19	Several teeth with each 1 denticle	3 to 4 ss, denticles absent	n/a
J35	ZMBN 87955	J. *tomentosa* lineage B	23x 28.0.28	One tooth with 5 denticles	3 to 4 ss, up to 5 denticles	TL = 880 µm
J46	ZMBN 127705	J. *tomentosa* lineage B	n/a	n/a	n/a	TL = 1000 µm

Table B. *Continued*.

Sample ID	Voucher no.	Species name	Remarks on caryophyllidia	Remarks on penial structure
J08	NTNU-VM-58891	*Jorunna* sp. nov.	Up to 6 long spicules	Round base, slender tip
J23	ZMBN 125946	*Jorunna* sp. nov.	Damaged due to preservation	Round base, slender tip. Flattened when dried.
J49	ZMBN 127749	*Jorunna* sp. nov.	Up to 6 long spicules	Slightly round base, slender tip
J39	ZMBN 127710	J. *tomentosa* lineage A	Damaged due to preservation	Diffuse base, slender, tilted tip
J47	ZMBN 127707	J. *tomentosa* lineage A	Damaged due to preservation	Diffuse base, slender, tilted tip
J48	ZMBN 127711	J. *tomentosa* lineage A	Up to 10 long spicules	Cone-shaped, rounded tip not tilted
J02	NTNU-VM-213	J. *tomentosa* lineage B	Up to 7 spicules, shorter	n/a
J14	ZMBN 125038	J. *tomentosa* lineage B	Damaged due to preservation	n/a
J19	ZMBN 125553	J. *tomentosa* lineage B	Up to 6 long spicules	Cone-shaped, rounded tip not tilted
J32	ZMBN 127603	J. *tomentosa* lineage B	Up to 8 long spicules	Destroyed when dried
J35	ZMBN 87955	J. *tomentosa* lineage B	Up to 7 long spicules	Cone-shaped, circular knob at tip
J46	ZMBN 127705	J. *tomentosa* lineage B	Up to 8 spicules, shorter	n/a